UNIVERSITÀ DEGLI STUDI DI MILANO

PhD Course in Molecular and Cellular Biology

XXIX Cycle

Unravelling the essential role of TgpA in the viability of *Pseudomonas aeruginosa*: a putative target for novel antimicrobial agents

Mónica Uruburu

PhD Thesis

Scientific tutor: Prof. Giovanni Bertoni

Scientific co-tutors: Mario Milani & Eloise Mastrangelo

Academic year: 2016-2017

SSD: BIO/19, BIO/10

Thesis performed at Department of Biosciences, Università degli Studi di Milano.

Contents

A. Abstract

The opportunistic pathogen *Pseudomonas aeruginosa* is a common agent of infectious disease in immunocompromised individuals, and a dominant pathogen in late-stage of cystic fibrosis disease. *P. aeruginosa* represents a prototype of multidrug resistant “superbug” due to intrinsic and acquired resistance to antimicrobials agents, for which effective therapeutic options are very limited. In order to overcome the current resistance mechanisms, the identification and characterization of new cellular functions that are essential for *P. aeruginosa* viability could drive the development of new antibacterial compounds with novel mechanisms of action.

The present PhD thesis is focused on the functional and structural characterization of the Transglutaminase protein A, TgpA, an inner membrane protein predicted to belong to the Transglutaminase-like family which contains a functional TG domain ($TG_{180–544}$), localized in the periplasmic side, suggested to take part in an essential function involved in envelope structure. The protein was recently described as essential for the viability of *P. aeruginosa*, and a promising candidate for the design of new specific antimicrobial compounds.

In Part I, the state of the art and main results are presented. First, the *in vivo* evaluation of the modulation of TgpA expression levels on the *P. aeruginosa* growth showed that, the increase of TgpA cellular levels dramatically affects the *P. aeruginosa* growth. On the other hand, the partial suppression of the chromosomal copy of the *tgpA* gene showed to compromised the envelope organization of the cells.

The subsequent structural characterization of the functional TG domain allowed confirming that TgpA belongs to the poorly characterized Transglutaminase-like family, in which many of the prokaryotic members are proteases. Also, the presence of a carbohydrate-binding domain at the N-terminal portion of the protein, suggests that the binding to polysaccharides present in the cell wall might constitute a mechanism of regulation of the enzymatic activity of TgpA. Moreover, the active site of the protein shares homology with cysteine proteases and endopeptidases with described action in the maintenance/biosinthesys of the bacterial peptidoglycan, suggesting that TgpA might be involved in the cell wall metabolism. The transglutaminase and proteolytic activity of the TG domain were evaluated *in vitro*, showing residual activity over generic substrates.

A manuscript in preparation, presented in Part II, describes in detail the characteristics found in the structure of the TG domain that are the foundations for the TgpA enzymatic activity.

Finally, in the search for possible inhibitory molecules of the activity of TgpA, the results of a preliminary *in silico* docking analysis with *in vivo* results are presented in Part III.

PART I

B. State of the Art

B.1. *Pseudomonas aeruginosa*

Pseudomonas aeruginosa is a rod-shaped gram negative and ubiquitous environmental bacterium. It belongs to the genus Pseudomonas that contains more than 120 species which are all-over in moist environments such as water and soil ecosystems and are infective to plants, animals and humans (Spiers *et al.*, 2000; Peix *et al.*, 2009).

P. aeruginosa is metabolically versatile and has been isolated from numerous nutrient-poor settings to the extent that it is able to survive even in distilled water. Its optimal temperature for growth is 37°C. However, it is able to tolerate temperatures as high as 50°C and is capable of growing under both aerobic and anaerobic conditions, using preferentially nitrate as a terminal electron acceptor (Schreiber *et al.*, 2007).

In humans*, P. aeruginosa* is an opportunistic pathogen, capable of acute, severe, invasive disease and persistent infections (eluding immune defences) (Kerr and Snelling, 2009). Serious infections are often in hospitalized patients, and nearly all associated with immunocompromised hosts such as in neutropenia, severe burns, urinary tract infections, AIDS, lung cancer, chronic obstructive pulmonary disease and cystic fibrosis (CF) (Driscoll *et al.*, 2007, Gellatly and Hancock, 2013). Infections caused by *P. aeruginosa* are not only common but also have been associated with high morbidity and mortality when compared with other bacterial pathogens (Harbarth *et al.*, 2002; Osmon *et al.*, 2004).

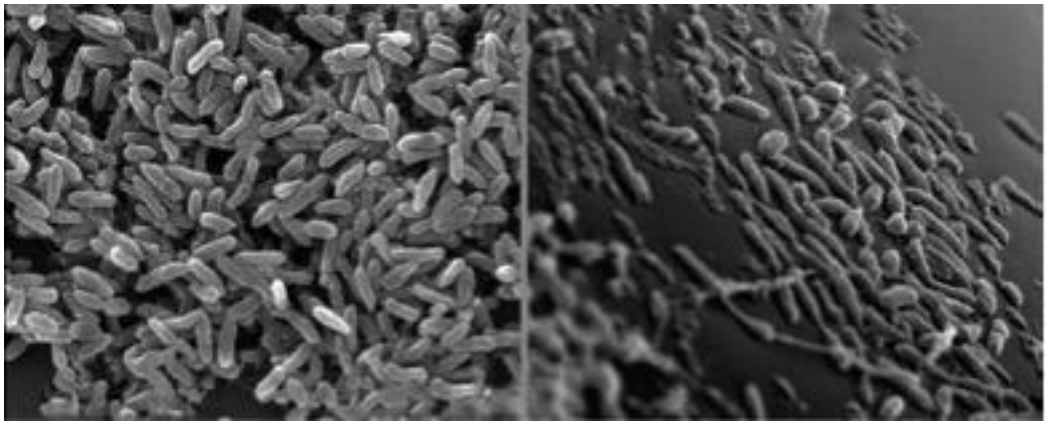

Figure B1. Scanning electron microscopy images of *P. aeruginosa* isolates attaching to glass surfaces.

The success of *P. aeruginosa* as an opportunistic pathogen is due to the versatility and adaptability encoded in its relatively large genome (> 6 Mbp), arranged in a core genome with a set of conserved regions (90%) interspaced by regions of high plasticity, containing genes that are found in only a few strains (Mathee *et al.*, 2008; Silby *et al.*, 2011; Gellatly and Hancock, 2013). In the pathogenic strain PAO1, the 10% of its genome encodes for regulatory proteins, many of them belonging to the two-component class of regulatory system, which allows the bacterium to rapidly adapt to environmental changes, and some others implicated in virulence and antibiotic resistance (Gellatly and Hancock, 2013).

B.1.1. Clinical importance

P. aeruginosa is largely associated with nosocomial infections, even reported as a worldwide healthcare issue (Rosenthal *et al.*, 2016). This pathogen is a prominent cause of health-care acquired pneumonia and ventilator-associated pneumonia, central line-associated bloodstream infection, urinary catheter-related infection and surgical/transplantation infections (Report from NNIS System, 2004; Nathwani *et al.*, 2014; Trubiano and Padiglione, 2015). Mortality rates can be significant (ranging from 7% to 62%), depending on host factors (pre-existing comorbidities, including alterations to normal physical barriers of the lung, and the presence of immunosuppression and bacterial factors, such as antimicrobial resistance and presence of virulence factors (Moore *et al.*, 2016).

In presence of pre-existing lung pathologies, such as certain chronic pulmonary diseases, the colonization with *P. aeruginosa* is very common. In patients with CF, the cause is multifactorial, but includes aberrant inflammatory responses, increased pathogen adhesion to the endothelium and altered host response to biofilm (Smith *et al.,* 2006; Hogardt and Heesemann, 2010; Moradali, 2017). *P. aeruginosa* will adapt to CF airways and persist as overwhelming, predominant and ineradicable infections to the end of patient's life in almost 70% of adults (Döring *et al.*, 2000).

The ability of *P. aeruginosa* to form biofilms extends to abiotic material and is a key virulence factor; colonization of and subsequent infection around prosthetic devices is a frequent complication. This ranges from intravascular device-associated bacteraemia (cannulae and central lines; particularly in critical care and among immunocompromised patients, such as those undergoing chemotherapy or dialysis), to prosthetic joint infections, through to in-

dwelling intrathecal or intracranial devices in neurology and neurosurgical patients associated with CNS infections (Smith *et al.*, 2006; Moore *et al.*, 2016).

Infection with *P. aeruginosa* can be also a serious complication of burns. In these patients the disruption of the tegument, combined with the local immunosuppression that comes with burnt tissue (where there is reduced T-cell activity, inflammatory cytokines and complement), the colonization frequently progresses to infection (Hogardt and Heesemann, 2010; Moore *et al.*, 2016).

The predilection of *P. aeruginosa* for moist areas means wounds, including foot wounds among patients with diabetes, which are frequently colonized with this organism and swab results commonly report its presence. However, the contribution of this organism to wound infections here is less clear; while *P. aeruginosa* has the potential to cause wound infections (including calcaneal osteomyelitis in diabetic foot infections), non-pathological colonization is more commonplace (Sadikot *et al.*, 2005; Kipnis *et al.,* 2006; Moore *et al.*, 2016).

B.2. Pathogenesis and virulence factors of *P. aeruginosa*

The pathogenesis of *P. aeruginosa* has been extensively studied and proven to be a multifactorial process mediated by quorum sensing (QS) (Sun *et al.*, 2016). This is a mechanism of communication between individual cells facilitated by specific chemical signals, called autoinducers (AIs), which are diffused through the membranes, and allows for a coordinated adaptation of a bacterial population to environmental changes. QS controls the behaviour of bacteria by multiple interconnected signalling pathways (LaSarre and Federle, 2013). The number of AIs molecules in the medium is proportional to the concentration of bacteria so, when a critical number of bacteria (i.e. “quorum”) is reached, the concentration of AIs triggers the activation of specified downstream genes which affects the entire bacterial population (Vasil, 2003). More than 10% of *P. aeruginosa* genes are regulated by QS. These genes are mainly involved in virulence factor production, motility, motility-sessility switch and biofilm development (Venturi, 2006; Williams and Camara, 2009; Barr *et al.*, 2015).

During pathogenesis *P. aeruginosa* QS plays a critical role for survival and colonization by coordinating phenotypic alterations at early stages of infection i.e., after attachment (González and Keshavan, 2006). Production of virulence factors is a survival strategy for pathogens to evade host immune defence resulting in progression of pathogenesis particularly at early stage of colonization or acute infection. QS upregulates the expression of genes involved in the production of some destructive virulence factors such as proteases (elastase, alkaline protease), pyocyanin, toxins (exotoxin A), rhamnolipids and hydrogen cyanide (Jaffar-Bandjee *et al.*, 1995; Lee and Zhang, 2015). Production of these toxic compounds is destructive to the host cells/tissues by impairing permeability barrier and by inhibiting protein production promoting cell death. Various modes of motility such as swimming and swarming involving flagella and twitching using type IV pili are associated with virulent traits in *P. aeruginosa* (Windstanley *et al.*, 2016). A motile cell is readily detectable by the host immune system via flagellar and other motility component mediating recognition and induction of signalling pathways that trigger inflammatory responses and phagocytosis (Amiel *et al.*, 2010).

The progress from acute to chronic infection is critically influenced by QS-dependent gene expression. Transition from motility to sessile lifestyle requires dynamic regulatory networks at transcriptional, post-transcriptional and post-translational levels resulting in coordinated timely expression of hundreds of genes. These events mainly arrest flagella based motility and the production of virulence factors such as exotoxins and proteases while positively regulating surface attachment, extracellular polymeric substances (EPS) production and biofilm maturation. The switching is a survival advantage by pathogenic bacteria like *P. aeruginosa* to evade stress and adverse conditions. They lose motility and attach to surfaces and form cellular aggregations embedded in EPS to protect bacteria from surroundings environment (Leid, 2009; Olsen, 2015). These structures, called biofilm, are characteristic of chronic infections and indicative of disease progression and long-term persistence (McDaniel *et al.*, 2015). The biofilm creates a niche in which bacteria establish intense cell-cell interaction and communication as well as a reservoir of metabolic substances, nutrients and energy (Flemming and Wingender, 2010). The exopolysaccharides and alginate are major constituents of the *P. aeruginosa* biofilm matrix involved in surface adhesion and together with extracellular DNA (eDNA) determine the biofilm architecture. These EPS play an important role in resistance to immune responses and antibiotic treatments (Ghafoor *et al.*, 2011; Gellatly and Hancock, 2013; Strempel *et al.*, 2013).

Genes involved in the progress of biofilm maturation and persistence are positively regulated by QS in *P. aeruginosa*. The rhamnolipids have been suggested to play an active role in the maintenance of the biofilm architecture by contributing to the formation of internal cavities allowing proper flow of water and nutrients (Davey *et al.*, 2003; Boles *et al.*, 2005; Dusane *et al.*, 2010; Chrzanowski *et al.*, 2012). Additionally, the production of polysaccharide (Jennings *et al.*, 2015), eDNA and QS-controlled production of pyocyanine (Das *et al*., 2013, 2015) are critical for biofilm maturation. Such molecular and cellular interactions in combination with other polymeric substances lead to establishment of a robust and mature biofilm.

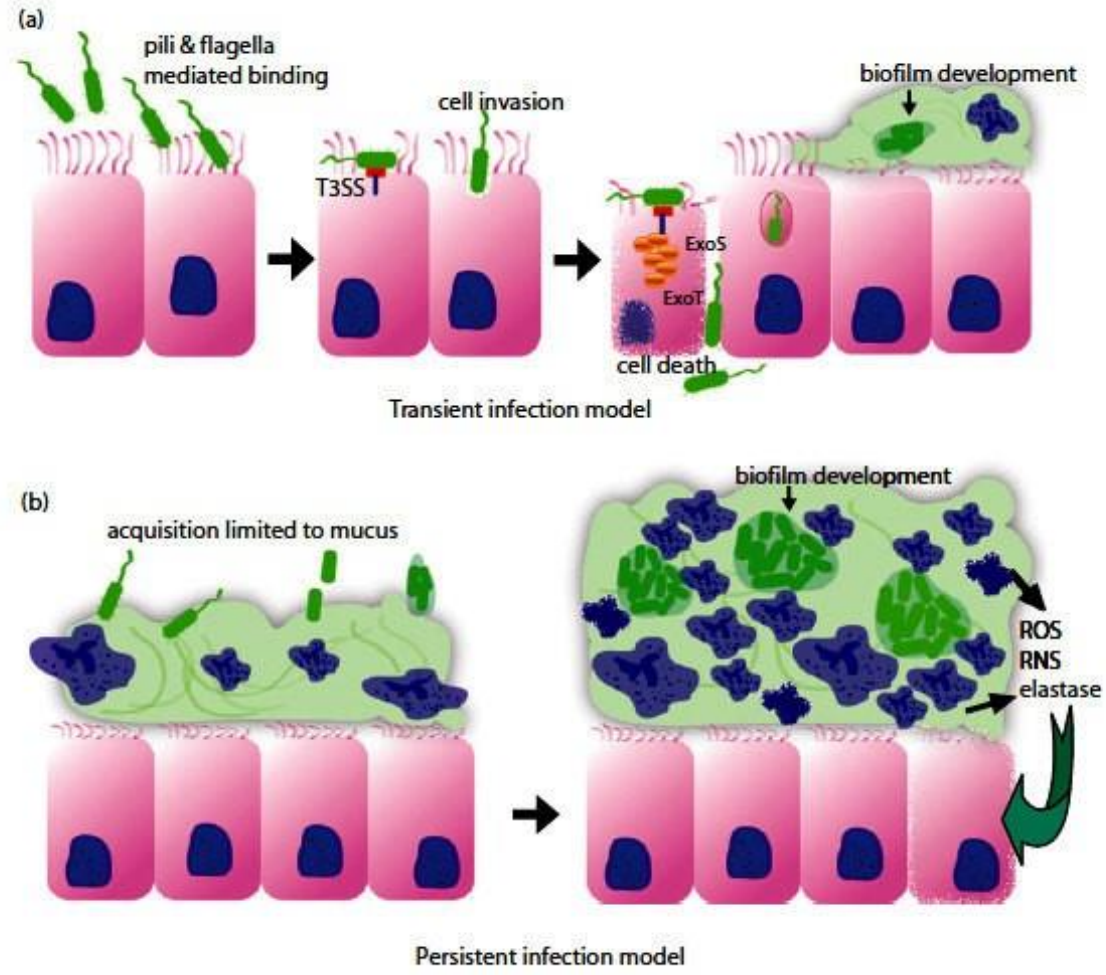

Figure B2. Model of establishment of *P. aeruginosa* infection. In (a) *P. aeruginosa* is equipped with a full arsenal of virulence traits including pili, flagella, type 3 secretion systems (T3SS) and secreted virulence factors. Toxin elaboration injures the surrounding host tissue. The significance of cytosolic invasion during human infections is not clear, but breach of the epithelial surface occurs after cell death from toxin injury. Epithelial injury also results in loss of mechanical clearance mechanisms and establishment of the pseudomonal biofilm leading to a persistent infection. In (b) *P. aeruginosa* infects an already inflamed surface with a defective muco ciliary elevator. The infecting organism mayor may not be piliated, and may already exist in a 'biofilm' state if acquired from another patient. The infection occurs strictly in the mucous layer where 'nests' of pseudomonads bind to cell debris and extracellular DNA rather than the epithelial surface. The pseudomonal micro-colonies are a strong inflammatory stimulus, but are resistant to the actions of neutrophils, which may injure surrounding tissue in their efforts to remove the stimulus. Neutrophil death may provide more substrate for pseudomonal growth. (Image source Williams, J. Dehnbostel, Sblackwell 2010. *Pseudomonas aeruginosa*: host defence in lung desease, Respirology).

B.3. Antibiotic resistance in *P. aeruginosa*

P. aeruginosa is intrinsically resistant to many antimicrobials, and capable of developing resistance to many others under the influence of previous antibacterial exposure. The emergence of antibiotic resistant bacteria is a global health issue, strongly associated with nosocomial infections, and a worldwide concern due to increasing development of Multidrug Resistant strains (MDR) (Streeter and Katouli, 2016).

B.3.1. Intrinsic resistance mechanisms

Like many gram-negatives bacteria, *P. aeruginosa* is intrinsically resistant to many β-lactams, macrolides, tetracyclines, cotrimazole and most fluoro-quinolones. Such intrinsic resistance mechanisms are derived from the presence of genes that encode inherent properties of cell structures and composition, providing protection against toxic molecules and antimicrobials (Lambert *et al.*, 2011; Blair *et al.*, 2015; Figure B3).

Some hydrophilic antibiotics, such as the broad-spectrum drugs carbapenems and cephalosporines, can enter the cell by diffusion through porin proteins in a non-specific manner. However, *P. aeruginosa* limits the antibiotic entry by reducing the expression of non-specific porins and replacing them with selective proteins for taking up required nutrients, resulting in the lowered permeability to toxic chemicals (Tamber and Hancock, 2003).

Another mechanism in *P. aeruginosa* that contributes to antibiotic resistance is based on the active multidrug efflux pumps, multi-protein complexes spanning the cell wall. They are responsible for the expelling of toxic materials and wide range of antimicrobials. However, they are substrate specific, so they show resistance against different classes of chemically unrelated antibiotics (Blair *et al.,* 2015, Venter *et al.*, 2015).

In *P. aeruginosa*, four active multidrug efflux pumps have been described:

1. MexAB-OprM
2. MexXY-OprM(OprA)
3. MexCD-OprJ
4. MexEF-OprN

MexAB-OprM and MexXY-OprM(OprA), are the most important, because their large prevalence in clinical strains. MexAB-OprM is stable and constitutively expressed in cells, guaranteeing a protective basal level that expels consistently a wide range of toxic molecules (Li *et al.,* 2015); therefore, it contributes to natural resistance to antibiotics. On the other hand, *mexXY-(oprA)* is mainly induced in response to protein inhibitors that target the ribosomal machinery (Matsuo *et al.*, 2004; Hay *et al.*, 2013). Both MexCD-OprJ and MexEF-OprN are not expressed in wild-type strains or are slightly expressed, and have been proposed not to contribute significantly to natural antimicrobial resistance (Llanes *et al.*, 2011; Li *et al.*, 2015).

P. aeruginosa produces β-lactamases: enzymes that hydrolyze the peptide bond of the β-lactam ring leading to their inactivation (Majiduddin *et al*., 2002). This pathogen is able to produce various β-lactamases, including extended-spectrum β-lactamases (ESBL), metallo-β-lactamases (MBL) and chromosomal cephalosporinase (AmpC) (Oliver *et al.,* 2015). AmpC differs from the other β-lactamases because the *amp*C gene is present in all strains of *P. aeruginosa*, although it requires a gene mutation to cause hyper production and antibiotic resistance (Juan *et al*., 2005). However, through adaptive or acquired resistance mechanisms AmpC can be overproduced, consequently conferring resistance to a wider range of antibiotics such as aminoglycosides and fluoroquinolones (Umadevi *et al.*, 2011).

B.3.2.Mechanisms of acquired resistance

P. aeruginosa can acquire resistance to antimicrobials through mutations of intrinsic genes or by horizontal acquisition of plasmids carrying genetic material encoding for antibiotic resistance (Davies, 1997; Davies and Davies, 2010). This type of resistance occurs in the presence of antibiotic compounds leading to irreversible resistance population transmittable to the progeny (Lee *et al.,* 2016). Mutations in regulatory pathways can increase the promoter activities resulting in unleashing gene expression and overproduction of proteins, even in genes that confer intrinsic resistance, such as AmpC or multi-drug efflux pumps that are regulated by regulatory pathways, causing higher level of resistance (Blair *et al*., 2015).

A clinically important and prevalent mutational alteration is attributed to OprD porin, a carbapenem-specific channel localized in the outer membrane of *P. aeruginosa*. Altered OprD reduces the permeability of the outer membrane, leading to the resistance to imipenem and reduced susceptibility to meropenem (Epp *et al.*, 2001; Gutiérrez *et al.*, 2007; Kao *et al.*, 2016).

Mutational changes within the fluoroquinolone targets i.e., DNA gyrase (gyrA and gyrB) and/or topoisomerase IV (parC and parE) or overproduction of active or inducible efflux pumps (Lee *et al.*, 2005; Sun *et al.*, 2014; Figure B3) explain the resistance to this kind of antibiotics in *P. aeruginosa*.

Also plasmids are potent vehicles for acquiring resistance genes against different kind of antibiotics in *P. aeruginosa* (Poole, 2011). Transferable plasmids carrying resistance genes can be mobile among a wide range of unrelated bacteria, increasing treatment complications (Hong *et al.,* 2015). So far, *P. aeruginosa* resistance via horizontal gene transfer has been reported for the genes encoding β-lactam-hydrolyzing enzymes known as the extended-spectrum β-lactamases and the carbapenemases, aminoglycoside-modifying enzymes, 16S rRNA methylases resulting in high-level pan-aminoglycoside resistance (Poole, 2011).
Genes encoding extended-spectrum β-lactamases and carbapenems, are important not only for their hydrolysing activity on a wide range of β-lactam but also for their worldwide prevalence (Paterson and Bonomo, 2005; Blair *et al.*, 2015; Sullivan *et al.*, 2015).

Recent findings reported the first evidence of plasmid-mediated colistin (or polymyxin E) resistance (Liu *et al.*, 2016). Members of the polymixin family have been the last resort for antibiotic treatment of carbapenem-resistant bacteria such as *P. aeruginosa* isolates (Falagas and Kasiakou, 2005). Resistance to polymyxins was previously reported to occur via chromosomal mutations (Moskowitz *et al.*, 2012; Gutu *et al.*, 2013), however, new evidence suggests plasmid-mediated resistance through the mobilization of the mcr-1 gene, first described in *Escherichia coli* strain SHP45 (Liu *et al.*, 2016).

B.3.3. Adaptive resistance mechanisms

The adaptive resistance mechanism in *P. aeruginosa* is not very well understood yet, however it is known as an unstable and transient form of resistance, induced in the presence of specific antibiotics or environmental stress, and reversible upon removal of the external stimuli leading to a re-gaining of susceptibility (Barclay *et al.*, 1992; Xiong *et al.*, 1996; Fernández *et al.*, 2011). This mechanism has been seen mediating the resistance of *P. aeruginosa* isolates to β-lactams, aminoglycosides, polymyxins and fluoroquinolones (Zhang *et al.*, 2001; Poole, 2005; Fernández *et al.*, 2010; Khaledi *et al.*, 2016).

Some *P. aeruginosa* isolates from CF patients, showed adaptive resistance to fluoroquinolones due to multiple mutations in known-resistance genes like *nfxB*, leading to a loss of function of the NfxB transcriptional repressor that regulates the expression of the MexCD-OprJ efflux pump. The consequent overproduction of MexCD-OprJ reduces the susceptibility to this kind of antibiotics (Wong *et al.,* 2012). Through adaptive mechanisms, *P. aeruginosa* can also acquire and lose resistance to aminoglycosides, polymyxins and cationic antimicrobial peptides, by altering the lipid A structure of the LPS (Barrow and Kwon, 2009; Fernandez *et al* 2012). Other forms of multidrug efflux pumps such as MexJK, MexGHI-OpmD, MexVW, MexPQ-OpmE, MexMN, and TriABC, are not expressed in wild-type strains but may contribute to adaptive resistance against antibiotic or biocide agents when expressed in resistant strains (Lister *et al.*, 2009; Avrain *et al.*, 2013).

The Figure B3 summarizes the different mechanisms of antibiotic resistance *in P. aeruginosa.*

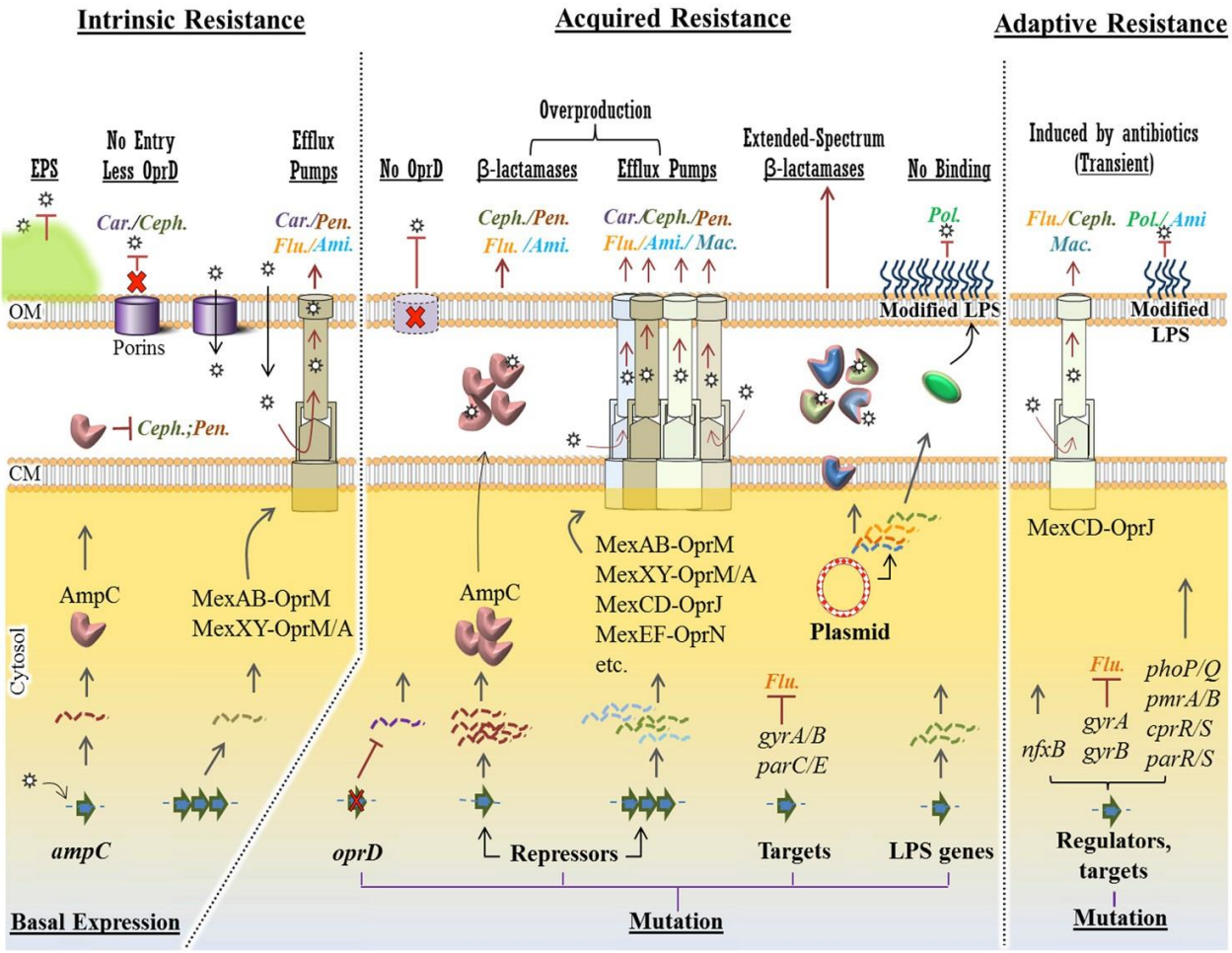

Figure B3. Intrinsic, acquired and adaptive mechanisms confer antibiotic resistance in *P. aeruginosa*. For each mechanism, various molecular strategies,which confer resistance to specific class of antipseudomonal antibiotics (Car., Carbapenems; Ceph., Cephalosporins; Pen., Penicillins; Ami., Aminoglycosides; Flu.,Fluoroquinolones; Mac., Macrolides and Pol., Polymyxins), were presented at the top of the figure (underlined) Intrinsic mechanisms such as structural barriers [e.g.,EPS (extracellular polymeric substances)], OprD reduction and basal production of AmpC b-lactamase and MexAB/XY efflux pumps confer a basal resistance to somegroup of antibiotics. However, in acquired resistance, mutational changes in the oprD gene, transcriptional repressors causingupregulation of resistance genes andefflux pumps conferring resistance against a wider spectrum of antibiotics. Plasmid-mediated resistance is very potent as a variety of resistance genes can beexchanged among bacteria. Either mediated by mutational changes in the genome or in plasmids, resistance to polymyxins occurs via modification of LPS (lipopolysaccharide) components hindering binding of the antibiotic to this layer. Adaptive resistance occurs in the presence of antibiotics mainly via mutation inregulatory genes. This is a transient and reversible resistance, which will reverse upon removal of antibiotics. Stars represent antibiotics and dashed/wavy linesrepresent transcriptional levels of each gene product. CM, cytoplasmic membrane; OM, outer membrane (Image source Moradali MF, Ghods S and Rhem BHA. 2017. *Pseudomonas aeruginosa* lifestyle: A paradigm for adaptation, survival and persistence. *Front Cell Infect Microbiol.* 7:39 doi: 10.3389/fcimb.2017.00039).

B.4. Multidrug resistance in *P. aeruginosa*

Resistance development in many human pathogens has taken place on an unprecedented scale, as resistance has evolved into multidrug resistance (MDR), leading to increased global morbidity and mortality (WHO, 2014). A MDR bacterium is defined as non-susceptible to at least one antimicrobial agent in three or more antimicrobial classes, while strains that are non-susceptible to all antimicrobials are classified as extreme drug-resistant strains (Kallen and Srinivasan, 2010). Bacterial strains belonging to the so-called "ESKAPE" group of pathogens (*Enterococcus faecium*, *Staphylococcus aureus, Klebsiella pneumoniae, Acinetobacter, P. aeruginosa* and *Enterobacter*) are of importance to this pandemic (Rice, 2008). These pathogens, both gram-positive and gram-negative bacteria, often carry MDR determining genes residing on genetic resistance islands of complex evolutionary origin that are encoded on the chromosome or plasmids (Toleman and Walsh 2011; Ellington *et al.,* 2015; Schmitz *et al.,* 1999). MDR gram-negative bacteria are by far the most important and costly in our society today, as they cause the vast majority of nosocomial infections (Livermore, 2012), being *P. aeruginosa* one of the most challenging superbugs (Boyle *et al.,* 2012).

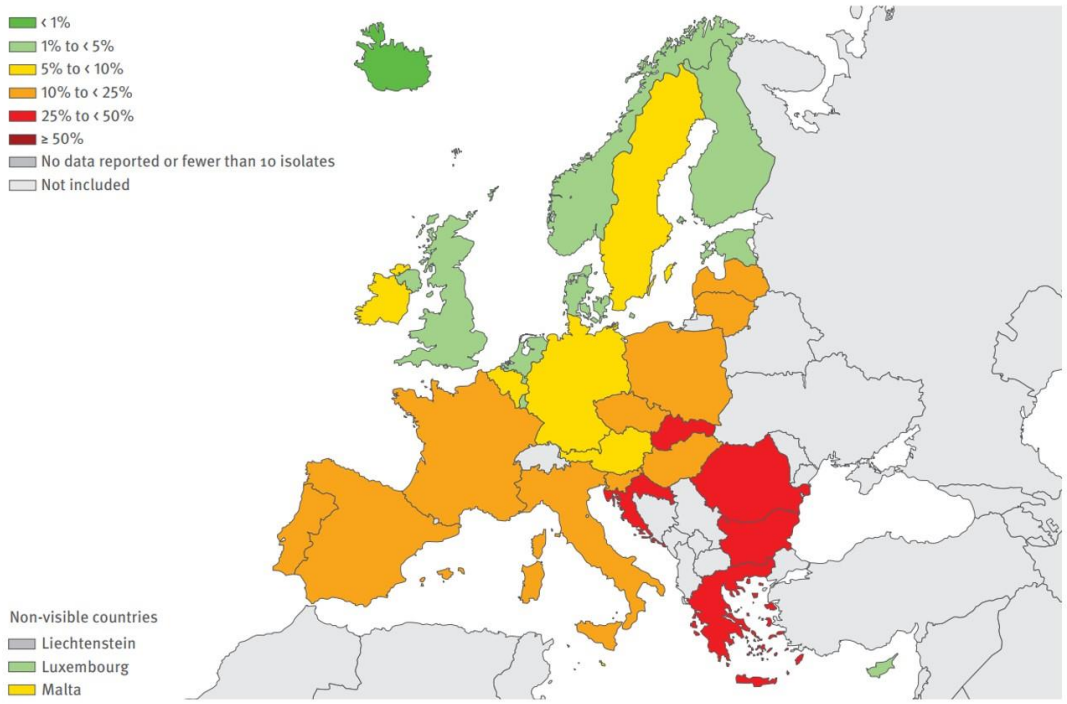

Figure B4. *P. aeruginosa* percentage of invasive isolates with combined resistance (to three or more antimicrobial groups among piperacillin + tazobactan, ceftazidime, fluoroquinilones, aminoglycosides and carbapenems) by country, EU/EEA countries, 2016. (Image source Antimicrobial Resistance Surveillance in Europe 2016 (http://www.ecdc.europa.eu))

According to the Antimicrobial Resistance Surveillance in Europe of 2016 (http://www.ecdc.europa.eu) high percentages of resistance in *P. aeruginosa* isolates were reported, with almost all the countries showing percentages above 10% for all antimicrobial groups under surveillance. Of special concern, 33.9% of the *P. aeruginosa* isolates reported in 2016 were resistant to at least one of the antimicrobial groups under regular surveillance (piperacillin ± tazobactam, fluoroquinolones, ceftazidime, aminoglycosides and carbapenems). The highest resistance percentage in 2016 was reported for piperacillin ± tazobactam (16.3%), followed by fluoroquinolones (15%), carbapenems (15%), ceftazidime (13%) and aminoglycosides (10%). Resistance for ceftazidime increased significantly between 2013 and 2016, while significantly decreases for fluoroquinolones, aminoglycosides and carbapenem resistance were reported during the same period of time. More specific analysis indicates that 4.9% of the isolates were resistant to at least three antimicrobial groups and 4.4% were resistant to all five antimicrobial classes (piperacillin, ceftazidime, fluoroquinolones, aminoglycosides and carbapenems) under the regular EARS-Net surveillance.

Carbapenems resistance has led to the introduction of peptides antibiotics, colistin (polymyxin E) and polymyxin B, rarely used due to their unattractive toxicity profile, but now utilized as last option antibiotics against MDR gram-negative infections that are resistant to all other antibiotics (Falagas and Kasiakou, 2005). However, currently little is known about their optimal dosing, pharmacokinetics and pharmacodynamics (Boucher *et al.,* 2009). A global survey of indications and regimens has found enormous inconsistencies in how and when colistin is used, including ways that are clearly suboptimal and could promote resistance to it and other polymixins (Wertheim *et al.,* 2013). In fact, resistance to polymyxins by *P. aeruginosa* strains that are normally susceptible to these drugs has been reported (Johansen *et al.,* 2008).

Development of novel antimicrobials against *P. aeruginos*a is therefore of the highest importance. At the beginning of 2017 a report made by the World Health Organization (WHO), about “Antibiotic-resistant priority pathogens list”, named the bacteria for which new antibiotics are urgently needed. International experts from the WHO and the University of Tübingen in Germany have identified them according to the level of resistance to excising treatment, mortality rates, prevalence in the community and burden on the health system. To convey the level of urgency, three priorities for research and development (R&D) were

settled: critical, high or medium. The critical priority category includes, in order, multi-resistant *Acinetobacter baumannii*, *P. aeruginosa* and *Enterobacteriaceae*.

The list is intended to spur governments to put in place policies that incentivize basic science and advanced R&D by both publicly funded agencies and the private sector investing in new antibiotic discovery. It will provide guidance to new R&D initiatives such as the WHO/Drugs for Neglected Diseases initiative (DNDi) Global Antibiotic R&D Partnership that is engaging in not-for-profit development of new antibiotics (WHO, 2017).

B.5. The crucial role of antibiotics

The discovery of penicillin in 1928 by Alexander Fleming, led devastating infectious diseases previously untreatable, such as streptococcal and chlamydia, suddenly to become treatable diseases. Without any doubt, the discovery of antibiotics sparked a new era in the treatment of infectious diseases and paved the way for modern medicine. Antibiotic treatment is the foundation for surgeries, cancer treatments and treatment of chronic diseases like diabetes and cystic fibrosis. Without efficacious antimicrobials, clinical medicine, as known today could be jeopardized (Lobanovska and Pilla, 2017).

During the “Golden era” of antibiotics drug discovery from 1940 to 1960, there was a huge expansion in the arsenal against bacterial infections through the continue discovery of new compounds, by two parallel and independent lines of discovery:

- Identification of small-molecule natural products with an observed antibacterial activity: penicillins and cephalosporins, the glycopeptides like vancomycin, and the aminoglycosides (Clardy *et al.*, 2009).
- Discovery of “man-made” molecules with antibiotic activity, such as aromatic sulfa scaffolds, originally from the chemical dyes industry or the fluoroquinolones (Blondeau, 2004).

During this relative short time period in history, most of today´s known classes of antibiotics were discovered (figure B5). From the 1960s to the 1970s, the rise of antibiotic resistance, especially in the hospital environment, led to a frantic search for new active compounds, but unfortunately screening programs mostly rediscovered existing antibiotics (Lewis, 2013). So, pharmaceutical companies developed new antibiotics by improving the already existing ones through chemical modifications, tailoring on the periphery of the major antibiotic classes, while leaving the core intact (Bérdy, 2005). However, resistance against the new versions of old-fashioned antibiotics quickly arise (Figure B5, bottom).

Simultaneously, the lack of success from natural compound screening led companies to redirect their efforts to small-molecule chemical libraries, obtaining, also in this case, a very poor return of new antibacterial agents. Thus, the development of brand new molecules with antibiotic effects must be a priority in microbiological research.

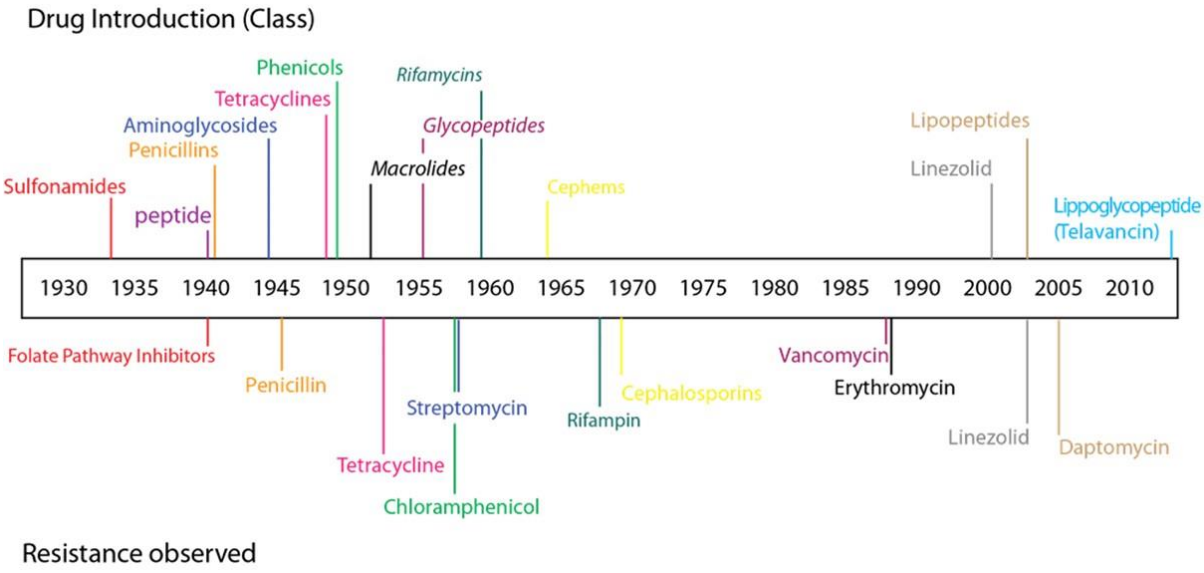

Figure B5. Top: Timeline showing the "Golden age" of antibiotic discovery (1940-1960) and "Golden age" of antibiotic medicinal chemistry (from 1960 to present). No new structural classes of antibiotics were introduced between 1962 and 2000, representing a serious innovation gap during the genomic era. Bottom: first time resistance to the class of antibiotics was observed in the clinical setting (Observation of resistance is not equal to loss of clinical efficacy against all clinical isolates. Not all classes or antibiotics are included). (Image source ClatworthyAE, Pierson E, Hung DT.2007.Targeting virulence: a new paradigm forantimicrobial therapy. *Nat Chem biol*; 3 (9):541-8).

B.5.1. Classic Antibiotic targets

Interestingly, most of the known antibiotics inhibit a relatively small number of vital cellular functions: I) cell wall synthesis inhibitors, II) protein synthesis inhibitors, III) Inhibition of DNA replication or RNA transcription, IV) Inhibition of Folic acid synthesis and V) Membrane disruption (Figure B6) (Lewis, 2013).

β-lactam antibiotics (Penicillins, cephalosporins, carbapenems and monobactams) represent the most important cell wall inhibitors, targeting the conserved penicillin binding proteins (PBPs). PBPs are involved in cross-linking of peptidoglycan precursor Lipid II in peptidoglycan synthesis (Typas *et al.*, 2012). Other inhibitors of cell wall synthesis include the glycopeptide antibiotic vancomycin that inhibits peptidoglycan synthesis through a different mechanism than β-lactams. Their applications result in changes to cell shape and size, induce cellular stress responses, and culminate in cell lysis (Tomasz, 1979; Barclay *et al.*, 1996).

A second category comprises the inhibition of DNA replication, most notably targeting DNA topoisomerase complexes by the synthetic quinolone class of antimicrobials, including the clinically relevant fluoroquinolone. These molecules interfere with the maintenance of chromosomal topology by hitting DNA gyrase and topoisomerase IV, trapping these enzymes at the DNA cleavage stage and preventing strand rejoining (Drlica *et al.*, 2008). The inhibition of RNA synthesis is due to the action of the Rifamycin class of semi-synthetic bactericidal antibiotics. These drugs inhibit DNA-dependent transcription by stable binding, with high affinity, to the subunit encoded by the *rpoB* gene and blocking RNA polymerase enzyme (Floss and Yu, 2005).

Protein synthesis inhibitors target either the 30S (aminoglycosides and tetracycline) or the 50S subunit (macrolides, chloramphenicol and clindamycin) of the 70S ribosome. Most of the antibiotics that inhibit the protein synthesis act on the elongation of the polypeptide synthesis (Wilson, 2013).

The last category of antimicrobials targets the folate biosynthetic pathway, responsible for the *de novo* synthesis of thymidine and other key cellular components. Folate analogues and sulfa derivate drugs, mostly used in combination, block two sequential steps in that biosynthetic pathway (Lange *et al.*, 2007).

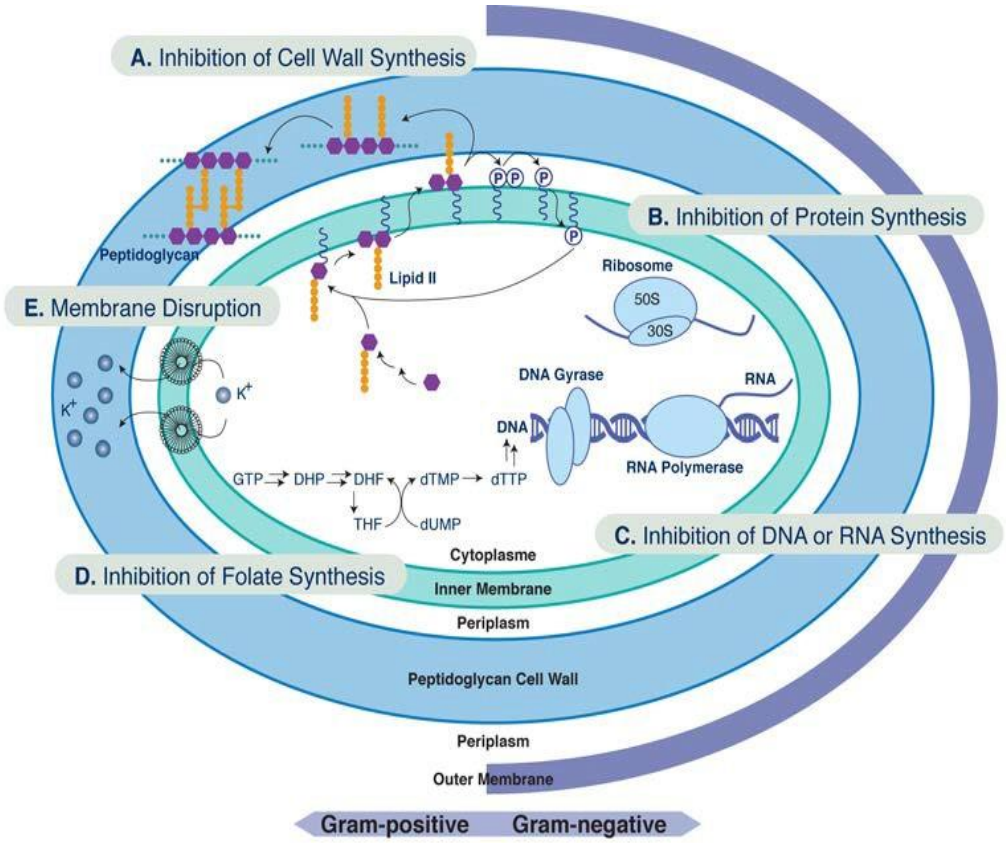

Figure B6. Overview of the cellular targets of most antibiotics, targeting either Gram-negative or Gram-positive bacteria. (A) The β-lactams (Penicillin's, cephalosporin's, carbapenem`s and monobactam`s) and glycopeptide`s inhibit cell wall synthesis; (B) Protein synthesis inhibitors include Aminoglycosides, tetracycline's, macrolides, chloramphenicol's and clindamycin, which interact with ribosomal subunits 30S and 50S; (C) Quinolones and fluoroquinolones inhibit the DNA gyrase and topoisomerase IV, Rifamycins (Rifampicin) inhibit DNA-dependent RNA polymerase; (D) Sulphonamides and Trimethoprim inhibit folic acid synthesis. Not all antibiotic drug classes are represented here. (Image sourceWalsh CT & Wencewicz TA. 2014. Prospects for new antibiotics: a molecule: entered perspective.*J Antibiot* 67, 7-22)

B.6. The urgent need for new antimicrobials

Nowadays the widespread antibiotic resistance is considered an important threat to modern medicine. In United States it is estimated that more than 2 million people acquire antimicrobial resistance infections every year, resulting in approximately 23.000 deaths (Fernandez, 2006). In Europe, drug resistant bacteria kill 25.000 people per year (Laxminaryan, 2014). The future global impact of antimicrobial resistance has the potential to be devastating.

The vast majority of current antibiotics target the same cellular processes as their natural or synthetic predecessors (Aminov, 2010). As described before, the range of these targets is limited to the components of translational machinery, cell wall biosynthesis, DNA/RNA metabolism and some other cellular processes.

It may seem obvious that efforts to develop new antibiotics with novel mechanism of action should be a priority. However, the development of new classes of antibiotics has lagged far behind the growing need for such drugs. A major factor contributing to the dwindling antibiotic pipeline is the decreasing number of companies within the pharmaceutical sector that continue to pursue the development of novel antimicrobials (Cooper and Shlaes, 2011), due to its decreasing profitability compared to other clinical indications that require longer term therapy. It is explicable also because the route to find new antibiotics and develop them into drugs is long and expensive. It costs around 1 billion dollars to bring a new drug to the market, and it takes on average over of 10 years for it to enter the clinic phase (Lobanovska and Pilla, 2017) (Figure B7).

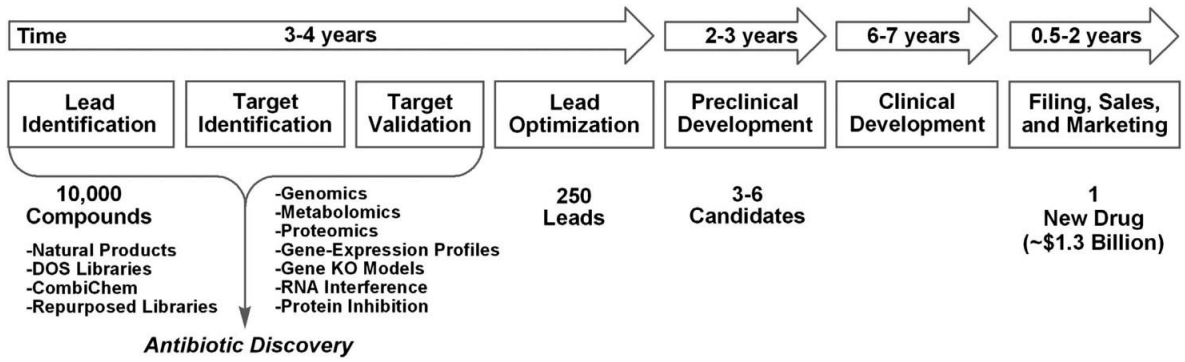

Figure B7. Antibiotic drug discovery and development flow chart. (Image sourceWalsh CT & Wencewicz TA. 2014. Prospects for new antibiotics: a molecule: entered perspective.*J Antibiot* 67, 7-22)

Despite the growing concern of clinicians about the very limited number of therapeutic options to mitigate the growing threat of antimicrobial resistance (AMR), a very small number of new drugs are currently in late stage of pre-clinical or clinical development (WHO 2017). A total of 51 antibiotics are in the clinical pipeline, but only eight of these belong to new antibiotic classes and have been classed as innovative by the WHO. Among them, Murepavidin, is the only one that showed specific activity against *P. aeruginosa* (including resistant strains) (De Winter *et al.*, 2017) and is a synthetic macrocyclic protegrin mimetic that inhibits the lipopolysaccharide-assembly protein (Giuliani and Rinaldi, 2011; Botos *et al.*, 2017) and has now completed phase-2 studies (NCT02096315, NCT02096328).

In this scenario, there is an impelling need for the identification of novel drug targets and the discovery of new-generation of antibiotics. Notably, the recent discovery of new promising antimicrobials with a completely new mechanism of action (Freire-Moran *et al.*, 2011; Ling *et al.*, 2015) indicates that we have only explored a fraction of the microbial targets that could be used for antibiotic drug discovery.

A rational development of antibacterial drugs with novel mechanisms of action requires the identification of new molecular targets that may emerge from a better understanding of cellular processes essential for cell survival and/or pathogenicity. In this view, large-scale systematic analysis of gene essentiality represented an important step towards the characterization of novel potential drug targets (Fernandez-Piñar *et al.*, 2015).

B.6.1. Novel essential genes as antimicrobial targets

In order to avoid being compromised by any of the current resistance mechanisms, it is desirable to develop compounds acting against unexploited targets (Tomaši and Peterlin. 2014). Over the last two decades the availability of genome sequencing techniques and transciptomics and proteomics approaches that permit the global characterization of bacterial components, have raised the possibility that antibiotic discovery can be performed by first identifying high value bacterial targets, like genes required for its growth and survival (Juhas *et al.,* 2012), and then developing compounds that inhibit these targets.

Although the genome sequences of approximately 2700 bacteria have already been released in public databases (Pagani *et al.*, 2012; Huang *et al.*, 2014), a number of crucial cellular pathways, such as secretion, cell division, and many other metabolic functions, remain uncharacterized and untargeted up to today (Kohanski *et al.*, 2010; WHO 2017).

It seems logical to assume that bacterial components necessary for growth and survival would serve as ideal targets for the identification of inhibitory compounds that demonstrate antibacterial activity. An essential gene is defined as one whose loss is lethal under a certain environmental condition (Xu *et al.*, 2011) but, regarding laboratory conditions where this essentiality is assessed, it typically refers to the ability to grow on solid media and form a colony in different experimental requirements (Fang *et al.*, 2005). So, the identification of essential genes plays a primary role not only in the research of potential targets for antimicrobial drug development but also in unravelling the minimal gene set for living organisms (Koonin, 2003; Gil *et al.*, 2004; Glass *et al.*, 2006) and deciphering bacterial relationships during evolution (Liao *et al.*, 2006; Koonin, 2009).

Furthermore, although important, many processes and pathways are not ubiquitous and, in most cases, are only shared by a subset of bacterial strains that are not well characterized (Jordan *et al.*, 2002). It is therefore evident that understanding and modelling the complexity of a living organism require global elucidation of gene function as well as the identification of the essential genes (de Berardinis *et al.*, 2008).

B.6.2. *P. aerug*inosa essential genes as antimicrobial targets

Recent analysis through different approaches, such as transposon mutagenesis, Tn-seq and Shotgun antisense, led to the identification of a number of general and condition-specific *P. aeruginosa* essential genes (Boutros and Ahringer, 2008; Christen *et al.*, 2011; de Berardinis *et al.*, 2008; French *et al.*, 2008; Gallagher *et al.*, 2011; Juhas *et al.*, 2012b; Langridge *et al.*, 2009; Lee *et al.*, 2015; McCutcheon and Moran, 2010; Moule *et al.*, 2014; Moya *et al.*, 2009; Rusmini *et al.*, 2014; Sigurdsson *et al.*, 2012; Skurnik *et al.*, 2013; Turner *et al.*, 2015).

A number of these genes are not essential in mammals cells therefore are considered as candidate drug target. That is the case for the genes implicated in asparagine-tRNA biosynthesis (Lee *et al.*, 2015). But more important, there are essential genes that have been described indispensable for *P. aeruginosa* but not for other bacteria, and are considered to be good targets for *P. aeruginosa* specific antibiotics. These include genes involves in the central carbon energy metabolism and protection from reactive oxygen species (Lee *et al.*, 2015), genes that are required for *P. aeruginosa* growth under clinically relevant conditions, such as cystic fibrosis sputum and genes necessary for pathogenesis (Turner *et al.,* 2015).

Recently, new antibiotics with novel mechanism of action support the idea that essential bacterial genes may be high valuable targets for the development of antimicrobials. The identification and characterization of inhibitors of the LpxC enzyme, a zinc-dependent deacetylase that catalyzes the first committed step in lipid A biosynthesis in gram negative bacteria (Barb *et al.*, 2008; Tomaras *et al.*, 2014) is one good example. LpxC inhibitors have shown potent *in vitro* activity against the multidrug resistant gram negative species *Klebsiella pneumoniae*, *Escherichia coli* and *P. aeruginosa* (Brown *et al.*, 2012; Montgomery *et al.*, 2012). Another successful example of an essential gene in *P. aeruginosa* targeted by an antimicrobial with novel mechanism of action is the recently developed peptidomimetic compound that targets the β-barrel of the outer membrane protein LptD, an essential gene for biogenesis of the cell envelope. In complex with the lipoprotein LptE, LptD transports LPS from the periplasm to the outer membrane (Wu *et al.*, 2005; Srinivas *et al.*, 2010; Wernebur *et al.*, 2012).

B.7. Transglutaminase Protein A –TgpA, a novel essential protein in *P. aeruginosa*

In *P. aeruginosa* was recently described a set of novel essential genes through Shotgun antisense RNA libraries (SALs). In this approach, essential genes are identified after shotgun-cloned genomic fragments and DNA sequencing of the growth-impairing fragments identifies those genes targeted by antisense RNA (Rusmini *et al.*, 2014).

The essentiality of a novel candidate, locus PA2873, encoding for Transglutaminase Protein A or TgpA, was further explored using different approaches such as insertional mutagenesis and conditional mutagenesis, demonstrating that the gene product TgpA, is indeed essential for the viability *P. aeruginosa* (Figure B8) (Milani *et al.,* 2012).

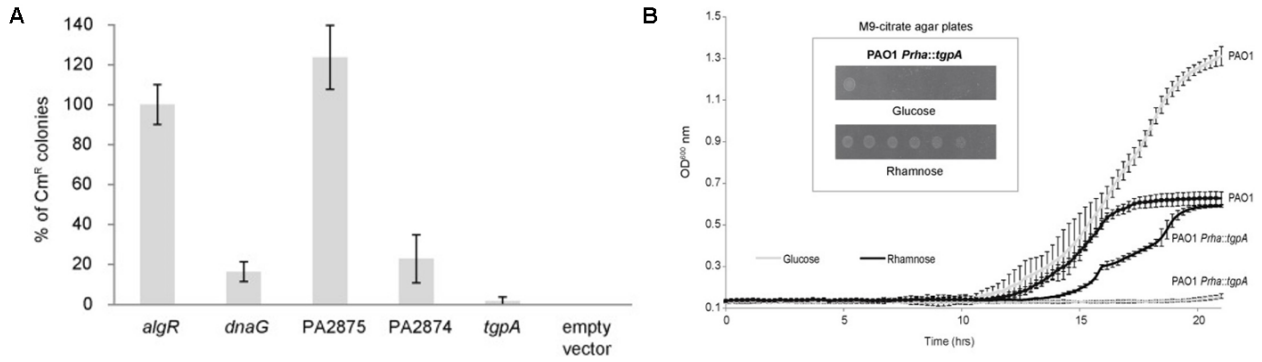

Figure B8. Mutagenesis analysis of locus PA2873 - *tgpA* gene. (A) Insertional mutagenesis on each indicated locus targeted for knock-out by homologous recombination-mediated cointegration of the suicide vector pDM4 carrying chloramphenicol resistance (CmR). The dnaG gene for DNA primase and the algR gene for a LytTR-type two-component response regulator were used respectively as positive and negative controls of essentiality. (B) Conditional mutagenesis. The rhamnose inducible/glucose repressible promoter PrhaB was inserted upstream to *tgpA* giving rise to PAO1 PrhaB::*tgpA* strain. Specificity of glucose/rhamnose effects on the growth of PAO1 PrhaB::*tgpA* was assessed by monitoring the PAO1 cultures in M9-citrate supplemented with either rhamnose or glucose. Note the opposite effects of glucose on growth of PAO1 PrhaB::*tgpA* and PAO1, respectively.(Image source Milani A, Vecchietti D, Rusmini R, Bertoni G. 2012. TgpA, a protein with a eukaryotic-like transglutaminase domain, plays a critical role in the viability of *Pseudomonas aerugnosa*. *PloS One*, 7(11): e50323 doi: 10.1371/journal.pone.0050323).

TgpA is a medium size inner membrane protein (668 amino acids, 75 KDa) (Vecchietti *et al.*, 2012) composed of six-seven transmembrane helices, a soluble periplasmic domain containing the functional domain (residues 180-544, 364 aa) and followed by an additional transmembrane helix and a small cytoplasmic domain (residues 561-668) (Figure B9).

The periplasmic portion of TgpA was predicted to display a eukaryotic-like transglutaminase domain (TG-like domain) (Makarova *et al.*, 1999) with unknown function, characterized by the presence of a conserved catalytic triad Cys, His, and Asp. It was suggested that TgpA can take part in an essential function linked to the cell wall, such as i) assembly of peptidoglycan structures ii) maturation/secretion of key periplasmic proteins iii) assembly of surface polypeptide structures, or iv) biogenesis/maturation of LPS.

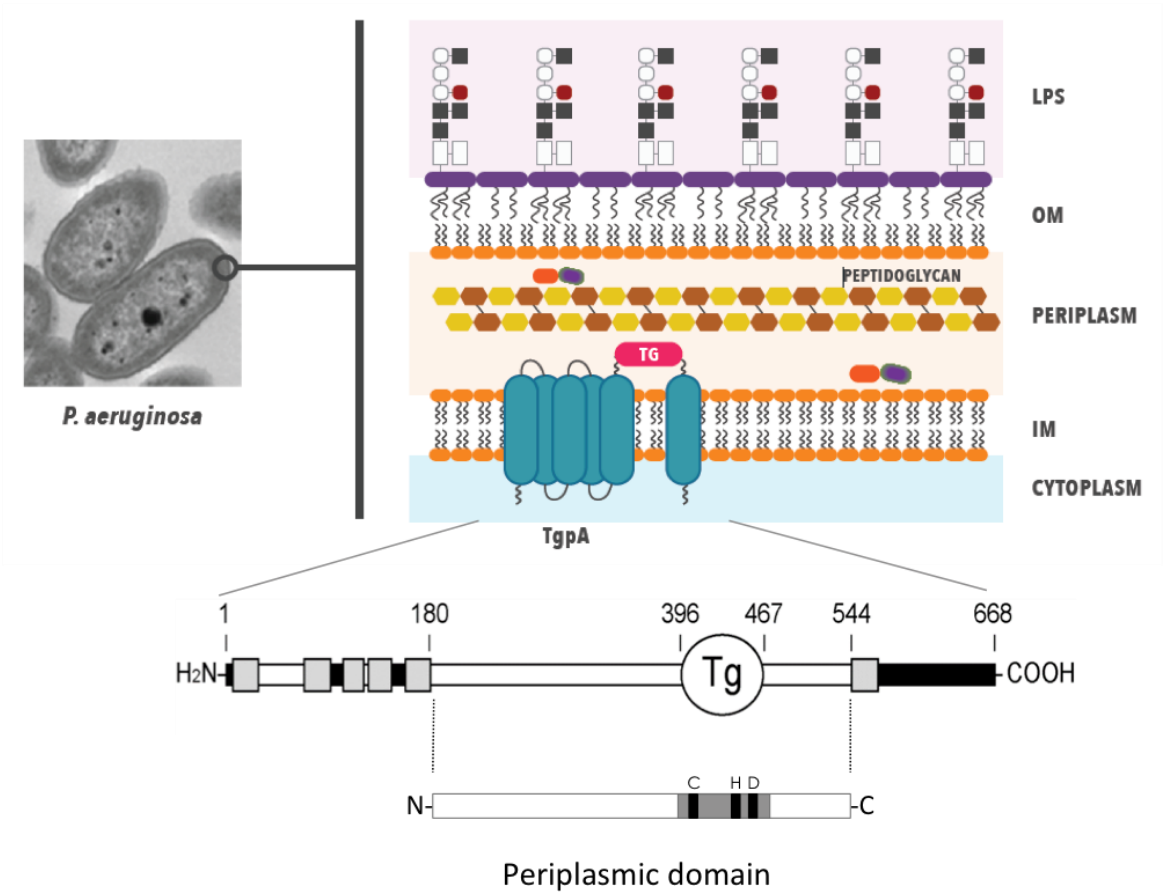

Figure B9. TgpA location and organization in the inner membrane of *P. aeruginosa*. The region TG180–544 that contain the functional TG domain have a high probability of being exposed on the outward face of cytoplasmic membrane, i.e. to protrude into the periplasmic space.

B.7.1. Transglutaminases

Transglutaminases (TG: EC 2.3.2.13, protein glutamine: amine γ-glutamyltransferase) are a group of thiol enzymes that catalyse the post-translational modification of proteins mainly by protein to protein cross-linking, but also through the covalent conjugation of polyamines, lipid esterification, or the deamidation of glutamine residues (Folk and Chung, 1973; Lorand and Conrad, 1984; Aeschlimann and Paulsson, 1994; Nemes *et al*., 1999).

Transglutaminases catalyze the calcium-dependent acyl-transfer reaction between a γ-carboxyamide group of glutamine and ε-amino group of lysine or other primary amines, which results in the formation of γ-glutamyl-ε-lysine peptide chains bridges (Lorand and Conrad, 1984). These enzymes thus establish either intramolecular or intermolecular cross-links in proteins. Transglutaminases are widely distributed among bacteria, plants and animals.

In general, TG employs a charge-relay Cys-His-Asp catalytic triad with the reaction involving formation of a covalent acyl-enzyme intermediate (Figure B10). During the reaction, (step 1) the thiolate ion nucleophilically attacks the Gln side chain (the acyl donor or Q substrate), leading to the formation of an oxyanion intermediate (step 2). Then, the regeneration of the carbonyl group of the tetrahedral intermediate leads to the release of ammonia and to the formation of the acyl−enzyme intermediate (Step 3); the catalytic His removes a proton from the primary amine of the Lys residue (Step 4), leading to the nucleophilic attack of the Lys residue on the carbonyl group of the acyl−enzyme intermediate formed in step 3 and to the formation of a second tetrahedral intermediate (Step 5). As the oxyanion intermediate regenerates the carbonyl group, the thioester bond is cleaved, regenerating the initial catalytic core and releasing the final, cross-linked, protein product (Step 6) (Fernandez *et al.*, 2015).

Interestingly, this reaction is the reversion of the proteolysis reaction catalysed by the thiol proteases that possess the same catalytic triad (Anantharama and Aravind, 2003).

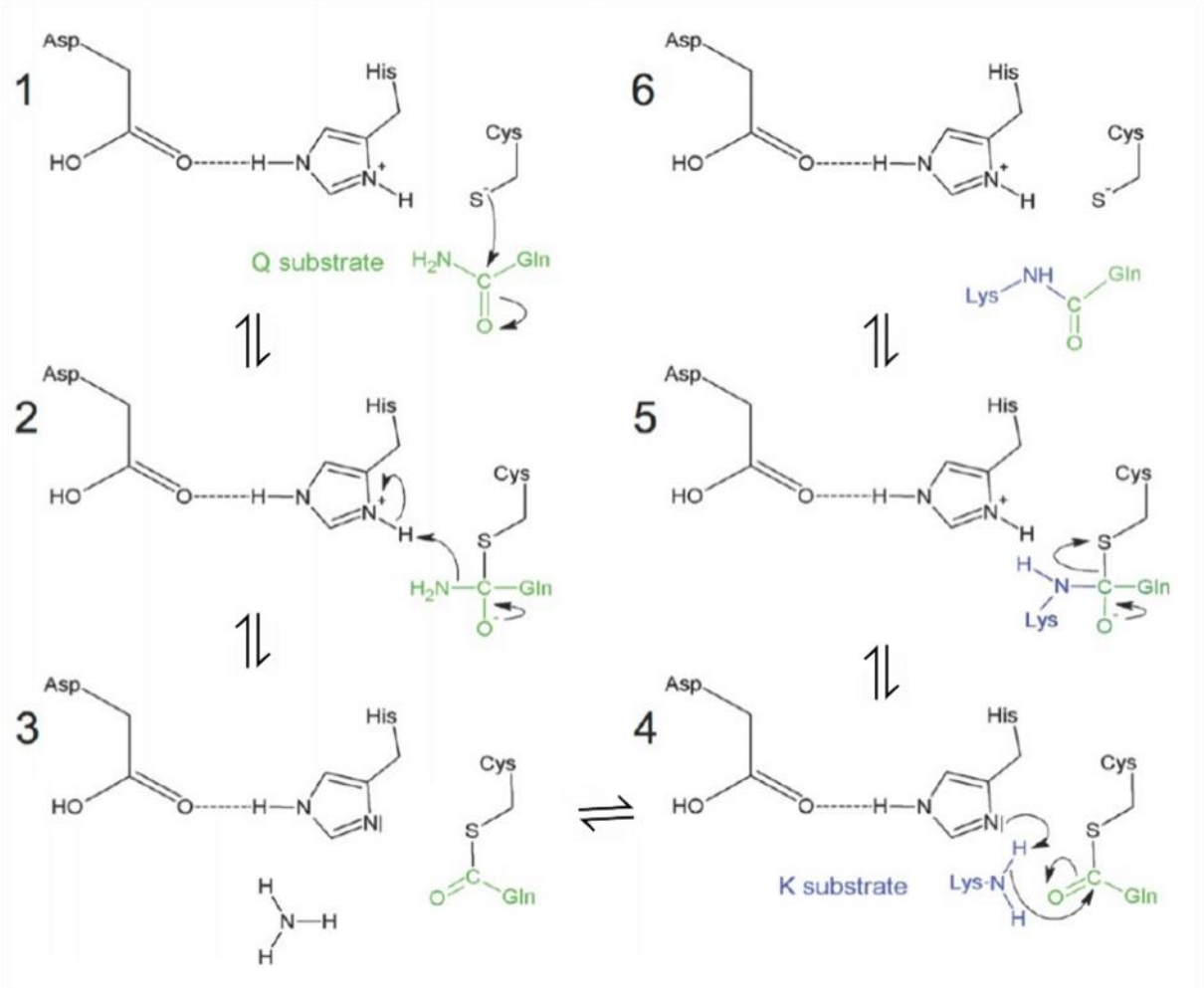

Figure B10. Proposed reaction mechanism of the animal TG on the basis of the similarity of their catalytic core to that of papain-like proteases (Image source Fernandez CG, Placido D, Lousa D, Brito JA, *et al*. 2015. Structural and Functional Characterization of an Ancient Bacterial Transglutaminase Sheds Light on the Minimal Requirements for Protein Cross-Linking. *Biochem* 54(37):5723-34doi: 10.1021/acs.biochem.5b00661)

The solved crystal structure of the human blood-clotting factor XIII (Yee *et al.,* 1994), a mammalian transglutaminase, allowed clarifying that transglutaminases and papain-like proteases shared core structural fold, and are classified into the same superfamily in the Structural of Proteins (SCOP) database (Hubbard *et al.,* 1999). It is suggested that, the catalytic core of TG derive from the minimal ancestral structural unit of the thiol-protease fold (Anantharaman and Aravind, 2003).

B.7.2. Transglutaminases-like superfamily of enzymes

Computational analysis allowed the identification of a superfamily of proteins, found in all archaea, bacteria, yeast and nematodes, that are homologous to eukaryotic transglutaminases. This family of large multidomain archeal proteins with predicted signal peptide and a globular domain (TG domain) that contains conserved cysteine, histidine and aspartate, which compose the catalytic core in the structurally characterized transglutaminase, human blood clotting factor XIIIa (Makarova *et al.,* 1999), which is also a reminiscent of the catalytic triad of a variety of thiol hydrolases (Anantharaman and Aravind 2003). The discovery of this superfamily suggests an evolutionary scenario for the origin of eukaryotic transglutaminases from ancient proteases.

In the sequenced euryarchaeal genomes at least one protein of the transglutaminase-like superfamily was found (Makarova *et al.*, 1999). The vast majority of these proteins have not been functionally characterized, but it has been predicted that many of the prokaryotic members are proteases, although it cannot be ruled out that some of them actually possess a transglutaminase activity. The presence of multiple transglutaminase homologs in *Mycobacteria* implies a possible role for these proteins in the development of the unusual surface structures found on them (Brennan and Nikaido, 1995). Some others have been functionally characterized with specific but non-essential functions at cell wall level. In the *Methanothermobacter* species, prophage proteins PeiW and PeiP act as pseudomurein endoisopeptidases (Steenbakkers *et al.*, 2006; Visweswaran *et al.*, 2010; Schofiel *et al.*, 2015). In the periplasm of *Bordetella bronchiseptica*, WbmE protein catalyzes the deamidation of uronamide-rich O chains of lipopolysaccharide (LPS) (King *et al.*, 2009).

B.7.3. Prokaryotic proteins with similar TG domain

B.7.3.1. Pseudomurein endoisopeptidases PeiW and PeiP

Pseudomurein is a kind of cell wall polymers present in Archaea, found only in Methanobacteriales and the genus *Methanopyrus* (Kurr *et al.*, 1991; Kandler and König, 1993; Kandler, 1993; Albers and Meyer, 2011). Structurally, is similar to the murein, predominant component of the bacterial cell wall, but differs for the presence of an archaeal-specific sugar, N-acetyltalosaminuronic acid in the glycan bond (instead of the bacterial N-acetylmuramic acid) linked by β(1-3) bonds to N-acetylglucosamine or N-acetylgalactosamine. The lack of D-amino acids in the peptide chain and the use of ε- and

γ-iso-peptide bond in both the peptide and interpeptidyl cross-link, are also important features that make the different between these two molecules (Hartmann and König, 1990; König *et al.*, 1993; Kandler and König, 1998).

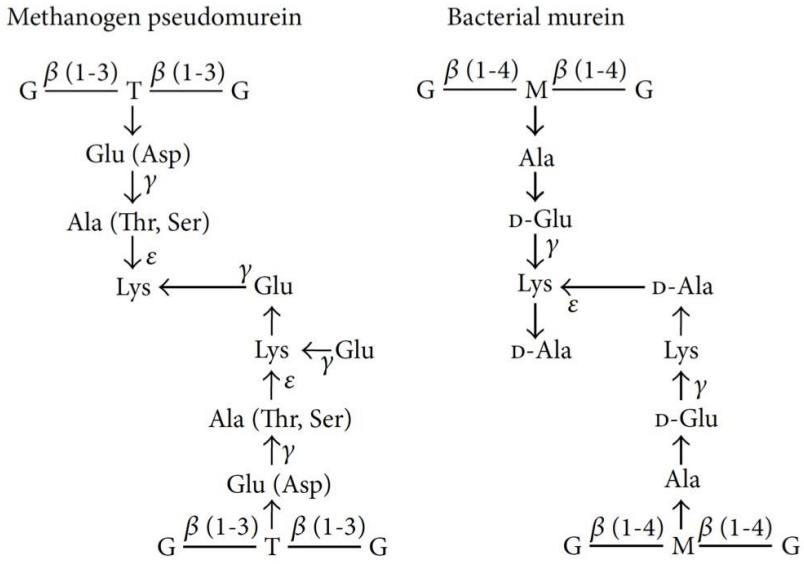

Figure B11. Composition of pseudomurein and murein cell walls. G:N-acetylglucosamine; T:N-acetyltalosaminuronic acid; M:N-acetylmuramic acid. Methanogen pseudomurein contains L-amino acids, *β* (1-3) bonds, and N-acetyltalosaminuronic acid in the glycan chain and several unusual isopeptide bonds. Asp can replace Glu; Thr or Ser can replace Ala, in some strains. Bacterial murein contains D- and L-amino acids and *β* (1-4) bonds and N-acetylmuramic acid in the glycan chain. (Image source Schofield LR, Beattie AK, Tootill CM, Dey D, et al., 2015. Biochemical characterization of phage Pseudomurein endoisopeptidases PeiW and PeiP using synthetic peptides. Archaea 2015:828693 doi 10.1155/2015/828693).

Pseudomurein endoisopeptidases (Pei), PeiW and PeiP, are two lytic enzymes that degrade the pseudomurein cell wall sacculi (Luo *et al.,* 2002). PeiW is encoded by the defective prophage ΨM100 of the thermophile *Methanothermobacter wolfei* (Luo *et al.*, 2001), and PeiP is encoded by phage ΨM1 and deletion mutant ΨM2 of the thermophile *Methanothermobacter marburgensis* (Stax *et al.*, 1992; Pfister *et al.*, 1998).

These two enzymes share the same catalytic triad of conserved cysteine, histidine and aspartate residues, as the transglutaminases and thiol proteases, located at the C-terminus of each enzyme. The N-terminus consists of a pseudomurein cell wall binding domain containing four pseudomurein-binding motifs (Visweswaran *et al.*, 2010; Steenbakkers *et al.*, 2006). Both enzymes causes lysis of the cell wall because they cleave the isopeptide bonds formed between the ε-amino group of an L-lysine residue and the α-carbonyl group

of an L-alanine residue in the oligopeptides linking sugar chains of pseudomurein (Kiener *et al.,* 1987). For this activity they require a divalent metal and have been shown enhanced thermal stability in presence of Ca^{2+} (Schofiel *et al.*, 2015).

B.7.3.2. WbmE of *Bordetella bronchiseptica*

The lipopolysaccharide (LPS) O antigen of the human pathogen *Bordetella bronchiseptica* contains a homopolymer of 2,3-dideoxy-2,3-diaceramido-L-galacturonic acid (L-GalNAc3NAcA), that can also be found in the uronamide form (L-GalNAc3NAcAN) (Di Fabio *et al.*, 2009). The expression of O antigen is required for full virulence in animal models of infection and for resistance to complement-mediated killing (Preston *et al.*, 2006).
In *B. bronchiseptica* the O antigen synthesis is encoded by the *wbm* locus that contains 24 coding sequences. The WbmE, a periplasmic deamidase protein, catalyzes the conversion of a proportion of deamidation of uronamide-rich O chains in LPS (L-GalNAc3NAcAN) to L-GalNAc3NAcA uronic acids. WbmE is a member of the papain-like transglutaminase superfamily, with conserved residues Cys-His-Asp, consistent as well with the deamidation role (King *et al.*, 2009). This enzyme probably constitutes a novel mechanism by which the *B. bronchiseptica* cell surface is modified in response to environmental stimuli.

B.7.3.3. AdmF, transglutaminase involved in the synthesis of Andrimid

AdmF is a protein expressed from a gene cluster related with the biosynthesis of Andrimid, a potent promising antibiotic with activity over unconventional targets such as the β-subunit of the acetyl-CoA carboxylase (ACC) (Needham *et al.*, 1994; Singh *et al.*, 1997; Freiberg *et al.*, 2004; Freiberg *et al.*, 2005).

The biosynthesis of this natural product is widely distributed in bacteria and involves a highly dissociated hybrid PKS/NRPS assembly line, with each carrier protein located on a separate subunit. Interesting features of this unusual pathway include the catalysis of peptide bond formation by transglutaminase-like enzymes, executed by AmdF (Fortin *et al*., 2007), a protein that contains the complete Cys-His-Asp catalytic triad characteristic of TG and that has shown the capacity to combine characteristics such as amide bond formation and involvement of an acyl-enzyme intermediate. *In vitro* biochemical assays with purified recombinant protein AdmF have demonstrated a broad substrate tolerance (Magarvey *et al.*, 2008).

B.8. Bacterial cell wall and peptidoglycan structure

The cell wall is of vital importance for bacteria because it determines the shape and the integrity of the cell, by surrounding the cytoplasmic membrane with a net-like macromolecule called peptidoglycan (PGN, or murein) sacculus (Weidel and Pelzer, 1964; Vollmer *et al.,* 2008a). The essential PGN is made of glycan chains cross-linked by short peptides, and is located in the periplasm of gram-negative bacteria as a thick monolayer or multi-layered wall in gram-positive species (Schleifer and Kandler, 1972; Vollmer and Bertsche, 2008b; Vollmer and Seligman, 2010).

The glycan strands are made of alternating N-acetylglucosamine (GlcNAc) and N-acetylmuramid acid (MurNAc) residues, linked by β-1,4 glycosidic bonds [GlcNAc-(β-1,4)-MurNAc], and having a pentapeptide, containing L- and D-aminoacids, attached to the D-lactyl moiety of each MurNAc. The pentapeptide sequence varies across bacteria species and can be L-Ala-D-γ-Glu-m-Dap-D-Ala-D-Ala (m-Dap, meso-diaminopimelic acid) in gram negatives species or L-Ala-D-γ-Glu-L-Lys-D-Ala-D-Ala in gram-positives, and participates in an interglycan cross-linking reaction between peptides of adjacent strands, building the three-dimensional PGN network (Schleifer and Kandler, 1972; Vollmer and Bertsche, 2008b; Vollmer and Seligman, 2010).

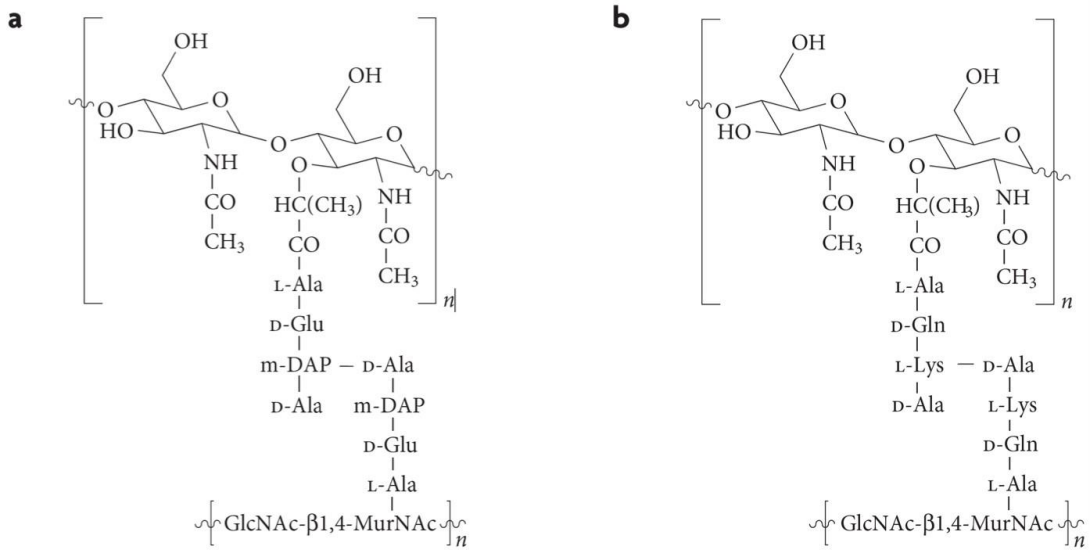

Figure B12. Peptidoglycan structure. (**A**) The polysaccharide backbone of peptidoglycan is linked by stem peptides. Gram-negative bacteria and Gram-positive Bacilli contain meso-diaminopimelic acid (m-DAP) as the third amino acid in the peptide linker. (**B**) Most other Gram-positive bacteria (including Gram-positive cocci) contain l-lysine as the third amino acid in the linker. GlcNAc, N-acetylglucosamine; MurNAc, N-acetylmuramic acid. (Image source Brown L, Wolf JM, Prados-Rosales R and Casadevall A. 2015. Through the wall: extracellular vesicles in Gram-positive bacteria, mycobacteria and fungi. *Nat Rev Microbiol*13, 620-630 doi: 10.1038/nrmicro3480

B.8.1. *P. aeruginosa* peptidoglycan structure

As gram-negative, the murein sacculus of *Pseudomonas* consists of the glycan moiety of β-1,4-linked alternating units of GlcNAc and MurNAc followed by the peptide L-Ala-D-γ-Glu-m-Dap-D-Ala-D-Ala.

The glycan reveals only a few variations such as acetylation of phosphorylation of the muramyl 6-hydroxyl groups and the occasional absence of a peptide of an N-acetyl substituent. In different *Pseudomonas* species the glycan length varies between 10 and 65 dissaccharide units in comparison to up to 30 in *E. coli* and 50-250 in the case of *Bacillus* sp. (Quintela et al., 1995); Margolin 2009; Dimitriev et al., 2005).

The peptide moiety is bound through its N-terminal to the carboxyl group of the MurNAc, followed by glutamic acid, which is linked by its γ-carboxyl froup to an L- m-Dap and finally D-Ala-D-Ala. Variations in peptidoglycan composition may involve amidation, hydroxylation, acetylation, and also the mode of cross-linkage of aminoacids and other groups at position 2 or 3 of the peptide moiety. These features allow to classify the peptidoglycan in the different categories established by Shleifer and Kandler, 1972. According to this, the peptidoglycan of *P. aeruginosa* is of classified as the “not amidated A1γ” chemotype, characterized by the lack of amidation at the C_1-carboxy group of D-Glu and L-m-Dap, as well as the 4-3 cross-link involving the stem peptide by L-m-Dap: the free aminoacid group (ω-amino group) of the L-m-Dap in position 3 forms a peptide linkage to the carboxyl group of D-Ala in position 4 of an adjacent peptide subunit (Figure B12a).

B.8.2. Peptidoglycan synthesis

The PGN layer has a flexible structure and is constantly remodelled during cell growth and division. Growth of the sacculus is a dynamic process that requires more than 20 enzymatic reactions (Lovering *et al.*, 2012), including synthases to make PGN and attach it to the existing sacculus and hydrolases to cleave the sacculus to allow insertion of the newly synthesized material (Höltje, 1998). The PGN synthesis takes place in the cytoplasm (synthesis of nucleotide precursors) and on the inner membrane and outer side of the cytoplasmic membrane (synthesis of lipid-linked intermediates and polymerization reactions) (Vollmer *et al.*, 2008c; Barreteau *et al.*, 2008).

In the cytoplasm, the conversion of fructose-6-phosphate to uridine diphosphate-N-acetyl glucosamine (UDP-GlcNAc) is taken in a four-step reaction catalysed sequentially by GlmS, GlmM and GlmU enzymes. UDP-MurNAc is then formed from UDP-GlcNAc in a reaction catalysed by MurA enolpyruvyl transferase and MurB reductase successively. Then MurC, MurD, MurE and MurF ligases mediate the assembly of the pentapeptide on the D-lactoyl group on UDP-MurNAc, giving rise to the formation of UDP-MurNAc-pentapeptide (Barreteau *et al.*, 2008).

On the cytoplasmic face of the inner membrane, MraY catalyzes the reaction of UDP-MurNAc-pentapeptide with undecaprenyl pyrophosphate to generate MurNac-pentapetide pyrophosphoryl undecaprenol or Lipid I, which is then coupled with GlcNAc by the MurG transferase to yield GlcNAc (pentapeptide) phosphoryl undecaprenol, also known as Lipid II (Bouhss *et al.*, 2008). Then, lipid II is translocate to the outer side of the cytoplasmic membrane. Both, MurJ and FtsW, have been proposed to be the lipid II flippase, yet remaining a matter of debate (Ruiz, 2008; Mohammadi *et al.*, 2011; Sham *et al.*, 2014). Once in the periplasm, lipid II is the disaccharide donor for glycan strand growth, catalyzed by the transglycosilase domain of Penicilling Binding Proteins (PBP). Cross-linking of the peptide stems occurs in a separate transpeptidase reaction, also mediated by PBP (Fisher *et al.*, 2005).

The transpeptidation is generally considered the last step in the PGN synthesis, but the structure of the cell wall suffers constant remodeling and modifications: for instance, O-acetylation is a mechanism against PGN-cleaving lysozymes and regulates glycan strand integrity against lytic transglycosilases cleavage (Moynihan and Clarke, 2011). Also the peptide stem undergoes important modifications. D-Ala-D-Ala carboxypeptidases remove the terminal D-Ala from the pentapeptide stem, in order to regulate the degree of final cross-linking, generating a tetrapeptide no longer suitable as a substrate for cross-linking by D-Ala-D-Ala transpeptidases (Zhang *et al.*, 2007; Shi *et al.*, 2008; Sauvage *et al.*, 2008).

B.8.3. Peptidoglycan turnover and recycling

As mentioned before, during growth and division the cell must keep its integrity. Initially, it was thought that the peptidoglycan grew with progressive elongation. However, it was later described a process in which both, growth of sidewalls and new septum of the bacteria, coincided with the release of the existing PGN as the incorporation of the new PGN occurred (Höltje, 1998; Park and Uehara, 2008). The process was described as a dynamic recycling of the released PGN, both in gram-negative and in gram-positive bacteria, but is yet less characterized in the last system (Reith and Mayer, 2011).

Briefly, the PGN turnover – the release of muropeptides to the medium – occurs through the simultaneous action of different PGN hydrolases, located in the periplasm and cytoplasm of the bacteria (Typas *et al.*, 2011). Lytic transglicosylases (LTs) are critical for the recycling of cell wall during growth (elongosome) and cellular division process (septation), and catalyze the cleavage of the glycan strand of the PGN, with the formation of N-acetyl 1,6-anhydromuramic acid. The LTs can cleave at the end of the glycan strand (exolytic LT) or in the middle of the PGN chain (endolytic LT).

The main reaction product is the N-acetyl-β-D-glucosamine-(1-4)-1,6-anhydro-N-acetyl-β-D-muramyl-peptide (NAG-anhNAM-peptide), which is internalized to the cytoplasm by AmpG permease. NagZ, a cytoplasmatic glucosaminidase, further hydrolyzes the glycosidic bond between NAG and anhNAM-peptide, and then AmpD (PGN amidase), releases the peptide stem from the anhNAM sugar. These products are then reincorporated to the PGN biosynthetic pathway (Fisher and Mobashery, 2014; Dominguez-Gil *et al.*, 2016).

The complexity of the events that occurrs in the cytosol, inner membrane, periplasm and outer membrane of the gram-negative bacteria related to the PGN synthesis, turnover and recycling are illustrated in Figure B13 from Fisher and Mobashery 2014.

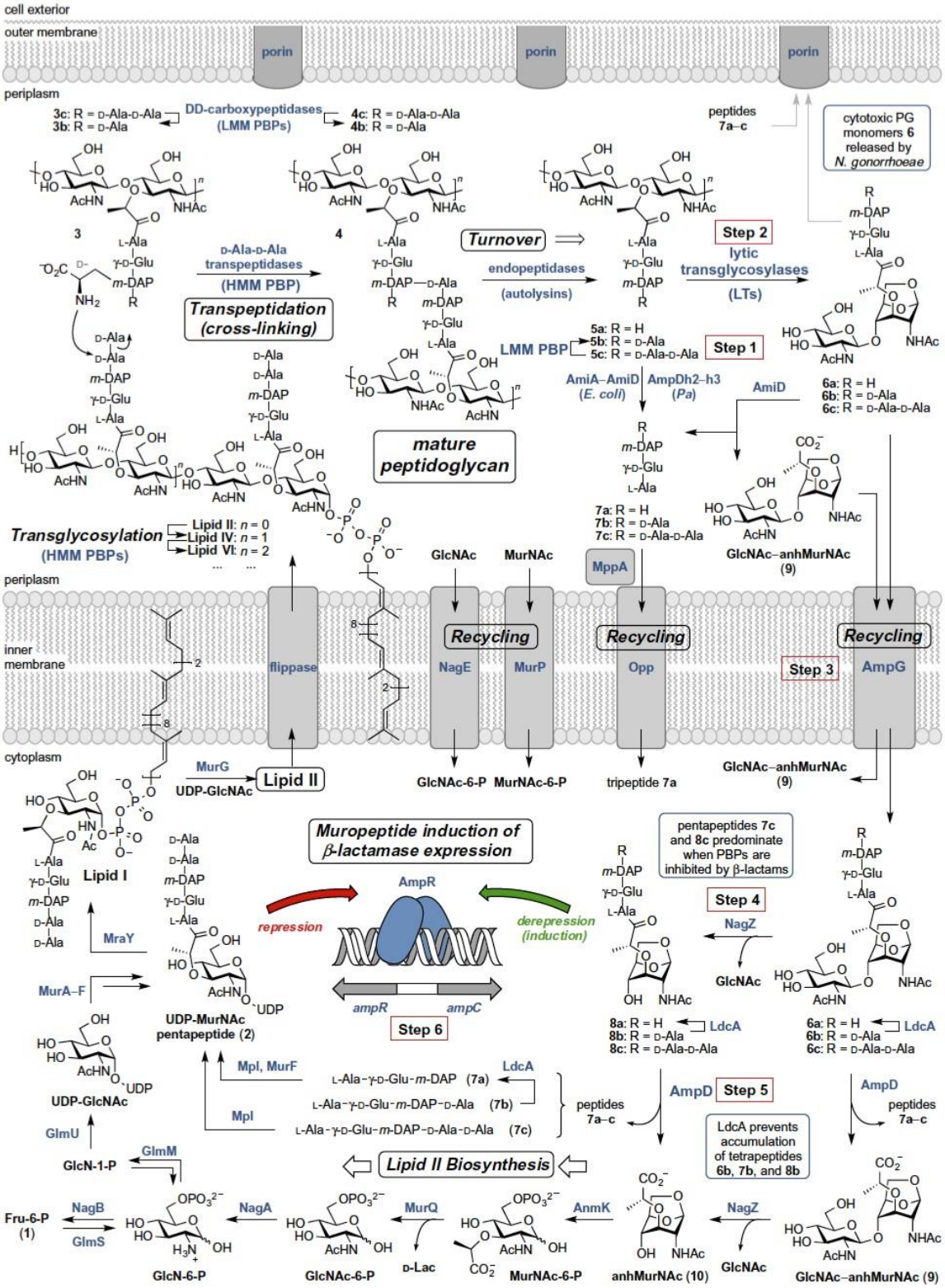

Figure B13. Events in the synthesis, turnover and recycling of PGN in Gram-negative bacteria. (Image source Fisher JF and Mobashery S. 2014.The sentinel role of peptidoglycan recycling in the β-lactam resistance of the Gram-negative enterobacteriaceae and *Pseudomonas aeruginosa*.*Bioorg Chem* 56:41-8 doi 10.1016/j.bioorg.2014.05.011)

C. Aim of the work

The characterization of new cellular functions that are essential for *P. aeruginosa* viability could drive the development of new antimicrobial compounds with novel mechanisms of action.

Therefore, during this PhD work the main aim was to gain knowledge about the crucial role played by the transglutaminase protein A, or TgpA, in the viability of *Pseudomonas aeruginosa,* and increase the rationale for targeting the activity as a novel approach to identify new antibacterial drugs.

To achive this goal, initially it was evaluated the impact of mutations that were predicted to knock down the TgpA activity on the growth of *P. aeruginosa*; and then, through the expression and purification of recombinant domains of TgpA, focusing on the periplasmic TG domain responsible for the catalytic activity of the enzyme, to characterize the protein at structural and biochemical level.

D. Main results

D.1. Evaluation of the impact of mutations predicted to knock-down TgpA activity on the growth of *P. aeruginosa* in different genetic systems

The first step of the analysis, aimed to evaluate whether ectopic expression of the wild type (wt) full-length TgpA protein and some variants with mutations in the predicted catalytic triad, could *per se* influence the growth of *P. aeruginosa* in the wt background of the PAO1 strain. Therefore, the wt *tgpA* gene (PA2873) was amplified from PAO1 genomic DNA and cloned into the broad host range expression vector pHERD28T (Qiu *et al.,* 2008) under the control of the arabinose-inducible P_{BAD} promoter. Mutations in the predicted catalytic triad Cys404 – His448 – Asp464, were generated through site-directed mutagenesis (Stratagene Kit) using as a template the pHERD28T vector expressing a wt full-length TgpA protein. A point mutant of the main residue Cys (Cys404Ala) and a double mutant in residues Cys and His (Cys404Ala-His448Asn) of the catalytic triad, were generated, as shown in Figure D1.

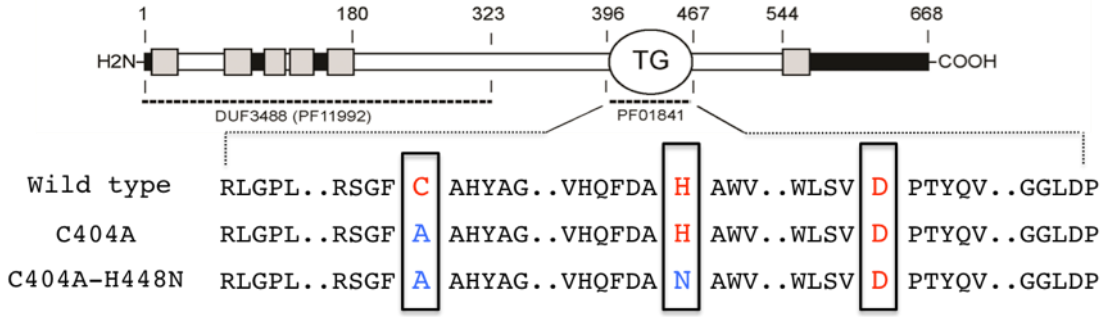

Figure D1. Panel of amino acid substitutions in the TG domain catalytic triad Cys404–His448–Asp 464

The generated constructs pHERD28T-TgpA and those carrying the respective mutation (pHERD28T-C404A and pHERD28T- C404A- H448N) were transferred from *E. coli* (where they were prepared) to *P. aeruginosa* PAO1 strain by triparental mating conjugation.

To test the hypothesis that unbalancing the *tgpA* expression could be deleterious for *P. aeruginosa*, the effects of the P_{BAD} promoter modulation on growth rate of PAO1-pHERD28T-TgpA and mutants relative to PAO1 carrying an empty vector pHERD28T were

assayed. Overnight cultures of PAO1- pHERD28T-TgpA and mutants in M9-citrate supplemented with trimethoprim 300 µg/ml were diluted to $OD_{600} = 10^{-6}$ and inoculated in microtiter wells filled with 200µl of growth medium and five different concentrations of Arabinose (0; 0.025; 0.05; 0.1 and 0.2%) for the induction of the P_{BAD} promoter.

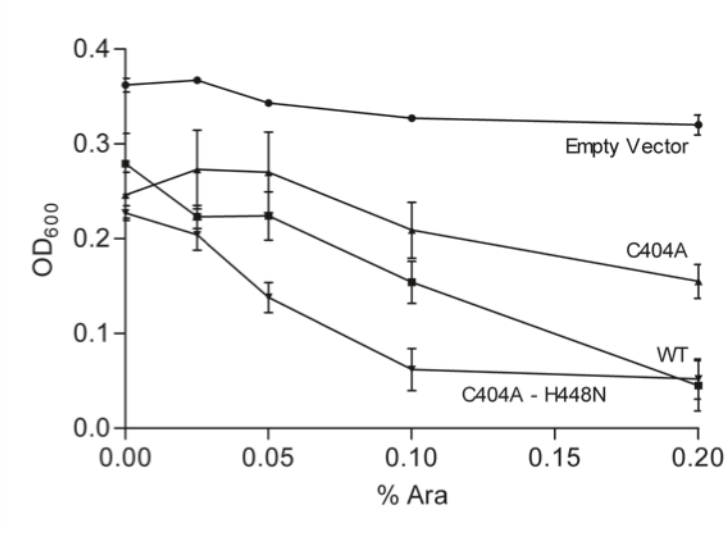

Figure D2. Effects of the ectopic expression of TgpA WT and mutants C404A and C404A-H448N on *P. aeruginosa* growth. The effects on growth were evaluated relative to PAO1 carrying the empty vector pHERD28T under five different concentrations of arabinose (0, 0.025, 0.05, 0.1 and 0.2%) for the induction of the P_{BAD} promoter. For each culture, the OD_{600} value after 16 hrs of growth (i.e. the onset of the stationary phase) was plotted with the corresponding concentration of arabinose.

The ectopic expression of WT and the two mutants proteins C404A and C404A-H448N resulted in an arabinose dose-dependent negative influence on *P. aeruginosa* growth (Figure D2). The overexpression of a wt copy of TgpA and the single mutant C404A leads to a decrease in the growth rate of *P. aeruginosa*, while the overexpression of the double mutant C404A-H448N dramatically decreased the growth of the cells, suggesting that an extra dosage of TgpA could be deleterious for the bacteria. The negative effects on the *P. aeruginosa* growth resulting from the ectopic expression were specific of TgpA. In fact, the ectopic expression from pHERD28T of another essential protein, YeaZ (Vecchietti *et al*., 2016), involved in tRNA modifications, did not result in significant negative effect on PAO1 growth (data not shown). These negative effects were evident and comparable among wt and the mutants, also in absence of arabinose (Figure D2). In fact, in this condition the TgpA expression was attributed to the basal activity of the P_{BAD} promoter.

Next, the levels of ectopic expression of the wt and mutants from pHERD28T, particularly in the absence of inducer arabinose were assessed by western blot analysis (Figure D3) and quantified it by Real time PCR (Table D1).

For western blot analysis, full-length C-terminal His-tagged constructs were generated using as template the wt and C404A already cloned in the pHERD28T vector, with appropriate primers adding the His-tag. Cultures with 0.1% arabinose and without arabinose were grown and the membrane fractions isolated by subcellular fractionation with ultracentrifugation at 37,000rpm, were used for the analysis. With a specific monoclonal anti-His antibody a unique band around 70 kDa, corresponding to TgpA-His (wt and mutant C404A), was detected relative to the absence of the band in the empty vector (Figure D3). The presence of a small band also in the absence of the arabinose inducer, both in the wt and the mutant C404A, provided evidence of the basal activity of the P_{BAD} promoter.

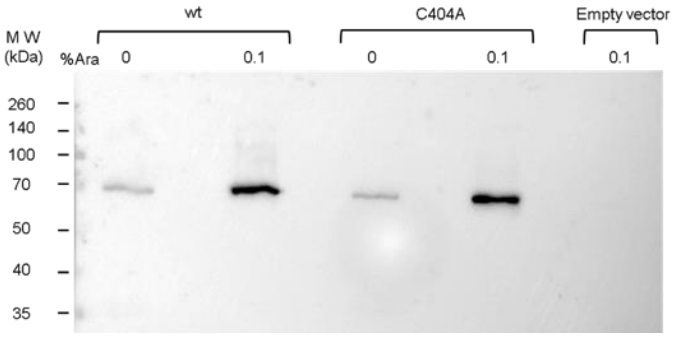

Figure D3. Western blot analysis of the ectopic expression of the TgpA wt and C404A full-length proteins in absence and presence arabinose. Ten microliters of total membrane fraction from the growth under each conditions were loaded onto 12% SDS-PAGE. Samples induced with 0.1% Ara are diluted 1:10 with respect to the sample without arabinose. MW = Molecular weight marker

The basal activity of the P_{BAD} promoter was further confirmed by Real time quantitative PCR (qRT-PCR) reactions. One millilitre from each of the samples produced for the western blot analysis was normalized at OD_{600} 0.8 and total RNA was extracted to further generate cDNA. Approximately 50ng of cDNA were used as a template for qRT-PCR. The calculation of the relative expression of the ectopic TgpA from plasmid pHERD28T versus the empty vector was performed as described by the $2^{-\Delta\Delta CT}$ method (Livak and Schmittgen, 2001), normalizing first mRNA amounts to 16S ribosome RNA (ΔCT) and relating the ΔCT in theTgpA wt and

C404A mutant ectopically expressed to the chromosomal copy (ΔΔ*C*T) (PAO1-pHERD28T empty vector).

In Table D1 are reported the $2^{-\Delta\Delta CT}$values of the ectopic expression of *tgpA* mRNAs. These values confirmed that in the absence of arabinose inducer, *tgpA* wt and mutated form are ectopically expressed more than ten times respect to the chromosomal copy due to the basal activity of the P_{BAD} promoter.

Table D1. Quantitative Real time PCR analyses of mRNA levels of ectopically overexpressed TgpA wt and C404A mutant

Strain	0% Ara	0.1% Ara
PAO1-pHERD28T	1*	1
PAO1-pHERD28T-TgpA wt	16	544
PAO1-pHERD28T-C404A	11	363

*Values represent $2^{-\Delta\Delta CT}$ values of the ectopic expression of *tgpA* mRNAs

Following the overexpression experiments in PAO1 background, vectors pHERD28T –TgpA wt and mutants C404 and C404A-H448N were transferred from *E. coli* to the PAO1 derivative strain PAO1- P_{rhaB}::*tgpA* (Milani *et al.,* 2012). This strain is a conditional mutant carrying a chromosomal copy of the *tgpA* gene under the control of the P_{rhaB} (rhamnose dependent) promoter. This strain is usually maintained in the presence of rhamnose that induces the expression of the *tgpA* from the P_{rhaB} promoter. However the P_{rhaB} promoter can be strongly down regulated by glucose addition in the medium. Consequently, PAO1 P_{rhaB}::*tgpA* is unable to growth in the presence of glucose unless functional TgpA is ectopically expressed from another promoter.

TgpA wt and mutants, ectopically expressed from vectors pHERD28T, were tested for the ability to complement a glucose-mediated down-regulation of the chromosomal *tgpA* gene in PAO1 P_{rhaB}::*tgpA*. As shown in Figure D4, wt *tgpA* allele expressed from pHERD28T-TgpA wt by the basal activity of P_{BAD} promoter (Ara 0%) is able to complement the forced repression by 1% glucose of the P_{rhaB} promoter. In fact, PAO1 P_{rhaB}::*tgpA* could grow with

1% glucose as much as with the permissive condition of 0.2% rhamnose. Differently from TgpA wt, both *tgpA* mutant alleles expressed from pHERD28T- C404A and pHERD28T-C404A-H448N, respectively, by the basal activity of P_{BAD} promoter (Ara 0%) could not complement the forced repression by 1% glucose of the P_{rhaB} promoter (Figure D4). Therefore, the mutations C404A andC404A-H448N impairs the *in vivo* functionality of TgpA.

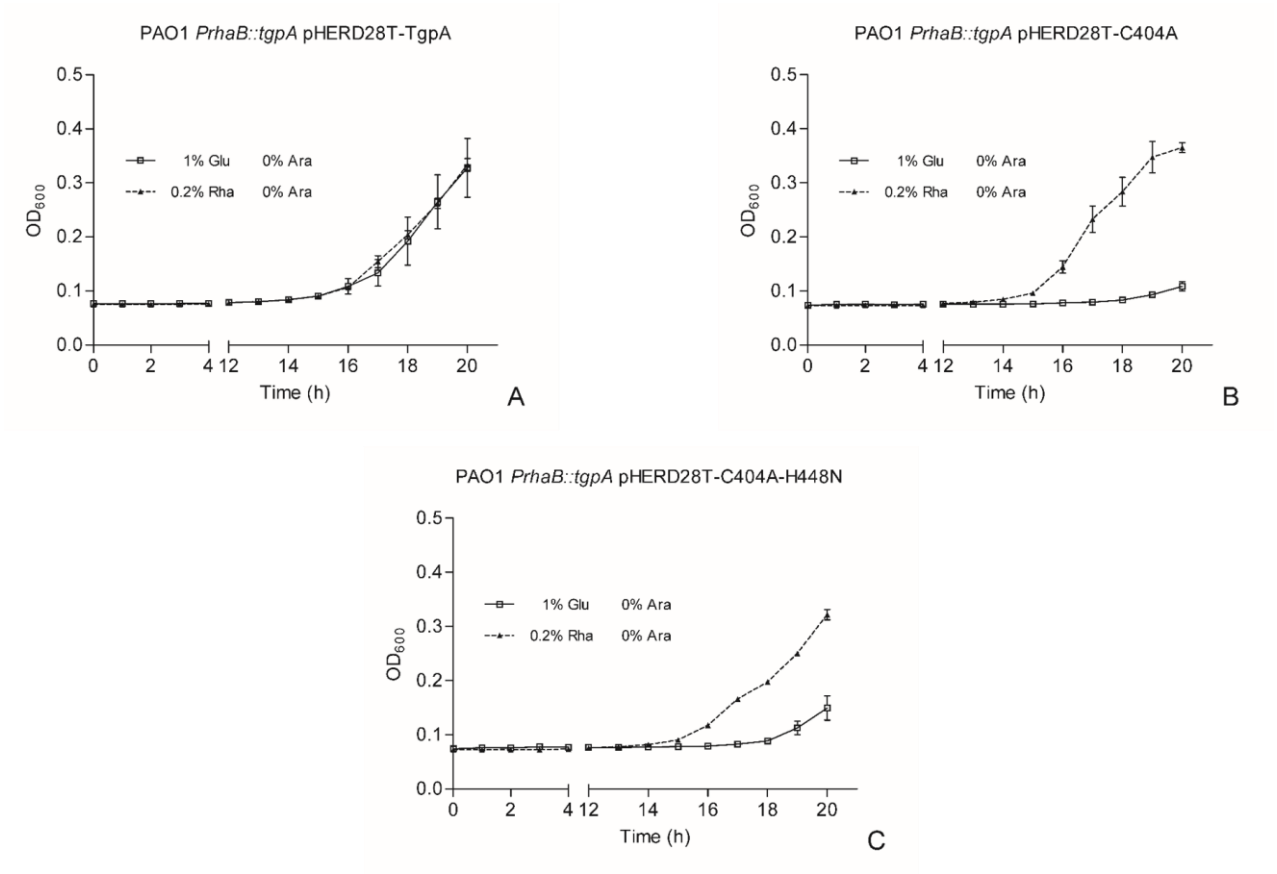

Figure D4. Tests of complementation of a glucose-mediated down-regulation of the chromosomal *tgpA* gene in PAO1 P_{rhaB}::*tgpA*. PAO1 P_{rhaB}::*tgpA* strains carrying pHERD28T-TgpA wt (**A**), pHERD28T- C404A (**B**) and pHERD28T- C404A-H448N (**C**) were grown for 20 hrs in micro-cultures of 200 µl with the indicated concentrations of arabinose, rhamnose and glucose concentrations. Cultures growth was monitored in real-time by absorbance measurement at OD_{600}.

The consequences in reducing the expression levels of TgpA were further investigated by Transmission Electron Microscopy - TEM. The conditional strain PAO1 *PrhaB::tgpA* was grown either in the absence or in the presence of a sub-lethal concentration of glucose that, although strongly reducing the growth-rate, gave rise to a sufficient amount of *P. aeruginosa* cells for TEM analysis. Figure D5 shows the results of these experiments.

PAO1 *PrhaB::tgpA* cells with glucose presented two abnormal morphological features:
1. The average cell length is greater than the reference condition with rhamnose.
2. The presence of “collapsed-zones” that might originate from the detachment of the inner membrane from upper layers of the envelope.

These results are consistent with the hypothesis that TgpA has a role at cell wall level, in particular the collapsed-zones visible following TgpA depletion suggests a role in anchoring inner membrane to upper layers of the envelope.

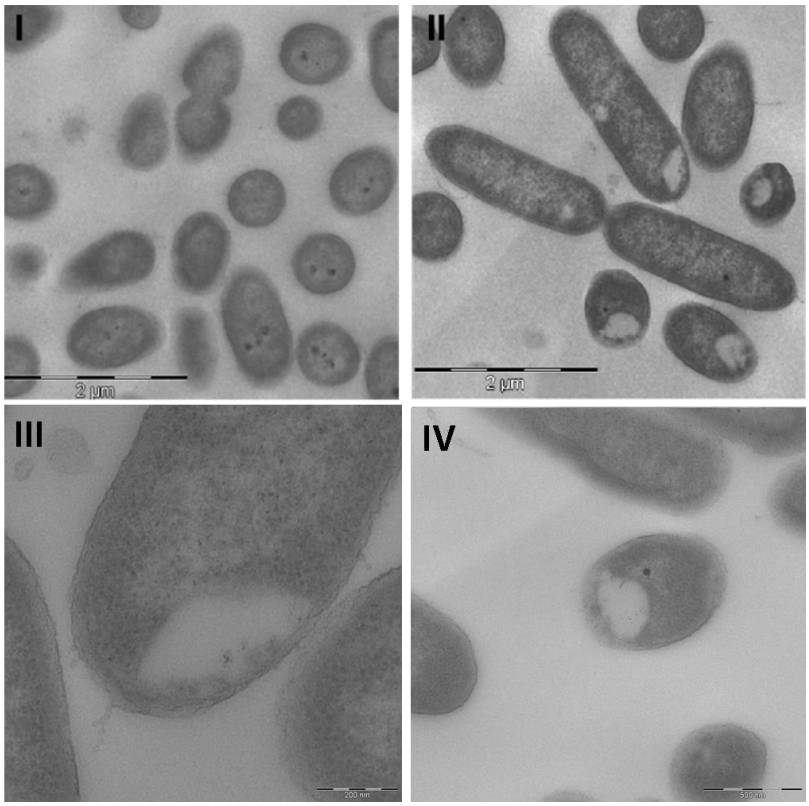

Figure D5. Morphological analysis of *P. aeruginosa* cells with reduced TgpA levels: I) PAO1 *PrhaB::tgpA* cells grown o/n in M9 medium with rhamnose; II) PAO1 *PrhaB::tgpA* cells grown o/n in M9 medium with glucose, 8000X magnification; III) PAO1 *PrhaB::tgpA* cells grown o/n in M9 medium with glucose, 12000X magnification; IV) PAO1 *PrhaB::tgpA* cells grown o/n in M9 medium with glucose, 16000X magnification.

D.2. Structural characterization of the TG domain

To gain knowledge about the organization and possible aspects of the function of the protein, was solved the structure of the soluble periplasmic domain (residues 180-544) containing the functional Transglutaminase (TG) domain, characterized by the presence of the conserved catalytic triad Cys – His – Asp.

D.2.1. Expression and purification of the TG domain

The periplasmic portion of TgpA, $TG_{180–544}$ (364aa), was cloned into the non-commercial p2N vector (PRIMM srl.; Ampicillin (Amp) resistance) expressing a N-terminally (His)10-tagged TG domain. The *E. coli* strain BL21CodonPlus (DE3) - RIPL was used for the expression of the TG domain, with overnight induction with 1 mM isopropyl β-D-thiogalactopyranoside (IPTG) at 17°C with 220 rpm agitation. The purification of the protein was performed by nickel affinity followed by size exclusion chromatography (SEC) (Figure D6, panel A and B). The concentrated protein (6 mg/ml) was used to perform crystallization trials with microbatch set-up using an Oryx-8 crystallization robot (Douglas Instruments, East Garston, UK). TgpA crystals were obtained after 48h at 20°C (Figure D6, panel C).

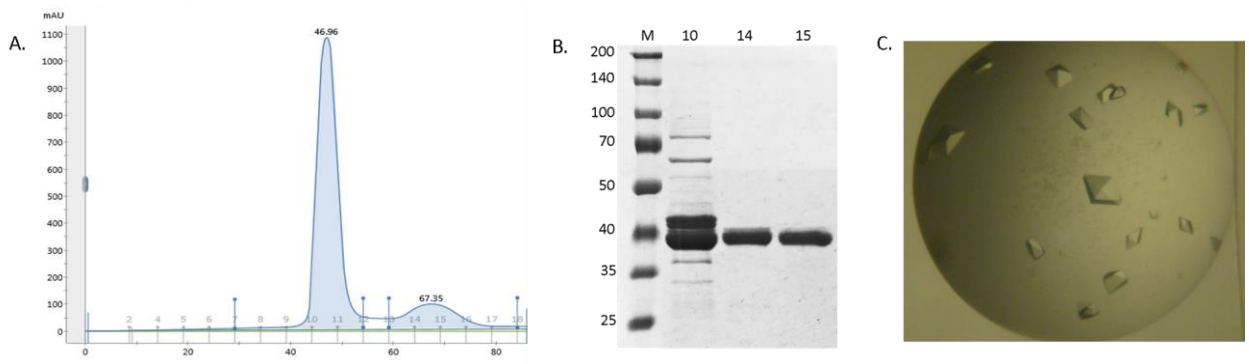

Figure D6. Summary of the purification and crystallization of the TG domain. (**A**) SEC elution profile of the TG domain; (**B**). SDS-PAGE showing the separation of the two bands of the TG domain during SEC, M) Molecular weight marker; the number of each line is representative of the indicated fraction from the SEC elution in panel A; (**C**). TG domain crystals

During the TG domain expression and purification, the protein showed the tendency to undergo proteolytic cleavage, evident by the presence of two bands around 40kDa (Figure D6 Panel B lane 1). Anti-His western blot analysis confirmed that both bands correspond to his-tagged proteins, suggesting that TgpA cleavage occurs at the C-terminal end. Such feature suggests a disordered nature of this part of the sequence.

For mass spectrometry analysis, both bands were digested with trypsin and other peptidases, and the pattern of fragmentation was compared with the overall sequence of the protein to identify the cleavage sites. As shown in Figure D7, the Band 1, corresponds to the expected molecular weight of the TGdomain (364aa, 44kDa), and the generated peptides covers up to seven amino acids before the end of the sequence. On the other hand, the Band 2, corresponds to a cleaved version of the TG domain, with fragments generated mainly by other peptidases different from trypsin. This truncated version of the protein, of approximately 39kDa, presents a region at the C-terminal portion that suffers proteolytic cleavage around Tyr499, generating different peptide fragments. Although it was not possible to identify a precise site of cleavage, it was possible to confirm that the protein loses more than 20 amino acids at its C-terminal end.

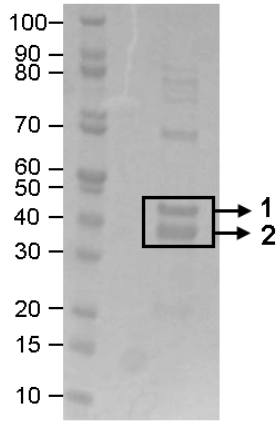

Band 1

MGSDKIHHHHHHHHHHGVR LGPLWSLPMP GNKGVTGLSE
201 SMAPGDIAEL GRSAELAFRV RFEGALPPRE QLYWRALTME RFDGRRWAQA
251 PQWSGEDALH WQKRGPELRY DVIMQPSSQP WLFALDVAQT DQTDTRLMSD
301 FHLQRRQPVE QRLFYRVSSW PQALRESSID PRTRWRNLQL PMHGNPRARA
351 LADELRQAHA QPQALVAALL QRFNHEPFAY TLKPPATGAD GVDDFLFDTR
401 SGFCAHYAGA MAFVLRAAGI PARVVAGYQG GELNPAGNYL LVHQFDAHAW
451 VEYWQPEQGW LSVDPTYQVA PERIEQGLEQ ALAGDSEYLA DAPLSPLRYR
501 GLPWLNDMRL AWDSLNYGWQ RWVLAYQGEQ QGAFLQRWFG GLDP

Band 2

MGSDKIHHHHHHHHHHGVR LGPLWSLPMP GNKGVTGLSE
201 SMAPGDIAEL GRSAELAFRV RFEGALPPRE QLYWRALTME RFDGRRWAQA
251 PQWSGEDALH WQKRGPELRY DVIMQPSSQP WLFALDVAQT DQTDTRLMSD
301 FHLQRRQPVE QRLFYRVSSW PQALRESSID PRTRWRNLQL PMHGNPRARA
351 LADELRQAHA QPQALVAALL QRFNHEPFAY TLKPPATGAD GVDDFLFDTR
401 SGFCAHYAGA MAFVLRAAGI PARVVAGYQG GELNPAGNYL LVHQFDAHAW
451 VEYWQPEQGW LSVDPTYQVA PERIEQGLEQ ALAGDSEYLA DAPLSPLRYR
501 GLPWLNDMRL AWDSLNYGWQ RWVLAYQGEQ QGAFLQRWFG GLDP

Figure D7. Mass spectrometry analysis of the two bands obtained during the TG domain purification. In Red are highlighte all the peptides generated by tripsin digestion and identified with mass analysis. In Green are highlithed those peptides generated by digestion with other peptidases different from trypsin

D.2.2. Solving the structure of the periplasmic TG domain

A detailed description and analysis of the structure of the TG domain is found in Part II in "manuscript in preparation".

The native TG domain crystals diffracted to a maximum resolution of 1.6 Å using synchrotron radiation at bem-line ID30a3 at the European Synchrotron Radiation Facility (ESRF-Grenoble, France). However, it was not possible to solve the structure through molecular replacement (MR), since TgpA has low homology respect to other proteins with structure already solved. In the cases where MR it is not possible, classic methods like heavy-atoms derivatization (where the crystals are soaked with heavy-atoms (HA) containing compounds) are used to create isomorphous HA derivatives (same unit cell, same orientation of the protein in cell). This strategy gave rise to measurable intensity changes that could be used to deduce the position of the heavy atoms (Taylor, 2010).

The TG domain crystals were soaked with mercury derivatives and collected data to a maximum resolution of 1.8 Å at beam-line BM14U (ESRF-Grenoble, France) (Figure D8).

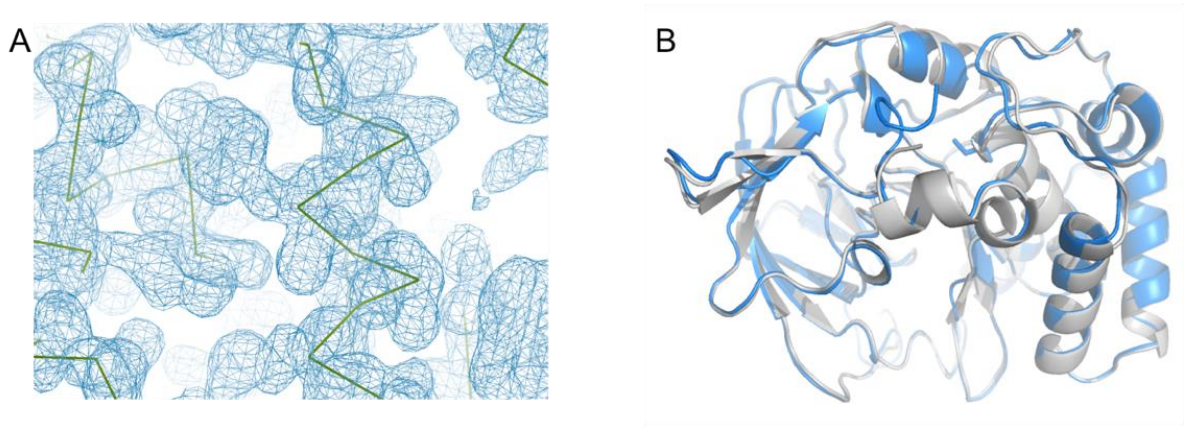

Figure D8. A. Electron density after heavy atom (Hg) phasing B. Superposition between the two TG domain structures: Blue native TG domain, grey mercury (Hg) derivative

X-ray diffraction data were indexed and scale using XDS (Kabsch, 2010) and the three-dimensional structure was solved using the SAD method based on mercury derivative, using the package SHELXC/D/E (Sheldrick, 2010) within the CCP4i interface (Potterton *et al.*, 2003). The obtained experimental electron density was used to trace an initial protein model with ARP/WARP (Lamzin and Wilson, 1997). The single TG domain molecule present in the crystal asymmetric unit was then subjected to manual (program COOT (Emsley *et al.*, 2010)

and constrained refined using REFMAC5 (Steiner *et al.*, 2003), and the model was used for molecular replacement to solve the structure of the native dataset (Vagin and Teplyakov, 1997). Additional refinements with BUSTER (Smart *et al.*, 2012) and REFMAC5 were subsequently performed for both datasets.

The experimental electron density of the TG domain allowed modelling all the protein sequence between Val195 and Leu482 that is around 17 amino acids upstream respect to the cleavage region (Figure D9). The TG domain is folded in a tripartite globular structure composed of two sub domains linked by a central antiparallel beta sheet composed of four strands. The N-terminal portion of the domain is mainly composed of β strands, with a major solvent exposed antiparallel β sheet (made by 6 strands), which could be considered as a putative regulatory domain. On the contrary, the C-terminal domain contains the conserved catalytic triad and is mainly composed of alpha helices (Figure D9).

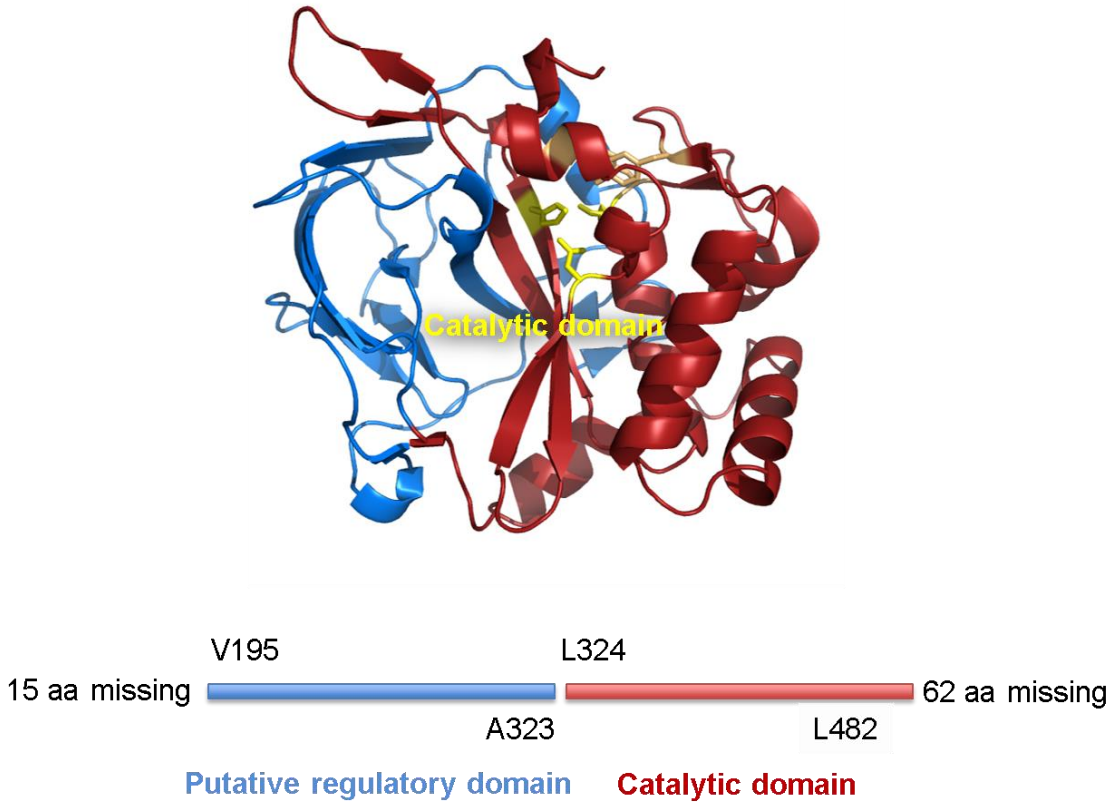

Figure D9. Blue N-terminal portion putative regulatory domain; yellow catalytic triad; red C-terminal catalytic domain

Structure-based analysis with DALI server (Holm, 2010) allowed identifying homology between the TG domain with the eukaryotic transglutaminase coagulation factor XIII (pdb-id 4kty, Z=6.4, id. 22%). The similarity is restricted to the conserved catalytic core with Cys-His-Asp residues, and also to the presence of certain residues in its proximities, like the presence of a Gly two amino acids upstream of the catalytic Cys and aromatic residues (Trp) two amino acids downstream of the catalytic His and also flanking the Asp from the N-terminal side. This led us to consider that TgpA belongs to the poorly characterized group of **Transglutaminase-like superfamily of enzymes**, typified by the structure of the human coagulating factor XIII (Makarova *et al.,* 1999).

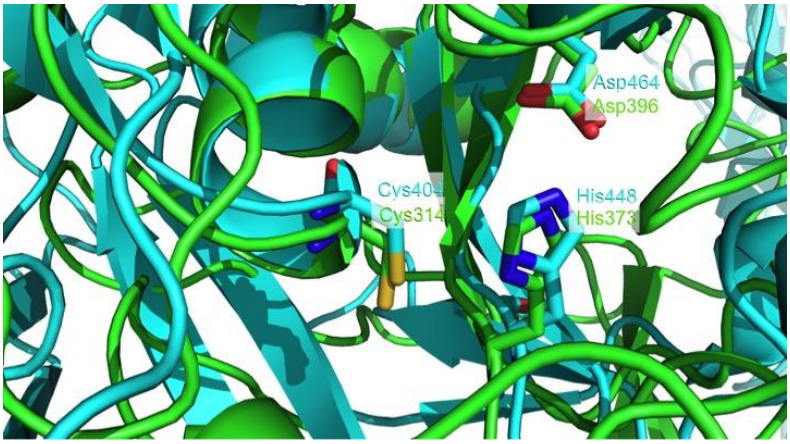

Figure D10. Superimposing catalytic triad of the human transglutaminase coagulation factor XIII (green) with TG domain (blue).

D.2.2.1. N-terminal portion: A regulatory domain?

Structural analysis restricted to the N-terminal portion of the protein (from Val195 to Ala323), established similarity with different carbohydrate binding domains like the chitin binding domain (chitinase, pdb-id 5dhe, Z=2.8, 13% identity (Hanazono *et al.*, 2016)), xylan binding domain (xylanase, pdb-id 1xbd, Z=2.7, 7% identity) and sugar binding (GH52 Beta-D-xylosidase; pdb-id 4rhh, Z=3.4, 7% identity), suggesting that this portion of the protein could be involved in the binding of polysaccharides presents in the cell wall and this might constitute a mechanism of regulation of the enzymatic activity of TgpA.

The major component of bacterial cell wall is the PGN, a complex polymer formed by long glycan chains cross-linked by peptide stems, which requires constant balance between synthesis and degradation, by a well-orchestrated set of proteins from different classes. Most of these proteins are PGN hydrolases that contains cell wall binding motives that recognize specific fragments of the cell wall. Such is the case of the well-characterized SPOR (PF05036), LysM (PF01476), SH3b (PF08460), PGN-binding domain type 1 (PF01471), DUF3393 (PF11873) or WxL (PF13731) domains (Alcorlo *et al.,* 2017). However, the mechanisms of PGN recognition and regulatory mechanisms of the enzymes involved in its metabolism are still largely unknown.

Considering these arguments, the ability of the TG domain to bind bacterial PGN was investigated by a pulldown assay (Wong *et al*, 2013). In such experiments the protein that binds to the PGN will coprecipitate with the ligand and is found in the pellet after centrifugation. As shown in Figure D11, in presence of increased concentrations of PGN from *P. aeruginosa* the TG domain localized in the pellet, suggesting interaction between the two molecules. In absence of PGN the TG domain remains soluble. The helicase from virus dengue was used as a control, showing no detectable binding.

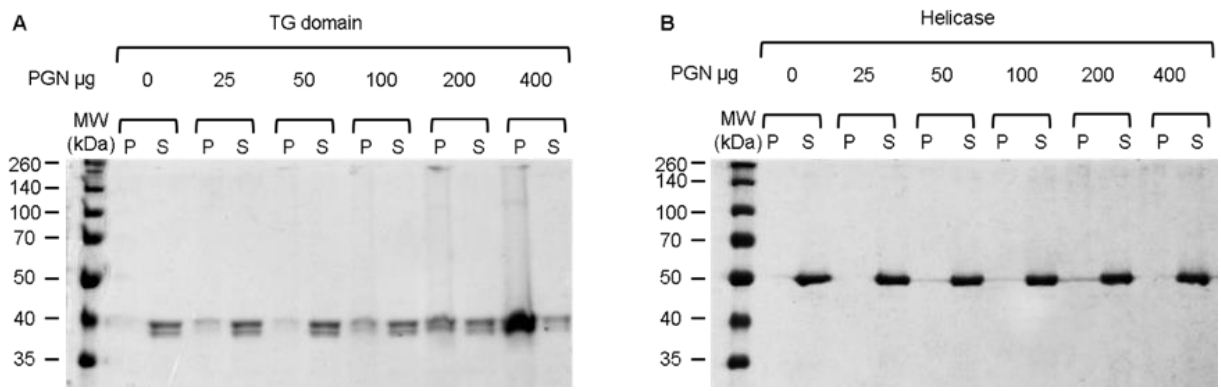

Figure D11. Pulldown experiments with insoluble PGN. The binding capacity of the (**A**) TG domain and (**B**) helicase were assayed by Pulldown assay with increasing concentrations of insoluble PGN from *P. aeruginosa*. The lanes are labelled as follows: MW = Molecular weight marker, P = Pellet, S = Supernatant

To further validate the binding capability of the TG domain, the specificity of the interaction was assessed through Microscale Thermophoresis – MST. For this purpose, the binding capacity of the TG domain was compared towards the sacculi from *P. aeruginosa* and. *B. subtilis* (Sigma), a gram-positive bacteria with PGN classified as amidated A1γ (L-m-Dap amidated). Negative controls of binding were performed with labelled helicase from dengue virus under the same conditions used for the TG domain.

Knowing the insoluble nature of the bacterial sacculi, a pilot experiment was carried out using the soluble fraction of the sacculi extracted from *P. aeruginosa* and *B. subtilis*. After centrifuging the mixture, the dry weight of the insoluble fraction of the PGN from *B. subtilis* allowed establishing that the 50% remains soluble (5mg/ml). A standard curve was set with the soluble fraction measuring the absorbance at 280nm (A 280nm), and an estimated concentration of the soluble fraction of the isolated PGN from *P. aeruginosa* was determined.

With the hypothesis that the binding between the the TG domain and PGN is given by the glycans present in each molecule of the muropeptide, the molecular weight of the disaccharide GlcNAc-MurNAc (496.466g/mol) was used to calculate a hypothetical dissociation constant (K_d).

The TG domain – PGN interaction was monitored by titrating PGN form *P. aeruginosa* from 0.125 mM to ~7.6 nm and higher concentration of *B. subtilis* were used to define better the curve, from 5 mM to ~150 nM. The TG domain and helicase labelled with the Kit RED-NHS (NanoTemper technologies, Munich, Germany), were kept at constant concentration 75 nM. The changes of the fluorescent thermophoresis signals were plotted and K_d values were determined using the NanoTemper analysis software, through non-linear curve fitting.

In this exploratory analysis, it was possible to conclude that the TG domain has the ability to bind the PGN, both from *P. aeruginosa* and *B. subtilis* (Figure D12). The affinity for both type of PGN is in the µM range, however the TG domain shows greater affinity for the PGN from *P. aeruginosa* (Table 2).

The negative control, helicase from dengue virus, does not bind the PGN from *P. aeruginosa*, but it binds to the PGN from *B. subtilis* with a K_d in the milimolar range, around 10 times the value of the K_d for the binding of the TG domain and the *B. subtilis* PGN.

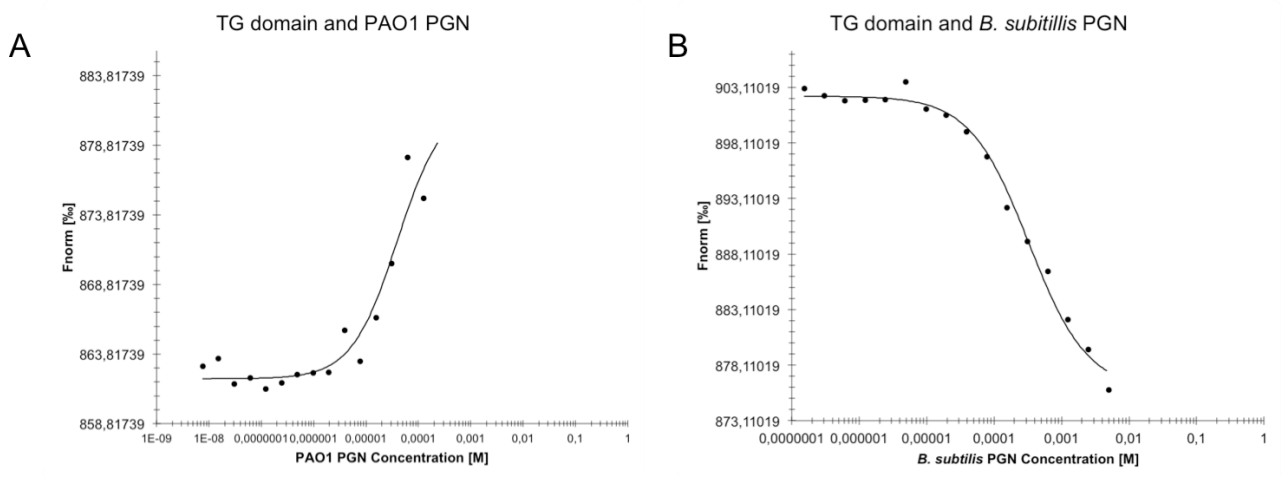

Figure D12. TG domain and PGN binding affinity was analysed by MST. The TG domain – PGN interaction was monitored by titrating PGN of (**A)**. PAO1 from 0.125 mM to ~7.6 nm, and (**B)**. *B. subtilis* from from 5 mM to ~ 0.1 nM, against 75 nM of TG domain labelled with the Kit RED-NHS (NanoTemper technologies, Munich, Germany). The changes of the fluorescent thermophoresis signals were plotted and K_d values were determined using the NanoTemper analysis software, through non-inear curve fitting. The change in MST signals was fitted to yield the hypothetical *Kd*.

Table D2. Binding constants for PGN ligands. The equilibrium dissociation constants (K_d) are given in µM. NS: Not significative

	K_d (µM)	
	P. aeruginosa	*B. subtilis*
TG domain	39± 2	210 ± 4
helicase	NS	1800± 390

These results suggest that the TG domain has the ability to bind PGN with greater affinity for *P. aeruginosa* samples. Although the PGN of *P. aeruginosa* and *B. subtilis* do not differ much structurally, only in the amidation on m-Dap in *B. subtilis*, it could be suggested that this difference was sufficient to establish a difference in binding affinity. However, more detailed analyses are required with different purified muropeptides oligomers to establish the specificity of the interaction. Likewise, it should be clarify the boundaries of the N-terminal domain to which PGN is bound and the residues involved in it.

Although it is true that the domain identified at the N-terminal end of the TG domain has no homology with the already known domains that bind to the bacterial PGN, the mechanisms of recognition of bacterial PGN and regulatory mechanisms of the enzymes involved in its metabolism are still largely unknown.

D.2.2.2. TG domain active site

A detailed description and analysis of the active site of the TG domain is found in Part II in "manuscript in preparation".

Structural analysis with DALI server restricted to the active site found homology with a transglutaminase-like putative cysteine proteases (pdb-id 3ISR, Z=9.8, id. 18%) and a putative protease (pdb-id 3KD4, Z=8.7, id. 17%), both from gram-negative bacteria; although these enzymes have not been functionally characterized they are classified as hydrolases. An additional analysis of the overall geometry of the active site residues using the LabelHash server (Moll et al., 2011) found homology with the active site of a Cys endopeptidase acting on muropeptides (Xu et al., 2009). Therefore all the structure-based analyses suggest that the protein might be somehow involved in the cell wall metabolism.

Interestingly, with the solved structure of the TG domain it was possible to establish that the active site Cys404 is buried inside the protein at about 10 Å from the protein surface (Figure D13), and that probably it becomes accessible when the right substrate is present. So far, it has not been possible to accurately define the specific substrate for the protein, but we hypothesized that, in a truncated version of the protein, in which a portion of the C-terminal end is removed, the catalytic site will be more exposed and accessible for generic substrates, and measurement of protein activity *in vitro* will be possible.

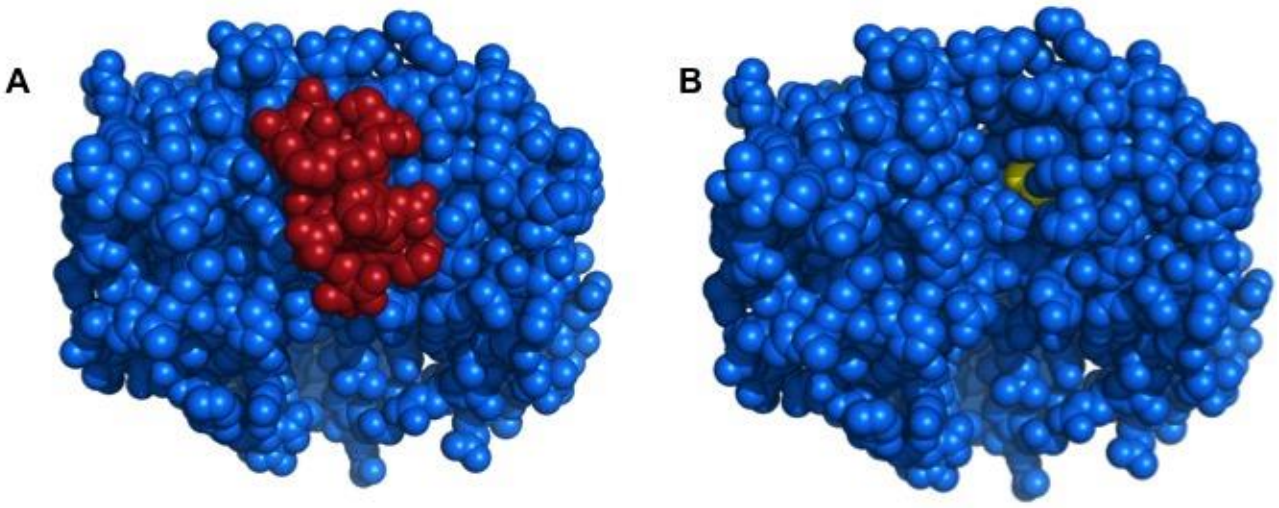

Figure D13. (**A**) TG domain structure. The C-terminal portion is colored in Red, showing how encloses the active site. (**B)** Cys residue is colored in Yellow

For this purpose, two shorter truncated forms of the TG domain were generated, considering also the previously described cleavage at the C-terminal end of the protein. One of the truncated forms terminates at the amino acid Pro471 (P471) and the other one at the amino acid Glu480 (Q480). Both constructs were cloned and expressed in the same manner as the wt TG domain (described above), and after affinity purification and size exclusion chromatography both proteins were observed as single bands on SDS-PAGE (Figure D14). However, both proteins were highly unstable and prone to precipitate. With the addition of 10% glycerol in the elution buffer the truncated form P471 remained soluble and available to be evaluated for activity *in vitro*.

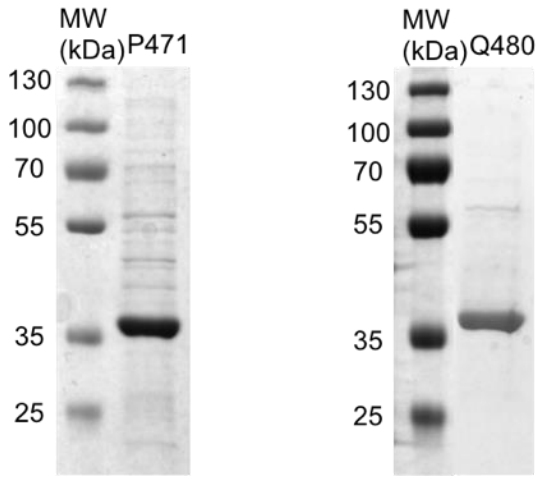

Figure D14. Purified recombinant truncated forms of TG domain, P471 and Q480. SDS-PAGE 12% MW = Molecular weight marker

D.2.3.*In vitro* activity assays

D.2.3.1. Ammonia release assay

Typically, transglutaminases catalyze an acyl-transfer reaction between the γ-carboxamide group of a protein- or peptide-bound glutamine and the ε-amino group of a lysine residue, releasing ammonia in the process. In the search for a method that would allow the measurement of transglutaminase activity of the TG domain for high throughput screening (HTS) purposes, a sensitive method has been modified and established for the detection of the ammonia released during the formation of acyl intermediates in the transglutaminase reaction. The reaction between ammonia and the fluorescent ortho-phthalaldehyde (OPA) produces coloured polymeric products that can be used for fluorescent detection and quantification.

Thus, the release of ammonia was assessed in a reaction between the TG domain and a commercially available substrate used to characterize transglutaminase activity, Z-Gln-Gly (Z-QG), which acts as a γ-glutamyl donor during the first step of the TG reaction. A human transglutaminase II, TG2, was used as a positive control, setting a standard curve with serial dilutions ranging from 200nM to 0.1 nM in reaction. The reaction between each enzyme and substrate was kept at 37°C for two hours. The reaction products were detected by the addition of OPA and the fluorescence intensity was read on TECAN after 1 additional hour. As blank, it was considered all the components of the reaction mixture except for the presence of the substrate. The fluorescence reading of the blank sample was substrated from the flouorescence value of each tested sample, and the enzymatic activity was compared to the standard curve. The substrate was also evaluated to verify that it did not contain ammonia contaminants that could affect the fluorescence reading.

As can be seen in the Figure D15, the fluorescence values due to the ammonia release are not comparable between the positive control TG2 and the two recombinant forms of the TG domain, wt and P471, when incubated with the substrate Z-QG. However, the fluorescence values observed with the TG domain and truncated form P471 (around 2000 fluorescent units) are not considered trivial; the small amount of ammonia released during the reaction may be due to the fact the Z-QG substrate is not specific for the TG domain. This can be considered as a residual transglutaminase activity that might be potentiated in the presence of the right substrate for the TG domain.

Therefore the ammonia release method with the substrate Z-QG is not the method of choice to measure the possible transglutaminase activity that the TG domain could have.

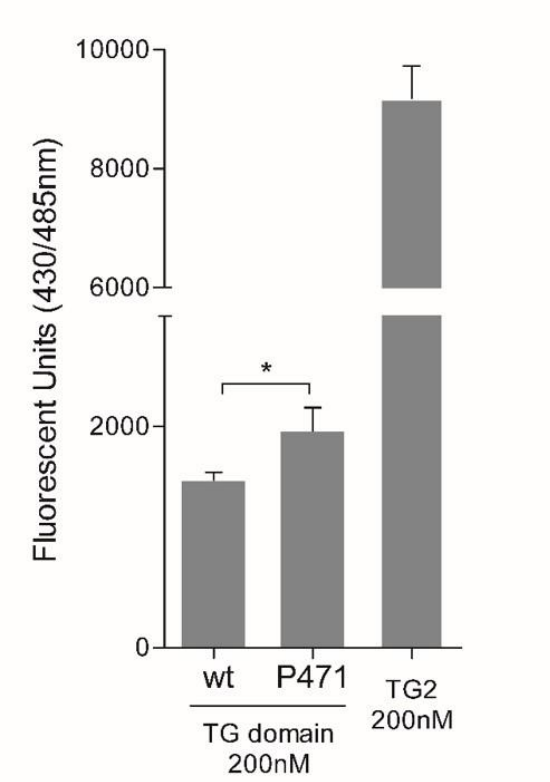

Figure D15. Ammonia release assay of TG domain. 200nM of purified protein, TG domain and P471, were tested for the ammonia release assay. For the positive control Human Transglutaminase 2, TG2, was established a standard curve using serial dilutions starting from 200nM to 0.1 nM in reaction. 20mM of the Z-QG substrate and 4mM of the fluorescent OPA reagent were used. In the figure are plotted the fluorescence product of the ammonia release of 200 nM of each protein, TG2, TG domain and P471. One asterisk represents *p*-value 0.03. The results are representative of three independent experiments.

D.2.3.2.Protease activity assay

The conserved catalytic triad Cys-His-Asp, also present in diverse enzyme families such as cysteine proteases and peptide N-glycanases (PNGases), which are all members of the transglutaminase protein superfamily, suggests that TG domain might have a cysteine protease activity.

To determine if the TG domain has cysteine protease activity *in vitro*, was used a kit designed for the detection of protease activity (serine, aspartic, cysteine and metalloproteinases) using fluorimetry based on the hydrolysis of casein labelled with

fluorescein isothiocyanate (FITC) as general substrate. A standard curve with the positive control Trypsin was established with serial dilutions from 2.5µg/ml to 0.15µg/ml in reaction. The TG domain and the truncated form P471 were tested at a concentration of 20 µg/ml. The proteolytic reaction was performed at 37°C and after 2 hrs was stopped with trichloroacetic acid (TCA) and after centrifuged the sample, the processed soluble fragments of fluorescent casein were measured. The blank of the proteolytic reaction was carried out in the same manner previously described for the ammonia release assay.

Through pulldown assay and MST experiments we demonstrated that TG domain can bind PGN from *P. aeruginosa*, so we speculated that this binding could act as a regulatory mechanism of the enzymatic activity and generate conformational changes in the protein, exposing and making the catalytic site accessible so that it can fullfils its function. For this reason, it was performed the proteolytic reaction in presence of 5µg of PGN from *P. aeruginosa*.

As shown in figure D16, the fluorescence product of the proteolytic activity is not comparable between the positive control and the TG domain. The trypsin enzyme used as a positive control showed much higher activity on the casein substrate than TG domain in its forms, wt and truncated P471. However, it is important to point out that in the presence of PGN from PAO1 the proteolytic activity of the truncated form P471 showed a significant increase in fluorescence with respect to the TG domain wt, which could be considered as a residual proteolytic activity. This suggests conformational changes in the TG domain structure due to the presence of PGN that allowed the casein substrate to be partially cleaved.

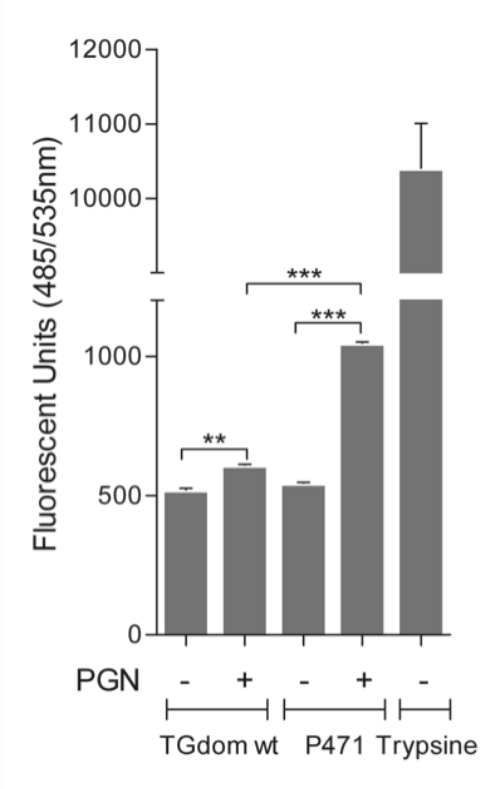

Figure D16. Protease activity on the general substrate FITC casein. 20µg/mlof TG domain and P471 were tested for protease activity on the casein FITC substrate, in presence of 5µg/mlof *P. aeruginosa* PGN. For the positive control, a standard curve with trypsin from 2.5µg/ml to 0.15 µg/ml. In the figure are plotted the fluorescence product of the proteolytic activity of 0.3 µg/ml of trypsin vs 20 µg/ml of TG domain and P471. The truncated form P471 shows residual protease activity on the general substrate casein. Three asterisk represents significant difference; *p*-value < 0.0001.The results are representative of three independent experiments.

D.3. Conclusions and perspectives

The current rise in multi-drug resistant *P. aeruginosa* is of particular concern. Nowadays, this ubiquitous bacterial pathogen is accepted worldwide as a public health risk due to its increasing prevalence in healthcare acquired infections combined with its ability to develop resistances to multiple classes of antibiotics. Urgent and novel strategies to discover new antibiotics are required and the study of essential genes has proved to be an interesting strategy in medicine for the identification of important antimicrobials targets.

This PhD work provides initial insights towards the characterization of TgpA, an essential protein for the viability of *P. aeruginosa,* and a promising target for the design of new specific antimicrobial compounds.

From the initial analysis, in which substitutions in the predicted main residues of catalytic triad Cys404 and His448were evaluated for their effects on the *P. aeruginosa* growth, it was possible to speculate about the importance of these two residues for the activity of the protein. The fact that PAO1 P_{rhaB}::*tgpA* strain was unable to growth in the presence of glucose unless functional TgpA was expressed ectopically from another promoter, confirmed the essentiality of the Cys404 and His448 residues for the activity of TgpA.

Regarding phenotypic effects, the results of the partial suppression of the chromosomal copy of the *tgpA* gene were consistent with the hypothesis that TgpA has an important role at the cell wall level; in particular the visible “collapsed-zones” following TgpA depletion suggest a possible role of anchoring inner membrane to upper layers of the envelope, or in the assembly of peptidoglycan structures. These results are also in agreement with the TgpA overexpression that could affect the envelope dynamic and thus leads to the growth impairment.

Metabolomic or proteomic profiles of the periplasm of *P. aeruginosa* with the PAO1 P_{rhaB}::*tgpA* strain could help to clarify the essential role that the protein plays for the viability of the cell. As well as the identification of possible natural substrates for the evaluation of the enzymatic activity.

On the other hand, the solved structure of the periplasmic TG domain showed the presence of two subdomains: The N-terminal, a possible regulatory domain linked to different carbohydrate binding domains, and the C-terminal hosting the conserved catalytic triad Cys404-His448-Asp464 involved in a specific enzymatic activity.

The exploratory analysis on the interaction between the TG domain and peptidoglycan resulted in directing the hypothesis about the regulatory role of the N-terminal subdomain and showing some hints on how the mechanism of ligand binding and activation of the C-terminal catalytic subdomain may occur in order to carry out its function. The binding between TG domain and peptidoglycan was found to be quite specific (in the μM range) when compared to the ability of the dengue virus helicase to bind to the same ligand. At the same time, the residual proteolytic activity observed with the generic substrate casein, when the reaction is conducted in presence of the peptidoglycan, suggest a mechanism of conformational changes in the TG domain structure when is bounded to the peptidoglycan that allows the exposure the catalytic site and this one can fullfil its function.

These results are yet preliminary and future studies are required to assess whether the binding to the peptidoglycan is at the N-terminal subdomain and also to describe the key residues involved in the binding. Also, the question remains open on what is the portion of the peptidoglycan to which the protein binds. Additional exploratory studies about the binding capacity of other molecules present in the cell wall (e.g. LPS) should be carried out to identify other possible protein substrates.

Evidences collected in this work show some key points that can direct the evaluation of the protein activity *in vitro*, which remains one of the priorities for future studies and for high throughput screening purposes. In particular, it seems interesting to analyse the importance of the presence of aromatic residues around the active site and how this are related with the activity of the protein. These residues could be also crucial for the inhibition of the activity, for which *in silico* docking studies are continuing.

Furthermore, it could be interesting to explore the importance of a C-terminal domain that is predicted to be cytoplasmic and that is found after the last transmembrane domain (residues 582-638 belonging to the DUF4129 superfamily) of the TgpA full-length protein. Preliminary analyses through bioinformatics tools, allow identifying that this domain is not characterized

yet, but is closely related to transglutaminases proteins. It could be a domain that facilitates the union of a cytoplasmic substrate / cofactor important for the regulation / function of the protein. Currently the C-terminal cytoplasmic domain is in the process of purification.

In conclusion, our results expanded the knowledge about the essentiality of TgpA for the viability of *P. aeruginosa*, providing initial evidence regarding the characterization of the protein at molecular, cellular, structural and biochemical level, valuable for the future design of novel antimicrobials acting specifically on *P. aeruginosa*.

E. References

Aeschlimann, D., and Paulsson, M. (1994). Transglutaminases: protein cross-linking enzymes in tissues and body fluids. *Thromb Haemost* **71**(4): 402-415.

Albers, S.V., and Meyer, B.H. (2011). The archaeal cell envelope. *Nat Rev Microbiol* **9**: 414.

Alcorlo, M., *et al*. (2017). Carbohydrate recognition and lysis by bacterial peptidoglycan hydrolases. *Curr Opin Struct Biol* **44**: 87-100.

Amiel, E., *et al*. (2010). *Pseudomonas aeruginosa* evasion of phagocytosis is mediated by loss of swimming motility and is independent of flagellum expression. *Infect Immun* **78**(7): 2937-2945.

Aminov, R.I. (2010). A Brief History of the Antibiotic Era: Lessons Learned and Challenges for the Future. *Front Microbiol* **1**.

Anantharaman, V., and Aravind, L. (2003). Evolutionary history, structural features and biochemical diversity of the NlpC/P60 superfamily of enzymes. *Genome Biol* **4**(2): R11.

Avrain, L., Mertens, P., and Van Bambeke, F. (2013). RND efflux pumps in *P. aeruginosa*: an underestimated resistance mechanism. *Antibiot Susceptib* **26321**: 26-28.

Barb, A.W., and Zhou, P. (2008). Mechanism and inhibition of LpxC: an essential zinc-dependent deacetylase of bacterial lipid A synthesis. *Curr Pharm Biotechnol* **9**(1): 9-15.

Barclay, M.L., Begg, E.J., and Chambers, S.T. (1992). Adaptive resistance following single doses of gentamicin in a dynamic in vitro model. *Antimicrob Agents Chemother* **36**(9): 1951-1957.

Barclay, M.L., *et al*. (1996). Adaptive resistance to tobramycin in *Pseudomonas aeruginosa* lung infection in cystic fibrosis. *J Antimicrob Chemother* **37**(6): 1155-1164.

Barr, H.L., *et al*. (2015). *Pseudomonas aeruginosa* quorum sensing molecules correlate with clinical status in cystic fibrosis. *Eur Respir J* **46**(4): 1046-1054.

Barreteau, H., *et al*. (2008). Cytoplasmic steps of peptidoglycan biosynthesis. *FEMS Microbiol Rev* **32**(2): 168-207.

Barrow, K., and Kwon, D.H. (2009). Alterations in two-component regulatory systems of phoPQ and pmrAB are associated with polymyxin B resistance in clinical isolates of *Pseudomonas aeruginosa*. *Antimicrob Agents Chemother* **53**(12): 5150-5154.

Berdy, J. (2005). Bioactive microbial metabolites. *J Antibiot (Tokyo)* **58**(1): 1-26.

Blair, J.M., *et al*. (2015). Molecular mechanisms of antibiotic resistance. *Nat Rev Microbiol* **13**(1): 42-51.

Blondeau, J.M. (2004). Fluoroquinolones: mechanism of action, classification, and development of resistance. *Surv Ophthalmol* **49 Suppl 2**: S73-78.

Boles, B.R., Thoendel, M., and Singh, P.K. (2005). Rhamnolipids mediate detachment of *Pseudomonas aeruginosa* from biofilms. *Mol Microbiol* **57**(5): 1210-1223.

Botos, I., Noinaj, N., and Buchanan, S.K. (2017). Insertion of proteins and lipopolysaccharide into

the bacterial outer membrane. *Philos Trans R Soc Lond B Biol Sci* **372**(1726).

Boucher, H. W., *et al*. (2009). Bad bugs, no drugs: no ESKAPE! An update from the Infectious Diseases Society of America. *Clin Infect Dis* **48**(1): 1-12.

Bouhss, A., *et al*. (2008). The biosynthesis of peptidoglycan lipid-linked intermediates. *FEMS Microbiol Rev* **32**(2): 208-233.

Boutros, M., and Ahringer, J. (2008). The art and design of genetic screens: RNA interference. *Nat Rev Genet* **9**: 554.

Boyle, B., *et al*. (2012). Complete Genome Sequences of Three *Pseudomonas aeruginosa* Isolates with Phenotypes of Polymyxin B Adaptation and Inducible Resistance. *J of Bacteriol* **194**(2): 529-530.

Brennan, P.J. and Nikaido, H. (1995). The envelope of mycobacteria. *Annu Rev Biochem* **64**: 29-63.

Brown, M.F., *et al*. (2012). Potent inhibitors of LpxC for the treatment of Gram-negative infections. *J Med Chem* **55**(2): 914-923.

Christen, B., *et al*. (2011). The essential genome of a bacterium. *Mol Syst Biol* **7**: 528.

Chrzanowski, L., Lawniczak, L., and Czaczyk, K. (2012). Why do microorganisms produce rhamnolipids? *World J Microbiol Biotechnol* **28**(2): 401-419.

Clardy, J., Fischbach, M., and Currie, C. (2009). The natural history of antibiotics. *Curr Biol* **19**(11): R437-441.

Clatworthy, A.E., Pierson, E., and Hung D.T. (2007). Targeting virulence: a new paradigm for antimicrobial therapy. *Nat Chem Biol* **3**(9): 541-548.

Cooper, M.A., and Shlaes, D. (2011). Fix the antibiotics pipeline. *Nature* **472**(7341): 32.

Das, T., *et al*. (2013). Pyocyanin facilitates extracellular DNA binding to *Pseudomonas aeruginosa* influencing cell surface properties and aggregation. *PLoS One* **8**(3): e58299.

Das, T., *et al*. (2015). Phenazine virulence factor binding to extracellular DNA is important for *Pseudomonas aeruginosa* biofilm formation. *Sci Rep* **5**: 8398.

Davey, M.E., Caiazza, N.C., and O'Toole, G.A. (2003). Rhamnolipid surfactant production affects biofilm architecture in *Pseudomonas aeruginosa* PAO1. *J Bacteriol* **185**(3): 1027-1036.

Davies J., and Davies, D. (2010). Origins and evolution of antibiotic resistance. *Microbiol Mol Biol Rev* **74**(3): 417-433.

Davies, J. E. (1997). Origins, acquisition and dissemination of antibiotic resistance determinants. *Ciba Found Symp* **207**: 15-27; discussion 27-35.

de Berardinis, V., *et al*. (2008). A complete collection of single-gene deletion mutants of *Acinetobacter baylyi* ADP1. *Mol Syst Biol* **4**: 174.

De Winter, B., *et al.* (2017). Population pharmacokinetics of Murepavadin (POL7080) and Monte Carlo simulations to develop clinical dosing regimens, including the renally impaired. 27th

European Congress of Clinical Micobiology and Infectious Diseases (ECCMID), Vienna, Austria, 22–25 April 2017. Basel: European Society of Clinical Microbiology and Infectious Diseases; 2017.

Di Fabio, J.L., *et al.* (1992). Characterization of the common antigenic lipopolysaccharide O-chains produced by *Bordetella bronchiseptica* and *Bordetella parapertussis*. *FEMS Microbiol Lett* **76**(3): 275-281.

Dmitriev, B., *et al*. (2005). Towards a comprehensive view of the bacterial cell wall. *Trends Microbiol* **13**(12): 569-574.

Dominguez-Gil, T., *et al.* (2016). Renew or die: The molecular mechanisms of peptidoglycan recycling and antibiotic resistance in Gram-negative pathogens. *Drug Resist Updat* **28**: 91-104.

Doring, G., *et al*. (2000). Antibiotic therapy against *Pseudomonas aeruginosa* in cystic fibrosis: a European consensus. *Eur Respir J* **16**(4): 749-767.

Driscoll, J.A., Brody, S.L., and Kollef M.H. (2007). The epidemiology, pathogenesis and treatment of *Pseudomonas aeruginosa* infections. *Drugs* **67**(3): 351-368.

Drlica, K., *et al*. (2008). Quinolone-Mediated Bacterial Death. *Antimicrob Agents Chemother* **52**(2): 385-392.

Dusane, D.H., *et al*. (2010). Quorum sensing: implications on rhamnolipid biosurfactant production. *Biotechnol Genet Eng Rev* **27**: 159-184.

Ellington, M.J., *et al.* (2015). Emergent and evolving antimicrobial resistance cassettes in community-associated fusidic acid and meticillin-resistant *Staphylococcus aureus*. *Int J Antimicrob Agents* **45**(5): 477-484.

Emsley, P., *et al.* (2010). Features and development of Coot. *Acta Crystallogr D Biol Crystallogr* **66**(Pt 4): 486-501.

Epp, S.F., *et al.* (2001). C-terminal region of *Pseudomonas aeruginosa* outer membrane porin OprD modulates susceptibility to meropenem. *Antimicrob Agents Chemother* **45**(6): 1780-1787.

Falagas, M.E., and Kasiakou, S.K. (2005). Colistin: the revival of polymyxins for the management of multidrug-resistant Gram-negative bacterial infections. *Clin Infect Dis* **40**(9): 1333-1341.

Fang, G., Rocha E., and Danchin, A. (2005). How essential are nonessential genes? *Mol Biol Evol* **22**(11): 2147-2156.

Fernandes, C.G., *et al*. (2015). Structural and Functional Characterization of an Ancient Bacterial Transglutaminase Sheds Light on the Minimal Requirements for Protein Cross-Linking. *Biochem* **54**(37): 5723-5734.

Fernandes, P. (2006). Antibacterial discovery and development--the failure of success? *Nat Biotechnol* **24**(12): 1497-1503.

Fernandez, L., Breidenstein E.B., and Hancock, R.E. (2011). Creeping baselines and adaptive resistance to antibiotics. *Drug Resist Updat* **14**(1): 1-21.

Fernandez, L., *et al.* (2010). Adaptive resistance to the "last hope" antibiotics polymyxin B and colistin in *Pseudomonas aeruginosa* is mediated by the novel two-component regulatory system ParR-ParS. *Antimicrob Agents Chemother* **54**(8): 3372-3382.

Fernandez, L., *et al*. (2012). The two-component system CprRS senses cationic peptides and triggers adaptive resistance in Pseudomonas aeruginosa independently of ParRS. *Antimicrob Agents Chemother* **56**(12): 6212-6222.

Fernández-Piñar, R., *et al.* (2015). *In vitro* and *in vivo* screening for novel essential cell-envelope proteins in *Pseudomonas aeruginosa*. *Sci Rep* **5**: 17593.

Fisher, J.F., Meroueh, S.O., and Mobashery, S. (2005). Bacterial resistance to beta-lactam antibiotics: compelling opportunism, compelling opportunity. *Chem Rev* **105**(2): 395-424.

Fisher, J.F. and Mobashery, S. (2014). The sentinel role of peptidoglycan recycling in the beta-lactam resistance of the Gram-negative Enterobacteriaceae and *Pseudomonas aeruginosa*. *Bioorg Chem* **56**: 41-48.

Flemming, H.C. and Wingender, J. (2010). The biofilm matrix. *Nat Rev Microbiol* **8**(9): 623-633.

Floss, H.G., and Yu, T.W. (2005). Rifamycin-mode of action, resistance, and biosynthesis. *Chem Rev* **105**(2): 621-632.

Folk, J.E., and Chung, S.I. (1973). Molecular and catalytic properties of transglutaminases. *Adv Enzymol Relat Areas Mol Biol* **38**: 109-191.

Fortin, P.D., Walsh, C.T., and Magarvey, N.A. (2007). A transglutaminase homologue as a condensation catalyst in antibiotic assembly lines. *Nature* **448**(7155): 824-827.

Freiberg, C., *et al*. (2004). Identification and characterization of the first class of potent bacterial acetyl-CoA carboxylase inhibitors with antibacterial activity. *J Biol Chem* **279**(25): 26066-26073.

Freiberg, C., Fischer, H.P., and Brunner, N.A. (2005). Discovering the Mechanism of Action of Novel Antibacterial Agents through Transcriptional Profiling of Conditional Mutants. *Antimicrob Agents Chemother* **49**(2): 749-759.

Freire-Moran, L., *et al.* (2011). Critical shortage of new antibiotics in development against multidrug-resistant bacteria-Time to react is now. *Drug Resist Updat* **14**(2): 118-124.

French, C.T., *et al*. (2008). Large-scale transposon mutagenesis of Mycoplasma pulmonis. *Mol Microbiol* **69**(1): 67-76.

Gallagher, L.A., Shendure, J., and Manoil, C. (2011). Genome-Scale Identification of Resistance Functions in *Pseudomonas aeruginosa* Using Tn-seq. *mBio* **2**(1):e00315-10. doi:10.1128/mBio.00315-10

Gellatly, S.L., and Hancock, R.E. (2013). *Pseudomonas aeruginosa*: new insights into pathogenesis and host defenses. *Pathog Dis* **67**(3): 159-173.

Ghafoor, A., Hay, I.D., and Rehm, B.H. (2011). Role of exopolysaccharides in *Pseudomonas aeruginosa* biofilm formation and architecture. *Appl Environ Microbiol* **77**(15): 5238-5246.

Gil, R., *et al*. (2004). Determination of the core of a minimal bacterial gene set. *Microbiol Mol Biol Rev* **68**(3): 518-537

Giuliani, A., and Rinaldi, A.C. (2011). Beyond natural antimicrobial peptides: multimeric peptides

and other peptidomimetic approaches. *Cell Mol Life Sci* **68**(13): 2255-2266.

Glass, J.I., *et al.* (2006). Essential genes of a minimal bacterium. *Proc Natl Acad Sci U S A* **103**(2): 425-430.

Gonzalez, J.E. and Keshavan, N.D. (2006). Messing with bacterial quorum sensing. *Microbiol Mol Biol Rev* **70**(4): 859-875.

Gutierrez, O., *et al*. (2007). Molecular epidemiology and mechanisms of carbapenem resistance in *Pseudomonas aeruginosa* isolates from Spanish hospitals. *Antimicrob Agents Chemother* **51**(12): 4329-4335.

Gutu, A. D., *et al*. (2013). Polymyxin resistance of *Pseudomonas aeruginosa* phoQ mutants is dependent on additional two-component regulatory systems. *Antimicrob Agents Chemother* **57**(5): 2204-2215.

Hanazono, Y., Takeda, K., and Miki, K. (2016). Structural studies of the N-terminal fragments of the WW domain: Insights into co-translational folding of a beta-sheet protein. *Sci Rep* **6**: 34654.

Harbarth, S., *et al*. (2002). Epidemiology and prognostic determinants of bloodstream infections in surgical intensive care. *Arch Surg* **137**(12): 1353-1359; discussion 1359.

Hartmann, E., and Konig, H. (1990). Comparison of the biosynthesis of the methanobacterial pseudomurein and the eubacterial murein. *Naturwissenschaften* **77**(10): 472-475.

Hay, T., *et al*. (2013). Antibiotic inducibility of the mexXY multidrug efflux operon of *Pseudomonas aeruginosa*: involvement of the MexZ anti-repressor ArmZ. *PLoS One* **8**(2): e56858.

Hogardt, M., and Heesemann, J. (2010). Adaptation of *Pseudomonas aeruginosa* during persistence in the cystic fibrosis lung. *Int J Med Microbiol* **300**(8): 557-562.

Holm, L., and Rosenstrom, P. (2010). Dali server: conservation mapping in 3D. *Nucleic Acids Res* **38**(Web Server issue): W545-549.

Holtje, J.V. (1998). Growth of the stress-bearing and shape-maintaining murein sacculus of *Escherichia coli. Microbiol Mol Biol Rev* **62**(1): 181-203.

Hong, D.J., *et al.* (2015). Epidemiology and Characteristics of Metallo-β-Lactamase-Producing *Pseudomonas aeruginosa*. *Infect Chemother* **47**(2): 81-97.

Huang, K., *et al.* (2014). MetaRef: a pan-genomic database for comparative and community microbial genomics. *Nucleic Acids Res* **42**(Database issue): D617-624.

Leid, J.C. (2009). Bacterial biofilms resist key host defenses. *Microbe* **4**: 66-70.

Jaffar-Bandjee, M.C., *et al*. (1995). Production of elastase, exotoxin A, and alkaline protease in sputa during pulmonary exacerbation of cystic fibrosis in patients chronically infected by *Pseudomonas aeruginosa*. *J Clin Microbiol* **33**(4): 924-929.

Jennings, L.K., *et al*. (2015). Pel is a cationic exopolysaccharide that cross-links extracellular DNA in the *Pseudomonas aeruginosa* biofilm matrix. *Proc Nati Acad Sci* **112**(36): 11353-11358.

Johansen, H.K., *et al*. (2008). Spread of colistin resistant non-mucoid *Pseudomonas aeruginosa* among chronically infected Danish cystic fibrosis patients. *J Cyst Fibros* **7**(5): 391-397.

Jordan, I.K., *et al.* (2002). Essential genes are more evolutionarily conserved than are nonessential genes in bacteria. *Genome Res* **12**(6): 962-968.

Juan, C., *et al*. (2005). Molecular mechanisms of beta-lactam resistance mediated by AmpC hyperproduction in *Pseudomonas aeruginosa* clinical strains. *Antimicrob Agents Chemother* **49**(11): 4733-4738.

Juhas, M., Eberl, L., and Church, G.M. (2012). Essential genes as antimicrobial targets and cornerstones of synthetic biology. *Trends Biotechnol* **30**(11): 601-607.

Juhas, M., *et al*. (2012b). High confidence prediction of essential genes in *Burkholderia cenocepacia*. *PLoS One* **7**(6): e40064.

Kabsch, W. (2010). XDS. *Acta Crystallogr D Biol Crystallogr* **66**(Pt 2): 125-132.

Kallen, A.J. and Srinivasan, A. (2010). Current epidemiology of multidrug-resistant Gram-negative bacilli in the United States. *Infect Control Hosp Epidemiol* **31 Suppl 1**: S51-54.

Kandler, O. (1993). Cell Wall Biochemistry and Three-Domain Concept of Life. *Syst Appl Microbiol* **16**(4): 501-509.

Kandler, O., and Konig, H. (1993). Chapter 8 Cell envelopes of archaea: Structure and chemistry. New Comprehensive Biochemistry, Elsevier. **26:** 223-259.

Kandler, O., and Konig, H. (1998). Cell wall polymers in Archaea (Archaebacteria). *Cell Mol Life Sci* **54**(4): 305-308.

Kao, C.Y., *et al.* (2016). Overproduction of active efflux pump and variations of OprD dominate in imipenem-resistant *Pseudomonas aeruginosa* isolated from patients with bloodstream infections in Taiwan. *BMC Microbiol* **16**(1): 107.

Kerr, K.G. and Snelling, A.M. (2009). *Pseudomonas aeruginosa*: a formidable and ever-present adversary. *J Hosp Infect* **73**(4): 338-344.

Khaledi, A., *et al*. (2016). Transcriptome Profiling of Antimicrobial Resistance in *Pseudomonas aeruginosa*. *Antimicrob Agents Chemother* **60**(8): 4722-4733.

Kiener, A., *et al.* (1987). Purification and use of *Methanobacterium wolfei* pseudomurein endopeptidase for lysis of *Methanobacterium thermoautotrophicum*. *J Bacteriol* **169**(3): 1010-1016.

King, J.D., *et al*. (2009). Post-assembly modification of Bordetella bronchiseptica O polysaccharide by a novel periplasmic enzyme encoded by wbmE. *J Biol Chem* **284**(3): 1474-1483.

Kipnis, E., Sawa, T., and Wiener-Kronish, J. (2006). Targeting mechanisms of *Pseudomonas aeruginosa* pathogenesis. *Med Mal Infect* **36**(2): 78-91.

Kohanski, M.A., Dwyer, D.J., and Collins J.J. (2010). How antibiotics kill bacteria: from targets to networks. *Nat Rev Microbiol* **8**(6): 423-435.

König, H., Hartmann, E., and Kärcher, U. (1993). Pathways and Principles of the Biosynthesis of Methanobacterial Cell Wall Polymers. *Syst Appl Microbiol* **16**(4): 510-517.

Koonin, E.V. (2003). Comparative genomics, minimal gene-sets and the last universal common ancestor. *Nat Rev Microbiol* **1**(2): 127-136.

Koonin, E.V. (2009). Darwinian evolution in the light of genomics. *Nucleic Acids Res* **37**(4): 1011-1034.

Kurr, M., *et al*. (1991). *Methanopyrus kandleri*, gen. and sp. nov. represents a novel group of hyperthermophilic methanogens, growing at 110°C. *Arch Microbiol* **156**(4): 239-247.

Lambert, M.L., *et al*. (2011). Clinical outcomes of health-care-associated infections and antimicrobial resistance in patients admitted to European intensive-care units: a cohort study. *Lancet Infect Dis* **11**(1): 30-38.

Lamzin, V.S., and Wilson, K.S. (1997). Automated refinement for protein crystallography. *Methods Enzymol* **277**: 269-305.

Lange, R.P., *et al*. (2007). The targets of currently used antibacterial agents: lessons for drug discovery. *Curr Pharm Des* **13**(30): 3140-3154.

Langridge, G.C., *et al*. (2009). Simultaneous assay of every Salmonella Typhi gene using one million transposon mutants. *Genome Res* **19**(12): 2308-2316.

LaSarre, B., and Federle, M.J. (2013). Exploiting quorum sensing to confuse bacterial pathogens. *Microbiol Mol Biol Rev* **77**(1): 73-111.

Laxminarayan, R. (2014). Antibiotic effectiveness: Balancing conservation against innovation. *Science* **345**(6202): 1299-1301.

Lee, J., and Zhang, L. (2015). The hierarchy quorum sensing network in *Pseudomonas aeruginosa*. *Protein Cell* **6**(1): 26-41.

Lee, J.K., *et al*. (2005). Alterations in the GyrA and GyrB subunits of topoisomerase II and the ParC and ParE subunits of topoisomerase IV in ciprofloxacin-resistant clinical isolates of *Pseudomonas aeruginosa*. *Int J Antimicrob Agents* **25**(4): 290-295.

Lee, J.Y., *et al.* (2016). Corrigendum: Evolved resistance to colistin and its loss due to genetic reversion in *Pseudomonas aeruginosa*. *Sci Rep* **6**: 30365.

Lee, S.A., *et al*. (2015). General and condition-specific essential functions of Pseudomonas aeruginosa. *Proc Natl Acad Sci U S A* **112**(16): 5189-5194.

Lenney, W., and Gilchrist, F.J. (2011). *Pseudomonas aeruginosa* and cyanide production. *Eur Respir J* **37**(3): 482-483.

Lewis, K. (2013). Platforms for antibiotic discovery. *Nat Rev Drug Discov* **12**(5): 371-387.

Li, X.Z., Plesiat, P., and Nikaido, H. (2015). The challenge of efflux-mediated antibiotic resistance in Gram-negative bacteria. *Clin Microbiol Rev* **28**(2): 337-418.

Liao, B.Y., Scott, N.M., and Zhang, J. (2006). Impacts of gene essentiality, expression pattern, and gene compactness on the evolutionary rate of mammalian proteins. *Mol Biol Evol* **23**(11): 2072-2080.

Ling, L.L., *et al*. (2015). A new antibiotic kills pathogens without detectable resistance. *Nature* **517**: 455.

Lister, P.D., Wolter, D.J., and Hanson, N.D. (2009). Antibacterial-resistant *Pseudomonas aeruginosa*: clinical impact and complex regulation of chromosomally encoded resistance mechanisms. *Clin Microbiol Rev* **22**(4): 582-610.

Liu, Y.Y., *et al*. (2016). Emergence of plasmid-mediated colistin resistance mechanism MCR-1 in animals and human beings in China: a microbiological and molecular biological study. *Lancet Infect Dis* **16**(2): 161-168.

Livak, K.J., and Schmittgen, T.D. (2001). Analysis of relative gene expression data using real-time quantitative PCR and the 2(-Delta Delta C(T)) Method. *Methods* **25**(4): 402-408.

Livermore, D.M. (2012). Fourteen years in resistance. *Int J Antimicrob Agents* **39**(4): 283-294.

Llanes, C., *et al.* (2011). Role of the MexEF-OprN efflux system in low-level resistance of *Pseudomonas aeruginosa*to ciprofloxacin. *Antimicrob Agents Chemother* **55**(12): 5676-5684.

Lobanovska, M., and Pilla, G. (2017). Penicillin's Discovery and Antibiotic Resistance: Lessons for the Future? *Yale J Biol Med* **90**(1): 135-145.

Lorand, L., and Conrad, S.M. (1984). Transglutaminases. *Mol Cell Biochem* **58**(1-2): 9-35.

Lovering, A.L., Safadi, S.S. and Strynadka, N.C. (2012). Structural perspective of peptidoglycan biosynthesis and assembly. *Annu Rev Biochem* **81**: 451-478.

Luo, Y., *et al.* (2001). The Genome of Archaeal Prophage ΨM100 Encodes the Lytic Enzyme Responsible for Autolysis of *Methanothermobacter wolfeii*. *J Bacteriol* **183**(19): 5788-5792.

Magarvey, N.A., *et al*. (2008). Gatekeeping versus promiscuity in the early stages of the andrimid biosynthetic assembly line. *ACS Chem Biol* **3**(9): 542-554.

Majiduddin, F.K., Materon, I.C. and Palzkill, T.G. (2002). Molecular analysis of beta-lactamase structure and function. *Int J Med Microbiol* **292**(2): 127-137.

Makarova, K.S., Aravind, L., and Koonin, E.V. (1999). A superfamily of archaeal, bacterial, and eukaryotic proteins homologous to animal transglutaminases. *Protein Sci* **8**(8): 1714-1719.

Margolin, W. (2009). Sculpting the bacterial cell. *Curr Biol* **19**(17): R812-822.

Mathee, K., *et al*. (2008). Dynamics of *Pseudomonas aeruginosa* genome evolution. *Proc Natl Acad Sci U S A* **105**(8): 3100-3105.

Matsuo, Y., *et al.* (2004). MexZ-mediated regulation of mexXY multidrug efflux pump expression in *Pseudomonas aeruginosa* by binding on the mexZ-mexX intergenic DNA. *FEMS Microbiol Lett* **238**(1): 23-28.

McCutcheon, J.P., and Moran, N.A. (2010). Functional convergence in reduced genomes of bacterial symbionts spanning 200 My of evolution. *Genome Biol Evol* **2**: 708-718.

McDaniel, C.T., Panmanee, W., and Hassett, D.J. (2015). An Overview of Infections in Cystic Fibrosis Airways and the Role of Environmental Conditions on *Pseudomonas aeruginosa* Biofilm Formation and Viability. Cystic Fibrosis in the Light of New Research. D. Wat. Rijeka, InTech**:** Ch.

08.

Milani, A., Vecchietti, D., Rusmini, R., and Bertoni, G. 2012. TgpA, a protein with a eukaryotic-like transglutaminase domain, plays a critical role in the viability of *Pseudomonas aeruginosa*. *PLoS One* **7**(11): e50323.

Mohammadi, T., *et al.* (2011). Identification of FtsW as a transporter of lipid-linked cell wall precursors across the membrane. *EMBO J* **30**(8): 1425-1432.

Moll, M., Bryant, D.H., and Kavraki, L.E. (2011). The LabelHash Server and Tools for substructure-based functional annotation. *Bioinformatics* **27**(15): 2161-2162.

Montgomery, J.I., *et al.* (2012). Pyridone methylsulfone hydroxamate LpxC inhibitors for the treatment of serious Gram-negative infections. *J Med Chem* **55**(4): 1662-1670.

Moore, L.S., Cunningham, J. and H. Donaldson (2016). A clinical approach to managing *Pseudomonas aeruginosa* infections. *Br J Hosp Med (Lond)* **77**(4): C50-54.

Moradali, M.F., Ghods, S., and Rehm, B.H. (2017). *Pseudomonas aeruginosa* Lifestyle: A Paradigm for Adaptation, Survival, and Persistence. *Front Cell Infect Microbiol* **7**: 39.

Moskowitz, S.M., *et al.* (2012). PmrB mutations promote polymyxin resistance of *Pseudomonas aeruginosa* isolated from colistin-treated cystic fibrosis patients. *Antimicrob Agents Chemother* **56**(2): 1019-1030.

Moule, M.G., *et al.* (2014). Genome-Wide Saturation Mutagenesis of *Burkholderia pseudomallei* K96243 Predicts Essential Genes and Novel Targets for Antimicrobial Development. *mBio* **5**(1).

Moya, A., *et al.* (2009). Toward minimal bacterial cells: evolution vs. design. *FEMS Microbiol Rev* **33**(1): 225-235.

Moynihan, P.J. and Clarke, A.J. (2011). O-Acetylated peptidoglycan: Controlling the activity of bacterial autolysins and lytic enzymes of innate immune systems. *Int J Biochem Cell Biol* **43**(12): 1655-1659.

Nathwani, D., *et al*. (2014). Clinical and economic consequences of hospital-acquired resistant and multidrug-resistant *Pseudomonas aeruginosa* infections: a systematic review and meta-analysis. *Antimicrob Resist Infect Control* **3**(1): 32.

Needham, J., *et al.* (1994). Andrimid and moiramides A-C, metabolites produced in culture by a marine isolate of the bacterium *Pseudomonas fluorescens*: structure elucidation and biosynthesis. *J Org Chem* **59**(8): 2058-2063.

Nemes, Z., *et al.* (1999). A novel function for transglutaminase 1: Attachment of long-chain ω-hydroxyceramides to involucrin by ester bond formation. *Proc Natl Acad Sci* **96**(15): 8402-8407.

Oliver, A., *et al.* (2015). The increasing threat of *Pseudomonas aeruginosa* high-risk clones. *Drug Resist Updat* **21-22**: 41-59.

Olsen, I. (2015). Biofilm-specific antibiotic tolerance and resistance. *Eur J Clin Microbiol Infect Dis* **34**(5): 877-886.

Osmon, S., *et al*. (2004). Hospital mortality for patients with bacteremia due to *Staphylococcus*

aureus or *Pseudomonas aeruginosa*. *Chest* **125**(2): 607-616.

Pagani, I., *et al*. (2012). The Genomes OnLine Database (GOLD) v.4: status of genomic and metagenomic projects and their associated metadata. *Nucleic Acids Res* **40**(Database issue): D571-579.

Park, J.T., and Uehara, T. (2008). How bacteria consume their own exoskeletons (turnover and recycling of cell wall peptidoglycan). *Microbiol Mol Biol Rev* **72**(2): 211-227

Paterson, D.L., and Bonomo, R.A. (2005). Extended-spectrum beta-lactamases: a clinical update. *Clin Microbiol Rev* **18**(4): 657-686.

Peix, A., Ramirez-Bahena M.H., and Velazquez, E. (2009). Historical evolution and current status of the taxonomy of genus *Pseudomonas*. *Infect Genet Evol* **9**(6): 1132-1147.

Pfister, P., *et al.* (1998). Molecular analysis of Methanobacterium phage psiM2. *Mol Microbiol* **30**(2): 233-244.

Poole, K. (2005). Aminoglycoside resistance in *Pseudomonas aeruginosa*. *Antimicrob Agents Chemother* **49**(2): 479-487.
Poole, K. (2011). *Pseudomonas Aeruginosa*: Resistance to the Max. *Front Microbiol* **2**: 65.

Potterton, E., *et al.* (2003). A graphical user interface to the CCP4 program suite. *Acta Crystallogr D Biol Crystallogr* **59**(Pt 7): 1131-1137.

Preston, A., *et al.*(2006). Complete Structures of *Bordetella bronchiseptica* and *Bordetella parapertussis* Lipopolysaccharides. *J Biol Chem* **281**(26): 18135-18144.

Qiu, D., *et al.* (2008). P(BAD)-Based Shuttle Vectors for Functional Analysis of Toxic and Highly Regulated Genes in *Pseudomonas* and *Burkholderia* spp. and Other Bacteria. *Appl Environ Microbiol* **74**(23): 7422-7426.

Quintela, J., *et al*. (1995). Variability of peptidoglycan structural parameters in Gram-negative bacteria. FEMS *Microbiol Letters* **125**(1): 95-100.

Reith, J., and Mayer, C. (2011). Peptidoglycan turnover and recycling in Gram-positive bacteria. *Appl Microbiol Biotechnol* **92**(1): 1-11.

Rice, L.B. (2008). Federal funding for the study of antimicrobial resistance in nosocomial pathogens: no ESKAPE. *J Infect Dis* **197**(8): 1079-1081.

Rosenthal, V.D., *et al.* (2016). International Nosocomial Infection Control Consortium report, data summary of 50 countries for 2010-2015: Device-associated module. *Am J Infect Control* **44**(12): 1495-1504.

Ruiz, N. (2008). Bioinformatics identification of MurJ (MviN) as the peptidoglycan lipid II flippase in *Escherichia coli. Proc Natl Acad Sci U S A* **105**(40): 15553-15557.

Rusmini, R., *et al.* (2014). A shotgun antisense approach to the identification of novel essential genes in *Pseudomonas aeruginosa*. *BMC Microbiol* **14**: 24.

Sadikot, R. T., *et al.* (2005). Pathogen-host interactions in *Pseudomonas aeruginosa* pneumonia. *Am J Respir Crit Care Med* **171**(11): 1209-1223.

Sauvage, E., *et al.* (2008). The penicillin-binding proteins: structure and role in peptidoglycan biosynthesis. *FEMS Microbiol Rev* **32**(2): 234-258.

Schleifer, K.H., and Kandler, O. (1972). Peptidoglycan types of bacterial cell walls and their taxonomic implications. *Bacteriol Rev* **36**(4): 407-477.

Schmitz, F.J., *et al.* (1999). The prevalence of aminoglycoside resistance and corresponding resistance genes in clinical isolates of staphylococci from 19 European hospitals. *J Antimicrob Chemother* **43**(2): 253-259.

Schofield, L.R., *et al.* (2015). Biochemical Characterisation of Phage Pseudomurein Endoisopeptidases PeiW and PeiP Using Synthetic Peptides. *Archaea* **2015**: 12.

Schreiber, K., *et al.* (2007). The anaerobic regulatory network required for *Pseudomonas aeruginosa* nitrate respiration. *J Bacteriol* **189**(11): 4310-4314.

Sham, L.T., *et al.* (2014). Bacterial cell wall. MurJ is the flippase of lipid-linked precursors for peptidoglycan biogenesis. *Science* **345**(6193): 220-222.

Sheldrick, G. (2010). Experimental phasing with SHELXC/D/E: combining chain tracing with density modification. *Acta Crystallogr D* **66**(4): 479-485.

Shi, Q., *et al.* (2008). Investigation of the mechanism of the cell wall DD-carboxypeptidase reaction of penicillin-binding protein 5 of *Escherichia coli* by quantum mechanics/molecular mechanics calculations. *J Am Chem Soc* **130**(29): 9293-9303.

Sigurdsson, G., *et al*. (2012). A systems biology approach to drug targets in *Pseudomonas aeruginosa* biofilm. *PLoS One* **7**(4): e34337.

Silby, M.W., *et al.* (2011). *Pseudomonas* genomes: diverse and adaptable. *FEMS Microbiol Rev* **35**(4): 652-680.

Singh, M.P., *et al.* (1997). Biological activity and mechanistic studies of andrimid. *J Antibiot (Tokyo)* **50**(3): 270-273.

Smart, O.S., *et al.* (2012). Exploiting structure similarity in refinement: automated NCS and target-structure restraints in BUSTER. *Acta Crystallogr D Biol Crystallogr* **68**(Pt 4): 368-380.

Smith, E.E., *et al*. (2006). Genetic adaptation by *Pseudomonas aeruginosa* to the airways of cystic fibrosis patients. *Proc Natl Acad Sci U S A* **103**(22): 8487-8492.

Spiers, A.J., Buckling, A., and Rainey, P.B. (2000). The causes of *Pseudomonas* diversity. *Microbiol* **146 (Pt 10)**: 2345-2350.

Srinivas, N., *et al.* (2010). Peptidomimetic antibiotics target outer-membrane biogenesis in *Pseudomonas aeruginosa*. *Science* **327**(5968): 1010-1013.

Stax, D., *et al*. (1992). The lytic enzyme in bacteriophage ψM1-induced lysates of *Methanobacterium thermoautotrophicum* Marburg. *FEMS Microbiol Lett* **100**(1): 433-438.

Steenbakkers, P.J., *et al*. (2006). Identification of pseudomurein cell wall binding domains. *Mol Microbiol* **62**(6): 1618-1630.

Steiner, R.A., Lebedev, A.A., and Murshudov, G.N. (2003). Fisher's information in maximum-

likelihood macromolecular crystallographic refinement. *Acta Crystallogr D* **59**(12): 2114-2124.

Streeter, K., and Katouli, M. (2016). *Pseudomonas aeruginosa*: A review of their Pathogenesis and Prevalence in Clinical Settings and the Environment. *Infect Epidemiol Microbiol* **2**(1): 25-32.

Strempel, N., *et al.* (2013). Human host defense peptide LL-37 stimulates virulence factor production and adaptive resistance in *Pseudomonas aeruginosa*. *PLoS One* **8**(12): e82240.

Sullivan R, *et al*. (2015). Extended Spectrum Beta- Lactamases: A Minireview of Clinical Relevant Groups. *J Med Microb Diagn* **4**: 203.

Sun, J., Deng, Z., and Yan, A. (2014). Bacterial multidrug efflux pumps: mechanisms, physiology and pharmacological exploitations. *Biochem Biophys Res Commun* **453**(2): 254-267.

Sun, S., *et al.* (2016). Quorum sensing systems differentially regulate the production of phenazine-1-carboxylic acid in the rhizobacterium *Pseudomonas aeruginosa* PA1201. *Sci Rep* **6**: 30352.

System, R. f. N. (2004). National Nosocomial Infections Surveillance (NNIS) System Report, data summary from January 1992 through June 2004, issued October 2004. *Am J Infect Control* **32**(8): 470-485.

Tamber, S., and Hancock, R.E. (2003). On the mechanism of solute uptake in *Pseudomonas*. *Front Biosci* **8**: s472-483.

Taylor, G.L. (2010). Introduction to phasing. *Acta Crystallogr D Biol Crystallogr* **66**(Pt 4): 325-338.

Toleman, M.A., and Walsh, T.R. (2011). Combinatorial events of insertion sequences and ICE in Gram-negative bacteria. *FEMS Microbiol Rev* **35**(5): 912-935.

Tomaras, A.P., *et al.* (2014). LpxC Inhibitors as New Antibacterial Agents and Tools for Studying Regulation of Lipid A Biosynthesis in Gram-Negative Pathogens. *mBio* **5**(5).

Tomasic, T., and Masic, L.P. (2014). Prospects for developing new antibacterials targeting bacterial type IIA topoisomerases. *Curr Top Med Chem* **14**(1): 130-151.

Tomasz, A. (1979). The mechanism of the irreversible antimicrobial effects of penicillins: how the beta-lactam antibiotics kill and lyse bacteria. *Annu Rev Microbiol* **33**: 113-137.

Trubiano, J.A., and Padiglione, A.A. (2015). Nosocomial infections in the intensive care unit. *Anaesth Intensive Care Med* **16**(12): 598-602.

Turner, K.H., *et al.* (2015). Essential genome of *Pseudomonas aeruginosa* in cystic fibrosis sputum. *Proc Natl Acad Sci* **112**(13): 4110-4115.

Typas, A., *et al*. (2011). From the regulation of peptidoglycan synthesis to bacterial growth and morphology. *Nat Rev Microbiol* **10**(2): 123-136.

Umadevi, S., *et al.* (2011). Detection of extended spectrum beta lactamases, Ampc beta lactamases and metallobetalactamases in clinical isolates of ceftazidime resistant *Pseudomonas aeruginosa*. *Braz J Microbiol* **42**(4): 1284-1288.

Vasil, M.L. (2003). DNA microarrays in analysis of quorum sensing: strengths and limitations. *J Bacteriol* **185**(7): 2061-2065.

Vecchietti, D., *et al.* (2012). Analysis of *Pseudomonas aeruginosa* cell envelope proteome by capture of surface-exposed proteins on activated magnetic nanoparticles. *PLoS One* **7**(11): e51062.

Vecchietti, D., *et al*. (2016). Crystal structure of YeaZ from *Pseudomonas aeruginosa*. *Biochem Biophys Res Commun* **470**(2): 460-465.

Venter, H., *et al.* (2015). RND-type drug e ffl ux pumps from Gram-negative bacteria: molecular mechanism and inhibition. *Front Microbiol* **6**: 377.

Venturi, V. (2006). Regulation of quorum sensing in *Pseudomonas*. *FEMS Microbiol Rev* **30**(2): 274-291.

Visweswaran, G.R., Dijkstra, B.W., and Kok, J. (2010). Two Major Archaeal Pseudomurein Endoisopeptidases: PeiW and PeiP. *Archaea* **2010**.

Visweswaran, G.R., Dijkstra, B.W., and Kok, J. (2011). A minimum of three motifs is essential for optimal binding of pseudomurein cell wall-binding domain of *Methanothermobacter thermautotrophicus*. *PLoS One* **6**(6): e21582.

Vollmer, W., Blanot, D., and de Pedro, M.A. (2008a). Peptidoglycan structure and architecture. *FEMS Microbiol Rev* **32**(2): 149-167.

Vollmer, W., and Bertsche, U. (2008b). Murein (peptidoglycan) structure, architecture and biosynthesis in *Escherichia coli*. *Biochim Biophys Acta* **1778**(9): 1714-1734.

Vollmer, W., *et al.* (2008c). Bacterial peptidoglycan (murein) hydrolases. *FEMS Microbiol Rev* **32**(2): 259-286.

Vollmer, W., and Seligman, S.J. (2010). Architecture of peptidoglycan: more data and more models. *Trends Microbiol* **18**(2): 59-66.

Walsh, C.T., and Wencewicz, T.A. (2014). Prospects for new antibiotics: a molecule-centered perspective. *J Antibiot (Tokyo)* **67**(1): 7-22.

Weidel, W., and Pelzer, H. (1964). Bagshaped macromolecules--A new outlook on bacterial cell wall. *Adv Enzymol Relat Subj Biochem* **26**: 193-232.

Werneburg, M., *et al.* (2012). Inhibition of lipopolysaccharide transport to the outer membrane in *Pseudomonas aeruginosa* by peptidomimetic antibiotics. *Chembiochem* **13**(12): 1767-1775.

Wertheim, H., *et al.* (2013). Global survey of polymyxin use: A call for international guidelines. *J Glob Antimicrob Resist* **1**(3): 131-134.

WHO (2014). Antimicrobial resistance: global report on surveillance 2014. 257.

WHO (2017). Global priority list of antibiotic-resistant bacteria to guide research, discovery, and development of new antibiotics. 7.

Williams, B.J., Dehnbostel, J., and Blackwell, T.S. (2010). *Pseudomonas aeruginosa*: host defence in lung diseases. *Respirology* **15**(7): 1037-1056.

Williams, P., and Camara, M. (2009). Quorum sensing and environmental adaptation in

Pseudomonas aeruginosa: a tale of regulatory networks and multifunctional signal molecules. *Curr Opin Microbiol* **12**(2): 182-191.

Wilson, D.N. (2013). Ribosome-targeting antibiotics and mechanisms of bacterial resistance. *Nat Rev Microbiol* **12**: 35.

Winstanley, C., O'Brien, S., and Brockhurst, M.A. (2016). *Pseudomonas aeruginosa* Evolutionary Adaptation and Diversification in Cystic Fibrosis Chronic Lung Infections. *Trends Microbiol* **24**(5): 327-337.

Wong, A., Rodrigue, N., and Kassen, R. (2012). Genomics of adaptation during experimental evolution of the opportunistic pathogen *Pseudomonas aeruginosa*. *PLoS Genet* **8**(9): e1002928.

Wong, J.E.M.M., *et al*. (2013). Cooperative binding of LysM domains determines te carbohydrate affinity of bacterial endopeptidase protein. *FEBS J* **281**(4):1196-1208

Wu, T., *et al.* (2005). Identification of a multicomponent complex required for outer membrane biogenesis in *Escherichia coli*. *Cell* **121**(2): 235-245.

Xiong, Y.Q., *et al.* (1996). Influence of pH on adaptive resistance of *Pseudomonas aeruginosa* to aminoglycosides and their postantibiotic effects. *Antimicrob Agents Chemother* **40**(1): 35-39.

Xu, P., *et al*. (2011). Genome-wide essential gene identification in *Streptococcus sanguinis*. *Sci Rep* **1**.

Xu, Q., *et al.* (2009). Structural basis of murein peptide specificity of a gamma-D-glutamyl-l-diamino acid endopeptidase. *Structure* **17**(2): 303-313.

Zhang, L., Li, X.Z., and Poole, K. (2001). Fluoroquinolone susceptibilities of efflux-mediated multidrug-resistant *Pseudomonas aeruginosa*, *Stenotrophomonas maltophilia* and *Burkholderia cepacia*. *J Antimicrob Chemother* **48**(4): 549-552.

Zhang, W., *et al.* (2007). Catalytic mechanism of penicillin-binding protein 5 of *Escherichia coli. Biochem* **46**(35): 10113-10121.

PART II

Manuscript in preparation

Crystal structure of the periplasmic domain of TgpA from *Pseudomonas aeuruginosa*: structural bases for enzyme activity.

Mónica Uruburu, Eloise Mastrangelo, Martino Bolognesi, Giovanni Bertoni, Mario Milani.

Crystal structure of the periplasmic domain of TgpA from *Pseudomonas aeruginosa*: structural bases for enzyme activity

Mónica Uruburu[1,†], Eloise Mastrangelo[1,2,†], Martino Bolognesi[1], Giovanni Bertoni[1,#], Mario Milani[1,2,*]

[1]*Dipartimento di Bioscienze, Università di Milano, Via Celoria 26, I-20133, Milano, Italy*

[2] *CNR-IBF, Istituto di Biofisica, Via Celoria 26, I-20133, Milano, Italy*

[†]*These authors have contributed equally to the studies presented*

*Address correspondence to:
Dr. Mario Milani,
CNR, Istituto di Biofisica,
Via Celoria 26, I-20133, Milano, Italy.
Tel. (+39) 0250314767
Fax. (+39) 0250314895
e-mail: mario.milani@unimi.it

[#]Address correspondence to:
Prof Giovanni Bertoni,
Dipartimento di Bioscienze, Università di Milano
Via Celoria 26, I-20133, Milano, Italy
Tel. (+39) 0250315027
Fax. (+39) 0250315044
e-mail: giovanni.bertoni@unimi.it

ABSTRACT

Pseudomonas aeruginosa is an opportunistic pathogen associated with severe diseases, such as like cystic fibrosis. During an extensive search for novel essential genes, we identified the gene *tgpA* (*locus* PA2873) in *P. aeruginosa* PAO1, which plays a critical role in the bacterial viability. TgpA is an internal membrane protein with a periplasmic soluble domain predicted to be endowed with a transglutaminase-like fold with a Cys, His, and Asp 'catalytic triad'. We present here that the Cys residue in such triad is required for the essential function of TgpA relative to *P. aeruginosa* viability.and the crystal structure of the TgpA soluble domain as a first step towards structure-activity analysis of a new target for the discovery of novel antibacterial compounds.

1. Introduction

Infections caused by resistant gram-negative bacteria are becoming increasingly prevalent, and a serious threat to public health worldwide, being associated with high morbidity and mortality rates. Colonization with resistant gram-negative bacteria is common among residents in long-term care facilities, particularly for patients with an indwelling device, causing serious concern in hospitals.

Pseudomonas aeruginosa is a gram-negative opportunistic pathogen responsible for many diseases such as chronic lung colonization in cystic fibrosis patients and acute infections in hospitals (Driscoll et al., 2007). *P. aeruginosa* infections are always difficult to treat due to the natural resistance of this

bacterium (Obritsch et al., 2005), consequently a therapy based on two or three antimicrobial agents is typically adopted (Lodise et al., 2007) (Szaff et al., 1983) (Valerius et al., 1991). Unraveling novel essential genes or pathways that have not yet been targeted by clinical antibiotics can foster the development of new effective antibacterials to overcome resistance. We recently discovered an essential gene for *P. aeruginosa* viability coding for the protein TgpA (Milani et al., 2012). TgpA is a medium size inner membrane protein (668 amino acids) composed of five transmembrane helices, a periplasmic domain (residues 180-544) followed by an additional transmembrane helix, and a small cytoplasmic domain (residues 561-668). The periplasmic portion of TgpA was predicted to host an eukaryotic-like transglutaminase domain (TG-like domain) (Makarova et al., 1999) of unknown function, characterized by the presence of a Cys, His, and Asp 'catalytic triad' .

In this work, we demonstrate that the Cys residue in such triad is required for the essential function of TgpA relative to *P. aeruginosa* viability.

Furthermore, we present here the crystal structure of the TgpA periplasmic domain, solved using SAD methods after soaking the crystal with a mercury compound. The periplasmic domain is composed of two sub-domains, one hosting the catalytic triad of the predicted TG-like domain, and the other structurally linked to different carbohydrate binding domains that may play a role in substrate recognition.

2. Materials and Methods

2.1 Construction of plasmids expressing His-tagged TgpA wt and the mutant C404A in the full-length protein

A plasmid expressing a His-tagged full length TgpA was prepared by amplifying the *tgpA* gene (*locus* PA2873) from *P. aeruginosa* PAO1 genomic DNA with primers 5'-TATCATGAACGCGATTCCGCGGGTC-3' and 5'-AGAAGCTTGTAAAGCTTTCAGTGGTGGTGGTGGTGGTGTGCCTGCTCCTCTC-3'. Amplicons were digested with *Bsp*HI and *Hind*III restriction enzymes and cloned into the broad host range vector pHERD28T (Qiu et al, 2008), digested with *Nco*I and *Hind*III, under the arabinose inducible promoter P_{BAD}, giving rise to the plasmid pHERD28T-TgpA.

The QuikChange II XL Kit (Stratagene) was used to generate the mutant Cys404Ala, using as a template the construct pHERD28T-TgpA, with the complementary primers carrying the mutated codon 5'-GCGCAGCGGCTTCGCCGCGCATTACGCC-3' and 5'-GGCGTAATGCGCGGCGAAGCCGCTGCGC-3'.

For overexpression, the constructs pHERD28T-TgpA-His and pHERD28T-C404A-His were moved from *E. coli* JM109 to PAO1 strain by triparental mating as described previously (Milani et al., 2012). PAO1 cells carrying pHERD28T-TgpA-His, pHERD28T-TgpA-C404A-His, or the pHERD28T empty vector were grown for 20 hrs in micro-cultures of 200 µl with increasing arabinose concentrations (0, 0.025, 0.05, 0.1 and 0.2%), for the induction of the P_{BAD}

promoter. Growth cultures were monitored in real-time by absorbance measurement at 600 nm (OD_{600}).

Western-Blot analysis

Overnight cultures of PAO1/pHERD28T-TgpA-His, PAO1/pHERD28T-C404A-His and PAO1/pHERD28T in LB media supplemented with 300 µg/ml trimethoprim (Tmp) were diluted to OD_{600} of 0.05, incubated at 37°C until OD_{600} of 0.4-0.6 and induced with 0.1% arabinose. A parallel culture of each strain was grown without the addition of arabinose. After two hours induction, the cells were harvested at 7000 rpm for 10 min at 4°C and the pellet from 100 ml of culture was resuspended in 1 ml of lysis buffer (10 mM Tris-HCl pH 7.8, 20 µg/ml RNAse and DNAse, 1 mM PMSF, 0.2 mg/ml lysozyme) and passed through a French press for cell disruption. The lysate was centrifuged at 5000 rpm for 20 min at 4°C and supernatant was ultracentrifuged at 37,000 rpm for 1 h at 4°C. The pellet, corresponding to the total membrane fraction, was resuspended in 200 µl of Tris-HCl pH 7.8. Ten microliters of the samples with no arabinose and of the samples induced with 0.1% arabinose diluted 1:10 were analysed on SDS-PAGE. For Western blot analysis, specific monoclonal anti-His antibodies (Roche®) in 0.05% PBS-T were used.

Quantitative RT-PCR analysis

Total RNA was purified with a Total RNA Extraction kit (RBC Bioscience). cDNA was generated by incubating 1 µg of RNA with Superscript II Reverse

Transcriptase (RT) (Invitrogen), 100 pg of random primers and buffer supplied by the manufacturer for 50 min at 42°C. RT was inactivated by incubation at 70°C for 15 min. As a control of DNA contamination in the subsequent quantitative RT-PCR (qRT-PCR) analysis, reactions were also run without RT. qRT-PCR amplifications were performed in duplicate reactions of 15 µl in tubes filled with iQ^{TM} SYBR Green Supermix (Bio-Rad) and 300 nM of each primer (see below) and run in an iCycler Real-Time PCR machine (Bio-Rad) as follows: 1 cycle at 95°C for 10 min, 50 cycles at 95°C for 15 s and 60°C for 40 s. The calculation of the relative expression of the *tgpA* gene from plasmid pHERD28T versus the empty vector was performed as described by the $2^{-\Delta\Delta CT}$ method (Livak and Schmittgen, 2001), normalizing first mRNA amounts to 16S ribosome RNA (Δ*C*T) and relating the Δ*C*T in the TgpA wt and C404A mutant ectopically expressed to the chromosomal copy (ΔΔ*C*T) (PAO1-pHERD28T Empty vector). To confirm PCR specificity, the PCR products were subjected to melting curve analysis in a temperature range spanning 55-95°C with 1 cycle at 55°C for 50 s and 80 cycles at 55°C for 10 s set with 0.5°C increments after the first cycle.

The primer pairs used for qRT-PCR were:

tgpA 5'-CGAAAGCGCTCTGCTGCAA-3'/ 5'-TCTTCGCAGTGGTGGTGGG-3'

16S 5'-TGTCGTCAGCTCGTGTCGTGA-3'/ 5'-ATCCCCACCTTCCTCCGGT-3'

2.2 Complementation assay

TgpA wild type (wt) and mutant C404A were tested for their ability to complement a glucose-mediated down-regulation of the chromosomal *tgpA* gene

in the PAO1 *P_{rhaB}::tgpA* strain (Milani et al., 2012), when expressed from the ectopic vectors pHERD28T-TgpA or pHERD28T-TgpA-C404A. For the complementation assays, pHERD28T-TgpA and pHERD28T-TgpA-C404A were moved from *E. coli* JM109 to the conditional mutant PAO1 *P_{rhaB}::tgpA* strain by triparental mating as described previously (Milani et al., 2012). Exconjugants *P_{rhaB}::tgpA* clones were selected on M9 minimal medium plates supplemented with 0.2% citrate (M9-citrate), 60 µg/ml gentamicin (Gm), 0.2% rhamnose and 300 µg/ml Tmp. This procedure generated the strains PAO1 *P_{rhaB}::tgpA*/pHERD28T-TgpA and PAO1 *P_{rhaB}::tgpA*/pHERD28T-TgpA-C404.

For both *PrhaB::tgpA*/pHERD28T-TgpA and PAO1 *PrhaB::tgpA*/pHERD28T-TgpA-C404, the conditional growth was assessed after an overnight growth at 37°C in M9-citrate supplemented with 60 µg/ml Gm, 300 µg/ml Tmp and 0.2% rhamnose. An aliquot of the overnight culture was centrifuged and the bacterial pellet was washed three times with sterile PBS, and diluted to an OD_{600} of 10^{-6} in fresh M9-citrate with appropriated antibiotics (60 µg/ml Gm and 300 µg/ml Tmp) and supplemented either with 0.2% rhamnose or 1% glucose. 200 µl of the different cultures were grown at 37°C with stirring and monitored in real time by OD_{600} measurement in microtiter reader (TECAN) for 20 hrs.

2.3 Expression and purification of TgpA periplasmic domain.

TgpA periplasmic domain (residues 180-544) was expressed in *E. coli* BL21CodonPlus (DE3) - RIPL (Agilent; chloramphenicol (Cm) resistance) as N-terminally (His)10-tagged proteins, from plasmid p2N (PRIMM srl.; ampicillin (Amp) resistance). The cells were grown at 37°C in 2 l of LB medium containing 100 µg/ml Amp and 34 µg/ml Cm, to an OD_{600} of 0.6. After induction with 1 mM isopropyl β-D-thiogalactopyranoside (IPTG), the incubation temperature was lowered to 17°C and cells were grown for 16 hours. Cells, harvested by centrifugation, were resuspended in lysis buffer (1x Phosphate buffer saline (PBS), 1% Triton, 5 mM $MgCl_2$, 0.25 mg/ml lysozyme, 20 µg/ml DNase, 1µg/ml Pepstatin A, 0.5 mM AEBSF and 1 tablet of complete Protease Inhibitor (Roche®)), lysed with a cell disruptor at 27 KPSI, and the soluble fraction was collected after centrifugation at 15,000 rpm for 1 h at 4°C (Beckman JA20).

The protein purification was performed at 4°C, using a Fast Protein Liquid Chromatography (FPLC) apparatus (ÄKTA system – GE Healthcare). After Ni-IMAC column (HisTrapTM FF crude 5 ml, GE Healthcare) equilibration with Buffer A (20 mM Phosphate buffer pH 7.5, 500 mM NaCl, 0.5 mM AEBSF and 1 tablet of complete Protease Inhibitor Roche®), the soluble cell extract was loaded at 1 ml/min and eluted at 250 mM imidazole. The protein was then loaded (1 ml/min flow-rate) on a SuperdexTM 75 column (GE Healthcare), previously equilibrated with Gel Filtration (GF) Buffer (20 mM Tris-HCl pH 7.5, 500 mM NaCl, 20 mM Imidazole, 0.5 mM AEBSF and 1 tablet of complete Protease Inhibitor Roche®).

The purified protein was concentrated up to 8 mg/ml using a centrifugal filter unit (10 kDa cut-off, Millipore).

2.4 Crystal structure TgpA periplasmic domain.

Microbatch crystallization experiments on TgpA periplasmic domain (6 mg/ml) were assembled with an Oryx-8 crystallization robot (Douglas Instruments, East Garston, UK), with 0.3 µl droplets containing 66/34% of the protein/precipitant solutions, covered with Al's oil. Crystals were obtained after 48 hours at 20°C, in 0.8 M NaH_2PO_4, 0.8 M KH_2PO_4, and 0.1 M Na HEPES pH 7.5. Before collecting crystals for flash freezing in liquid nitrogen, about 0.1 µl glycerol was added to the crystal drop as cryoprotectant. The TgpA native crystals diffracted to a maximum resolution of 1.6 Å using synchrotron radiation at beam-line ID30a3 at the European Synchrotron Radiation Facility (ESRF-Grenoble, France). Additional crystals ($(NH_4)H_2PO_4$ 0.7 M, 0.1 M Na HEPES pH 7.2) were selected for soaking with mercury derivatives. The crystals were soaked in a stabilizing solution ($(NH_4)H_2PO_4$ 0.7 M, 0.1 M Na HEPES pH 7.6) with 5 mM ethylmercurithiosalicylic acid sodium salt for 60 min, then washed (in stabilizing solution) and transferred into a cryoprotectant solution ($(NH_4)H_2PO_4$ 0.7 M, 0.1 M Na HEPES pH 7.6, glycerol 25%) and flash frozen. TgpA derivative crystal showed a nice absorption peak for mercury at 12.3 keV (1.008 Å) and diffracted to a maximum resolution of 1.8 Å at beam-line BM14U (ESRF-Grenoble, France). For both native and derivative crystals, X-ray diffraction data were indexed and scaled using XDS (Kabsch, 2010) (Table 1).

The three-dimensional structure of TgpA was solved using the SAD method based on the mercury derivative (X-ray wavelength 1.00775 Å) using the program package SHELXC/D/E (Sheldrick, 2010) within the CCP4i interface (Potterton et al., 2003). Briefly, SHELXC detected an anomalous signal up to ~1.9 Å; SHELXD (at 2 Å resolution) found 6 possible heavy atoms sites (CC All/Weak 42.8/25.1, CFOM 67.9, best 67.9, PATFOM 16.28), and SHELXE calculated the initial phases and performed density modification (FOM=0.582, Pseudo-free CC=63.71%). The obtained experimental electron density was then used to trace an initial protein model with ARP/WARP (Lamzin and Wilson, 1997). The single TgpA molecule present in the crystal asymmetric unit was then subjected to manual (program COOT (Emsley et al., 2010)) and constrained refinements using REFMAC5 (Steiner et al., 2003), and the partially refined model was used for molecular replacement to solve the structure of the native dataset (Vagin and Teplyakov, 1997). Additional refinements with BUSTER (Smart et al., 2012) and REFMAC5 were subsequently performed for both datasets. Data collection, refinement statistics as well as stereochemical quality of the two models are summarized in Table 1. Atomic coordinates and structure factors have been deposited in the PDB (Berman et al., 2000), with accession codes **...**.

2.5 Cell wall peptidoglycans isolation

A published method (Desmarais et al., 2014) with minimum modifications was followed for the isolation of cell wall peptidoglycans (PGN) from *P. aeruginosa*. Cells were harvested from an exponential phase culture (OD_{600} of 0.8) by

centrifugation, washed two times with phosphate-buffered saline (PBS). The final pellet was resuspended in 3 ml of PBS, slowly added to boiling 6% SDS solution and boiled for 2 h; the mixture was then stirred overnight at room temperature. Cell walls were recovered by ultra-centrifugation at 400.000 x g, washed six times with ultrapure water at room temperature and then digested with 100 µg/ml of Pronase E (Sigma - Aldrich) for 2 h at 60°C. The reaction was stopped with the addition of 200 µl of 6% SDS and incubation for 30 min at 100°C. Additional washes by ultra-centrifugation at 400.000 x g were performed until the excess of SDS was removed. The final cell walls were resuspended in 50 mM MOPS, pH 7.0 and stored at -20°C.

2.6 Insoluble peptidoglycan pulldown assay

For PGN binding assay, we slightly modified a procedure already described (Wong et al., 2014). In a 50 µl reaction mixture, 50 µg of purified TG domain was added to increasing amounts of PGN (25, 50, 100, 200 and 400 µg) in the assay buffer: 50 mM Tris-HCl, pH 8, 1 M NaCl, 5 mM β-mercaptoethanol, 1% tween-20. The reaction was incubated for 30 min at 25°C, and then centrifuged at 10,500 *g* for 45 min. The supernatant was collected, and the insoluble PGN pellet was washed three times in assay buffer. Ten microliters of supernatant and resuspended pellet solution were analysed on a 10% SDS-PAGE gel. As a reaction control, three different proteins (BSA, DNAse (Sigma) and helicase from dengue virus) were used in reaction with the PGN at the same conditions as TG domain. A negative control was performed with 50 µg of each protein under the

same conditions but without PGN, to ensure that the proteins were not precipitating on their own.

2.7 Cell wall binding affinity - Microscale thermophoresis

To evaluate the binding ability of the TG domain to cell wall components, we used PGN isolated from both *Bacillus subtilis* (Sigma – Aldrich) and *P. aeruginosa*.

Protein interactions with PGN were measured through Microscale thermophoresis (MST). The soluble fraction of the sacculi from *P. aeruginosa* and *B. subtilis* was separated from the insoluble portion by ultracentrifugation (15000*g*). With the dry weight of the insoluble fraction of the PGN it was possible to stablish that the 50% of the mixture remains soluble (5mg/ml). Serial dilutions of the soluble fraction were prepared to set a standard curve with the absorbance at 280nm (A 280nm) of each dilution. The curve was used to stimate a concentration of the soluble fraction of the isolated PGN from *P. aeruginosa*.

With the hypothesis that the interaction between TG domain and the PGN was due to the glycans (N-Acetylglucosamine [GlcNac] and N-acetylmuramic acid [MurNAc]) present in each molecule of the muropeptide, we used the molecular weight of the disaccharide GlcNac - MurNAc (496.466g/mol) to calculate a hypothetical dissociation constant (K_d).

The TG domain and the helicase from dengue virus were labelled with the monolith NT^{TM} Protein labelling Kit RED-NHS (NanoTemper technologies, Munich, Germany) to achieve a 1:1 molar ratio of labelled protein to dye. The concentration of labelled TG domain and helicase were constant at 75 nM, in thermophoresis MST buffer (50 mM Tris-HCL pH 7.4, 150 mM NaCl, 10 mM $MgCl_2$, 0.05% Tween-20). Serial dilutions of the PGN were prepared in MST buffeer: PGN from *P. aeruginosa* varied from 0.125 mM to ~7.6 nm, and higher concentration of *B. subtilis* were used to define better the curve, from 5 mM to ~150 nM. MST measurements were performed at 24°C on a Monolith NT.115 instrument (NanoTemper Technologies) using Premium coated capillary. Binding curves were obtained from the thermophoresis, with MST power 60%.

3. Results

3.1 Cys404 in the periplasmic TG-like domain is critical for TgpA cell activity

TgpA is endowed with a periplasmic region harboring a structural domain predicted to belong to the transglutaminase-like superfamily (TG-like domain), a group of archaeal, bacterial and eukaryotic proteins homologous to animal transglutaminases (Makarova et al., 1999). The TG-like domain is characterized by the presence of a conserved catalytic triad Cys404-His448-Asp464. To assess whether the TgpA essential function (Milani et al., 2012) for *P. aeruginosa* viability resided in the TG-like domain, we generated a substitution of residue Cys404 with Ala (C404A mutant) in the full length protein, and evaluated the ability of such mutant to complement an induced down-regulation of the chromosomal *tgpA* gene in the *P. aeruginosa* conditional mutant PAO1 P_{rhaB}*::tgpA* (Milani et al., 2012).

Frist of all, we evaluated the ectopic expression also in the absence of inducer arabinose using Western blot analysis (Fig. 1) and Real time PCR (Table 1). Cell cultures without / with arabinose (0.1%) were grown and the membrane fractions were used for the analysis. With a specific monoclonal anti-His antibody, a unique band around 70 kDa corresponding to TgpA-His (wt and mutant C404A) was detected (absence of the band in the empty vector) (Fig. 1). The presence of the band also in the absence of the arabinose inducer, both in the wt and the mutant C404A, provided evidence of the basal activity of the P_{BAD} promoter.

Quantification of mRNA levels of the ectopically expressed TgpA wt and C404A mutant genes, relative to the chromosomal copy, was determined by quantitative Real-Time PCR on total RNA, isolated from the growth in the absence and presence of 0.1% arabinose (Table 2). A level of basal activity of the P_{BAD} promoter was confirmed by this analysis.

We then evaluated whether ectopic expression of TgpA wt or C404A mutant could *per se* influence the growth of *P. aeruginosa* (PAO1 strain) under five concentrations of arabinose (0, 0.025, 0.05, 0.1 and 0.2%). As shown in Fig. 2, the ectopic expression of TgpA wt and C404A mutant resulted in an arabinose dose-dependent negative influence on *P. aeruginosa* growth. The negative effects, evident also in the absence of arabinose (Fig. 2), can be explained with the basal activity of the P_{BAD} promoter.

The two vectors pHERD28T-TgpA or pHERD28T-TgpA-C404A were then transferred to a conditional mutant carrying a chromosomal *tgpA* gene under the control of the P_{rhaB} promoter (Milani et al., 2012). This strain is usually maintained in the presence of rhamnose (0.2%) that induce the expression of *tgpA*. However, the P_{rhaB} promoter can be strongly down regulated by glucose addition in the medium. Consequently, PAO1 P_{rhaB}*::tgpA* is unable to grow in the presence of glucose unless functional TgpA is ectopically expressed (Milani et al., 2012).

As shown in Fig. 3A, TgpA wt expressed by the basal activity of the P_{BAD} promoter (Ara 0%) is already able to complement the forced repression of the *PrhaB* promoter by 1% glucose. In fact, PAO1 P_{rhaB}::*tgpA* is able to grow with 1% glucose as well as in the permissive condition of 0.2% rhamnose. Differently from TgpA wt, the basal expression of the C404A mutant (Ara 0%) does not complement the forced repression of wt protein (Fig. 3B). Together, these results show that Cys404 is critical for the essential function of TgpA.

3.2 Crystal structure of the periplasmic domain of TgpA.

During the expression and purification, the recombinant TgpA periplasmic domain was susceptible to proteolytic cleavage, evident by the presence of two bands around 40kDa. Such feature suggests a disordered nature of this part of the sequence. Mass analysis confirmed the loss of more than 20 amino acids at the C-ter end; although it was not possible to identify a precise site of cleavage, the produced peptides indicated different cleavage sites around Tyr499 (Fig S1 in the supplementary information).

The experimental electron density allowed to model the protein periplasmic domain between residues Val195 and Leu482, that is ~17 amino acids upstream the cleavage region. The domain is folded in a tripartite globular structure (with average dimensions 50x45x30 $Å^3$) resembling a heart built by two sub-domains (*right and left ventricles*) linked by a central antiparallel beta sheet composed of four strands (*the septum*). The *right ventricle* (mostly formed by the N-terminal

portion of the domain) is primarily composed of β strands, with a major solvent exposed antiparallel β sheet (composed of 6 strands). On the contrary, the *left ventricle* that, together with the *septum* contains the conserved catalytic triad, is mainly composed of alpha helices (Fig. 4). Interestingly, N-and C-terminal ends of the domain are located on the same side of the protein, in agreement with its internal membrane anchoring.

A structure based homology search, over the whole domain and through the DALI server (Holm and Rosenstrom, 2010), identified two putative cysteine proteases (pdb-id 3ISR, Z=9.8 id. 18%; and pdb-id 3KD4, Z=8.7 id. 17%) from gram-negative bacteria, and the transglutaminase coagulation factor XIII (pdb-id 3KD4, Z=6.4 id. 22%). A new search for similar folds using the CATH server (http://www.cathdb.info) (Sillitoe et al., 2015) identified the pantoate-beta-alanine ligase functional family (Pantothenate synthetase 2, CATH-ID 3.30.1300) for the C-terminal domain, and the immunoglobulin-like domain or Cellulose-binding family II for the N-terminal extension, respectively.

Limiting the structural search to the N-terminal portion of the domain (residues Val195 to Ala323) yielded structural similarity to different carbohydrate binding domains, such as the chitin binding domain (chitinase, pdb-id 5DHE, Z=2.8, 13% identity (Hanazono et al., 2016)) and the xylan binding domain (xylanase, pdb-id 1XBD, Z=2.7, 7% identity), pointing to a possible involvement in binding to the cell wall peptidoglycan. In particular, the chitinase domains

(ChBD2 and ChBD3) belong to the carbohydrate binding domain family-II type (IPR001919, CBM2). CBM2 is further classified into two subfamilies according to substrate specificities: CBM2a that binds cellulose, and CBM2b interacting specifically with xylan. Like other CBM domains CBM2 is a beta-sheet domain containing a planar surface able to bind its ligand(s) via a hydrophobic strip of aromatic residues.

A DALI structural search based on residues corresponding to *right ventricle* yielded again a protein involved in sugar binding (GH52 Beta-D-xylosidase; pdb-id 4RHH, Z=3.4, 7% identity) that hydrolyses Beta-D-xylans. Conversely, searching for structural homologs of the C-ter portion of the protein with CATH (http://www.cathdb.info) we found (in addition to Pantoate--beta-alanine Ligase) 3.30.460.10 Beta Polymerase, domain 2 and v-type ATP synthase like domains.

Active site

Cys404 has been shown above to be critical for the essential activity of TgpA in *P. aeruginosa* growth. Cys404 is hosted in the C-terminal portion of the periplasmic domain, forming a typical catalytic triad with His448 and Asp464. While His and Asp side chain positions are restrained by a mutual H-bond (2.8 Å), the Cys side chain is not involved in any electrostatic interactions with other residues or water molecules (shorter distance 3.4 Å with main chain nitrogen of Ala449). The environment around Cys404 is characterized by the presence of

several aromatic and polar residues, *e.g.* Tyr380, Phe403, Arg473, and Thr466. Around His448 a network of H-bonds is found involving (besides Asp464) residues Thr466, Arg473 and Tyr380 bridged by two water molecules and linked to the main chains of residues Phe445 and Ala447.

The active Cys404 is buried inside the protein domain (at about 10 Å from the surface) but it may become accessible when the right substrate is present or in the full length protein. Such feature is supported by analysis of the Hg derivative structure, where, in order to accommodate the ethyl-mercury moiety linked to Cys404, Phe403 side chain rotates by ~135° around its χ1 angle, widening the active site cavity. Moreover, in the heavy atom bound structure the C-ter end of the protein (478-480) displays a conformational change (starting from Gly477), and becomes more mobile (first defined amino acid in the electron density is Leu478 *vs.* Ala483 in the native structure), yielding a wider entrance path to the active site. Interestingly, together with the ethyl-mercury sustituent, a phosphate ion is present within the active site cavity, H-bonded to His268 and Tyr200, with electroststic compensation by Hg and Arg473.

A different smaller cavity (N-terminal helix amino acids 205-212) is present in the native structure, where a phosphate ion (3.9 Å from the Sulphur of Cys404) is H-bonded to the main chain N-atoms of Gly205, Ile207, Ala208 and Ala405, and to the side chain of His406. The native and the heavy atom bound structures

together allow to propose a gating mechanism regulating substrate accessibility to the active site that would involve: 1. C-terminal helix. 2. N-ter helix, 3. Phe403 (Fig. 5).

Analysis of the overall geometry of the active site residues using the LabelHash server (Moll et al., 2011) identified structural homology with the active site of a Cys endopeptidase acting on muropeptides (Xu et al., 2009). Therefore, all the structure-based analyses point to a protein involvement in muropeptide binding and cell wall remodelling.

3.3. TgpA Binding to Peptidoglycan

Structural analysis restricted to the N-terminal portion of the protein (from Val195 to Ala323) displays some homology with two carbohydrate binding domains (ChBD), like chitin binding domain, fitting with the families ChBD2 and ChBD3, that bind chitin and cellulose.

Cellulose, chitin and peptidoglycan (PGN) are major polymers in living organisms, consisting of a long chain of carbohydrates linked with β-1,4 glycosidic bonds. Principles and regulatory mechanism of the enzymes involved in metabolism of these polymers are still unknown; however, there is growing available structural and biochemical information on how synthesis, chemical modifications and hydrolysis processes may occur.

In bacteria, there are well-characterized domains that bind cell wall components, tightly related with enzymes that participate in the peptidoglycan degradation and remodelling.

Since the major component of the bacterial cell wall is a complex polymer formed by glycan chain cross-linked by peptide stems, we investigated the hypothesis that the TgpA TG domain might be able to bind to PGN. To this end, we performed PGN pulldown assays; proteins binding the insoluble PGN would coprecipitate with them in the pellet after centrifugation. SDS-PAGE was used to analyse the amount of PGN bound proteins.

Pulldown experiments (Fig. 7) shows that in the presence of increasing concentrations of PGN, the amount of TG domain present in the pellet increased, in keeping with the TG capability to bind the PGN from *P. aeruginosa*. On the contrary, the helicase from Dengue virus, used as a negative control, showed no detectable PGN binding. Similar negative results were obtained with both BSA or DNase (data not shown).

3.4 . MST measurements

To further analyse the binding affinity between TG domain and PGN, we assessed the specificity of the interaction through Microscale thermophoresis - MST. For this purpose, we compared the binding capacity of the TG domain towards the sacculi from both *B. subtilis* and *P. aeruginosa*. Negative controls

were performed with helicase from Dengue Virus under the same conditions.

We observed that the TG domain has the ability to bind both PGN from *P. aeruginosa* and *B. subtilis* (Fig. 8), with affinity in the μM range (estimated with the hypothesis that the binding is given by the interaction with the glycans presents in each molecule of muropeptide; see Materials and Methods). However the TG domain shows slightly greater affinity for the PGN from *P. aeruginosa*. The helicase does not bind the PGN from PAO1 but it binds the PGN from *B. subtilis* with a Kd in the millimolar range, i.e. around 10 times lower affinity than the value observed for TG domain (Table 3).

4. Discussion

Nowadays, *P. aeruginosa* is considered a public health risk due to its ability to develop resistances to multiple classes of antibiotics. Urgent and novel strategies to discover new antibiotics are required and the study of essential genes has proved to be an interesting strategy for the identification of important antimicrobials targets.

TgpA is an essential protein for the viability *P. aeruginosa*, proven through insertional and conditional mutagenesis (Milani et al, 2012) and is composed of an N-terminal domain with 5 transmembrane (TM) helices (residues 11-321 belonging to the DUF3488 superfamily), a periplasmic domain (residues 180-548), and an additional TM helix (residues 549-567) terminating into a small C-

terminal cytoplasmic domain (residues 582-638 belonging to the DUF4129 superfamily).

Our structural investigation shows that the periplasmic portion of TgpA is composed of two subdomains linked by a central β-sheets (*the septum*): the N-ter domain, rich of β-strands, likely endowed with regulatory and/or substrate-binding activity, and the α-helices at C-ter domain, hosting a conserved catalytic triad likely involved in specific enzymatic activity. In keeping with these hypotheses, using inducible expression and complementation experiments of the wt TgpA and the Cys404Ala mutant, we demonstrated the crucial the role of Cys404 for the (so far unknown) TgpA activity required for bacterial growth.

Considering the periplasmic localization of the protein and the evidence that the N-ter subdomain is structurally linked to different carbohydrate binding domains, our structural results suggest a probable involvement of the protein in cell wall (re)modelling. Accordingly, we proved that the TG domain is able to interact with PGN (pulldown experiments) with an estimated affinity in the uM range (MST experiments). Such degree of affinity was previously described by Wong *et al*, 2013, with the evaluation of the affinity of the LysM domain for different fragments of PGN, also estimated in the low macromolar range (μM). LysM is a well characterized carbohydrate-binding domain with affinity for GlcNac polymers and often associated with proteins involved in PGN synthesis or remodeling. Although the carbohydrate binding module at the N-terminal end of

the TG domain does not share homology with LysM or other already known domains that binds the bacterial PGN, the mechanisms of bacterial PGN recognition and regulatory mechanisms of the enzymes involved in its metabolism are still largely unknown. Further specific analysis must be done in order to identify the residues involved in the interaction with the PGN, in addition to the exploration of other possible substrates of the protein presents in the cell wall.

The motility of the domain C-ter end, suggested by analysis of the crystal structures, could be related to tuning of the protein activity via substrate(s) recognition, allowing the opening of the active site cleft toward the solvent only when the right substrate is present. In particular, the two structures available suggest a gating mechanism regulating the substrate accessibility to the active site involving: N and C-ter portions of the domain, together with Phe403. Since the terminal ends of the domain are linked to the inner transmembrane portions of the enzyme, protein-membrane interaction might play a role in regulation of substrate accessibility and/or enzymatic activity. Furthermore, a regulative role might be also played by the small C-ter cytoplasmic domain of the protein. Finally, the observed binding of phosphate ions might suggest a possible role for phosphorylated substrates.

All the microbiology, structural and biochemical data reported contributed to start unravelling the function of a new protein essential for *P. aeruginosa* viability, which represents a valuable target for the development of novel antibacterial therapies.

ACKNOWLEDGEMENTS

We are grateful to the beam line scientists from the ESRF facility for support during data collections, to C. Rotella, D. Vecchietti and E. Breukink for technical assistance and helpful discussion and to S. Ferrara for helpful discussion.

FUNDING INFORMATION

The European Commission (grant NABATIVI, EU-FP7-HEALTH-2007-B contract number 223670) funded this work. This funder had no role in study design, data collection and analysis, decision to publish, or preparation of the manuscript.

REFERENCES

Berman, H. M., J. Westbrook, Z. Feng, G. Gilliland, T. N. Bhat, H. Weissig, I. N. Shindyalov and P. E. Bourne (2000). "The Protein Data Bank." Nucleic Acids Res**28**(1): 235-242.

Desmarais, S. M., F. Cava, M. A. de Pedro and K. C. Huang (2014). "Isolation and preparation of bacterial cell walls for compositional analysis by ultra performance liquid chromatography." J Vis Exp(83): e51183.

Driscoll, J. A., S. L. Brody and M. H. Kollef (2007). "The epidemiology, pathogenesis and treatment of Pseudomonas aeruginosa infections." Drugs**67**(3): 351-368.

Emsley, P., B. Lohkamp, W. G. Scott and K. Cowtan (2010). "Features and development of Coot." Acta Crystallographica Section D**66**(4): 486-501.

Hanazono, Y., K. Takeda, S. Niwa, M. Hibi, N. Takahashi, T. Kanai, H. Atomi and K. Miki (2016). "Crystal structures of chitin binding domains of chitinase from Thermococcus kodakarensis KOD1." FEBS Lett**590**(2): 298-304.

Holm, L. and P. Rosenstrom (2010). "Dali server: conservation mapping in 3D." Nucleic Acids Res**38**(Web Server issue): W545-549.

Kabsch, W. (2010). "Xds." Acta Crystallogr D Biol Crystallogr**66**(Pt 2): 125-132.

Lamzin, V. S. and K. S. Wilson (1997). "Automated refinement for protein crystallography." Methods Enzymol**277**: 269-305.

Lodise, T. P., Jr., B. Lomaestro and G. L. Drusano (2007). "Piperacillin-tazobactam for Pseudomonas aeruginosa infection: clinical implications of an extended-infusion dosing strategy." Clin Infect Dis**44**(3): 357-363.

Makarova, K. S., L. Aravind and E. V. Koonin (1999). "A superfamily of archaeal, bacterial, and eukaryotic proteins homologous to animal transglutaminases." Protein Sci**8**(8): 1714-1719.

Milani, A., D. Vecchietti, R. Rusmini and G. Bertoni (2012). "TgpA, a protein with a eukaryotic-like transglutaminase domain, plays a critical role in the viability of Pseudomonas aeruginosa." PLoS One**7**(11): e50323.

Moll, M., D. H. Bryant and L. E. Kavraki (2011). "The LabelHash server and tools for substructure-based functional annotation." Bioinformatics**27**(15): 2161-2162.
Obritsch, M. D., D. N. Fish, R. MacLaren and R. Jung (2005). "Nosocomial infections due to multidrug-resistant Pseudomonas aeruginosa: epidemiology and treatment options." Pharmacotherapy**25**(10): 1353-1364.
Potterton, E., P. Briggs, M. Turkenburg and E. Dodson (2003). "A graphical user interface to the CCP4 program suite." Acta Crystallogr D Biol Crystallogr**59**(Pt 7): 1131-1137.
Sheldrick, G. M. (2010). "Experimental phasing with SHELXC/D/E: combining chain tracing with density modification." Acta Crystallogr D Biol Crystallogr**66**(Pt 4): 479-485.
Sillitoe, I., T. E. Lewis, A. Cuff, S. Das, P. Ashford, N. L. Dawson, N. Furnham, R. A. Laskowski, D. Lee, J. G. Lees, S. Lehtinen, R. A. Studer, J. Thornton and C. A. Orengo (2015). "CATH: comprehensive structural and functional annotations for genome sequences." Nucleic Acids Res**43**(Database issue): D376-381.
Smart, O. S., T. O. Womack, C. Flensburg, P. Keller, W. Paciorek, A. Sharff, C. Vonrhein and G. Bricogne (2012). "Exploiting structure similarity in refinement: automated NCS and target-structure restraints in BUSTER." Acta Crystallographica Section D**68**(4): 368-380.
Steiner, R. A., A. A. Lebedev and G. N. Murshudov (2003). "Fisher's information in maximum-likelihood macromolecular crystallographic refinement." Acta Crystallographica Section D**59**(12): 2114-2124.
Szaff, M., N. Hoiby and E. W. Flensborg (1983). "Frequent antibiotic therapy improves survival of cystic fibrosis patients with chronic Pseudomonas aeruginosa infection." Acta Paediatr Scand**72**(5): 651-657.
Vagin, A. and A. Teplyakov (1997). "MOLREP: an automated program for molecular replacement." Journal of Applied Crystallography**30**: 1022-1025.

Valerius, N. H., C. Koch and N. Hoiby (1991). "Prevention of chronic Pseudomonas aeruginosa colonisation in cystic fibrosis by early treatment." Lancet**338**(8769): 725-726.

Wong, J. E., H. M. Alsarraf, J. D. Kaspersen, J. S. Pedersen, J. Stougaard, S. Thirup and M. Blaise (2014). "Cooperative binding of LysM domains determines the carbohydrate affinity of a bacterial endopeptidase protein." FEBS J**281**(4): 1196-1208.

Xu, Q., S. Sudek, D. McMullan, M. D. Miller, B. Geierstanger, D. H. Jones, S. S. Krishna, G. Spraggon, B. Bursalay, P. Abdubek, C. Acosta, E. Ambing, T. Astakhova, H. L. Axelrod, D. Carlton, J. Caruthers, H. J. Chiu, T. Clayton, M. C. Deller, L. Duan, Y. Elias, M. A. Elsliger, J. Feuerhelm, S. K. Grzechnik, J. Hale, G. W. Han, J. Haugen, L. Jaroszewski, K. K. Jin, H. E. Klock, M. W. Knuth, P. Kozbial, A. Kumar, D. Marciano, A. T. Morse, E. Nigoghossian, L. Okach, S. Oommachen, J. Paulsen, R. Reyes, C. L. Rife, C. V. Trout, H. van den Bedem, D. Weekes, A. White, G. Wolf, C. Zubieta, K. O. Hodgson, J. Wooley, A. M. Deacon, A. Godzik, S. A. Lesley and I. A. Wilson (2009). "Structural basis of murein peptide specificity of a gamma-D-glutamyl-l-diamino acid endopeptidase." Structure**17**(2): 303-313.

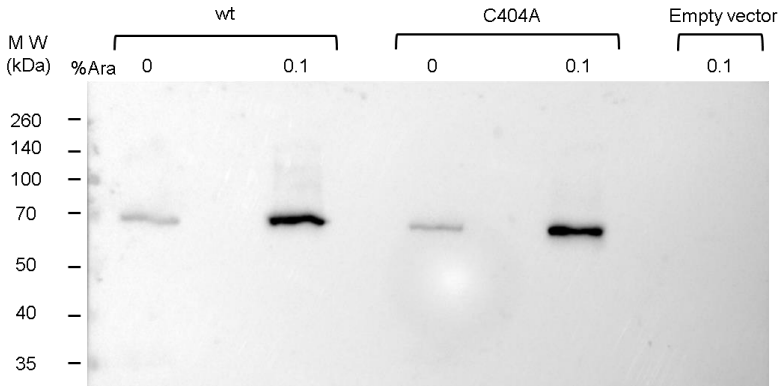

Fig. 1 Western Blot analysis of the ectopic expression of the TgpA wt and C404A full-length proteins in absence and presence of arabinose. 10 ul of total membrane fraction from the growth under each condition were loaded onto 12% SDS-PAGE. Samples induced with 0.1% Ara are diluted 1:10 with respect to the samples without arabinose. MW = Molecular weight marker.

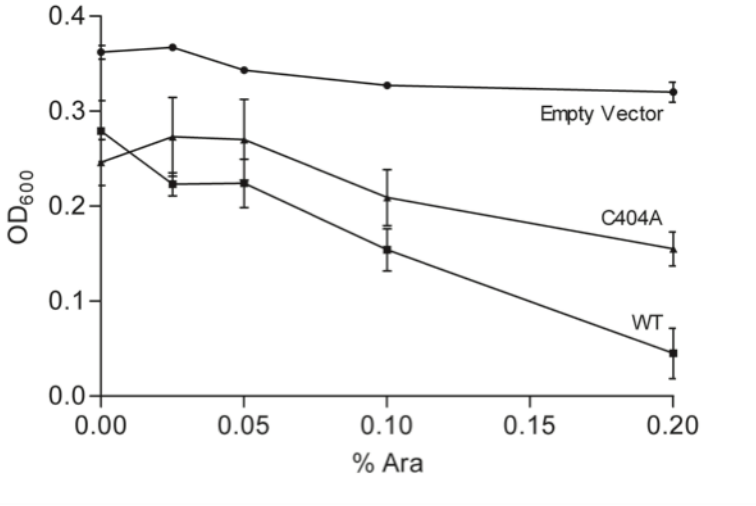

Fig. 2 Effects of ectopic expression of TgpA wt and mutant C404A on *P. aeruginosa* growth. The effects on growth were evaluated relative to PAO1 carrying the empty vector pHERD28T under five different concentrations of arabinose (0, 0.025, 0.05, 0.1 and 0.2%) for the induction of the P_{BAD} promoter. For each culture, the OD_{600} value after 16 hrs of growth (i.e. the onset of the stationary phase) was plotted with the corresponding concentration of arabinose.

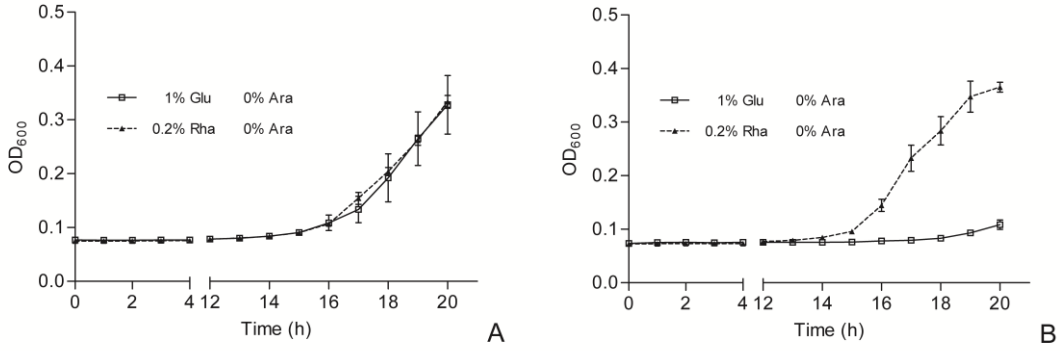

Fig. 3 Tests of complementation of a glucose-mediated down-regulation of the chromosomal *tgpA* gene in PAO1 *P_{rhaB}::tgpA*. PAO1 *P_{rhaB}::tgpA* strains carrying pHERD28T-TgpA wt (A), pHERD28T-TgpA-C404A (B) were grown in micro-cultures of 200 µl with the indicated concentrations of arabinose, rhamnose and glucose. Cultures growth was monitored in real-time by absorbance measurement at 600 nm (OD_{600}).

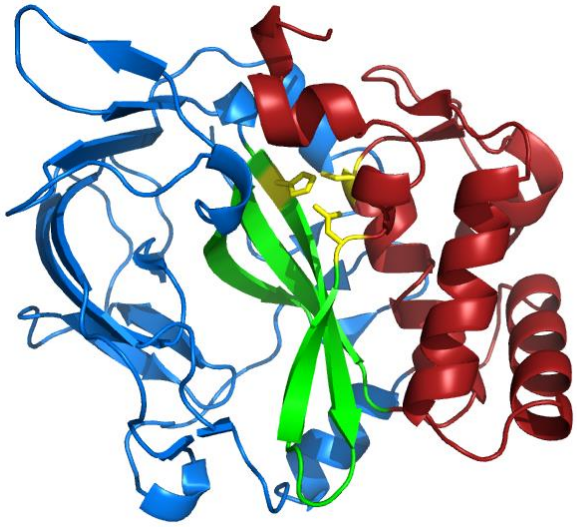

Fig. 4 Blue *right ventricle;* green *septum*; red *left ventricle; catalytic triad as yellow sticks*

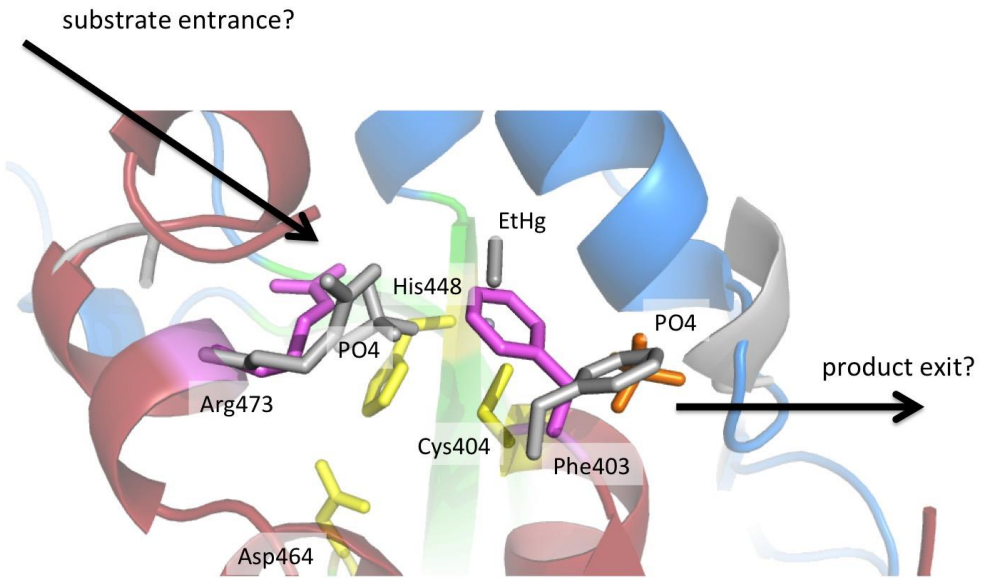

Fig. 5 Proposed substrate gating mechanism: entrance of the substrate from C-ter helix and Arg473, exit of the product toward N-terminal helix. Gating controlled by the position of Phe403.

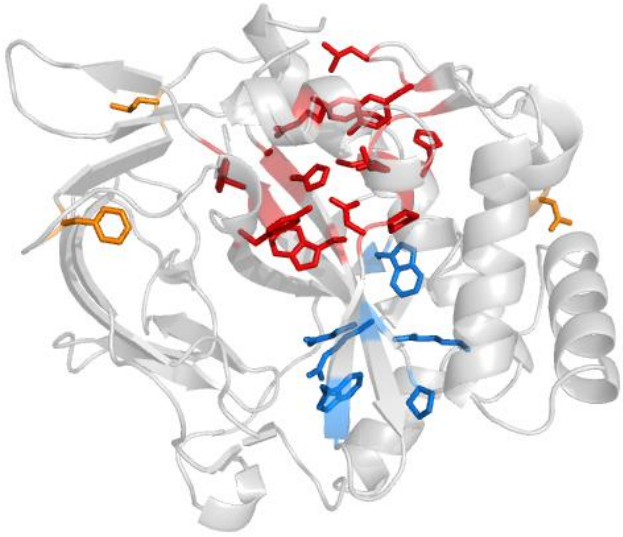

Fig. 6 strictly conserved residues in an alignment done with members of the gammaproteobacteria class (excluding pseudomonadales order) (lower seq. identity 45%) Active site cluster red, structural cluster blue, isolated residues (orange)

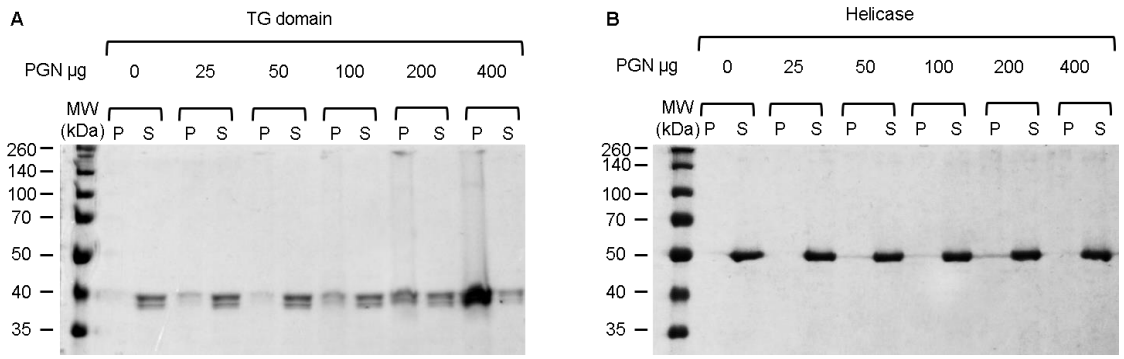

Fig. 7 Pulldown experiments with insoluble PGN. The binding capacity of the (**A**) TG domain and (**B**) Helicase were assayed by pulldown assay with increasing concentrations of insoluble PGN from *P. aeruginosa*. The lanes are labelled as follows: MW = Molecular weight marker, P = Pellet, S = Supernatant.

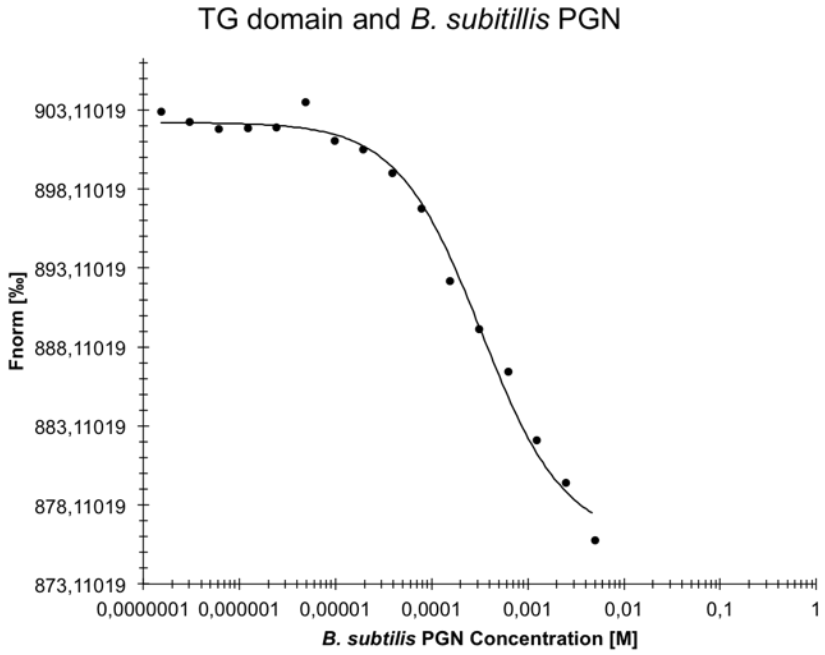

Fig. 8 TG domain-PGN interaction analyzed by MST. The TG domain – PGN interaction was monitored by titrating PGN form *B. subtilis* from 5 mM to ~0.1 nM against 75 nM of TG domain labelled with the Kit RED-NHS (NanoTemper technologies, Munich, Germany). The changes of the fluorescent thermophoresis signals were plotted and K_d values were determined using the NanoTemper analysis software, through non linear curve fitting.

Table 1. X-ray data-collection and refinement statistics

Data collection	TgpA Hg derivative	TgpA native
Beam line & wavelength (Å)	ESRF BM14U 1.00775 Å	ESRF ID30a-3 0.96770
Space group	$P4_32_12$	$P4_32_12$
Unit-cell parameters (Å)	a=b=72.5; c=157.5	a=b=71.6; c=164.3
Molecules in a.u.	1	1
Resolution (Å)	48.7 – 1.8	43.5 – 1.6
Mosaicity (°)	0.2	0.2
Unique reflections	74,217 (5,444)[a]	57,370 (4,156)[b]
Completeness (%)	99.9 (99.1)	99.9 (100)
Redundancy	7.1 (3.8)	7.5 (7.8)
Rmeas[†] (%)	9.1 (127.5)	6.4 (146.8)
CC(1/2) (%)	99.9 (42.5)	99.9 (73.9)
Average I/σ (I)	15.5 (1.1)	17.6 (1.7)
Final model		
R factor[‡]/Rfree[§] (%)	15.4/19.0	15.4/18.8
r.m.s. bonds (Å)	0.024	0.024
r.m.s. angles (°)	1.21	1.21
Average protein *B* fac.(Å^2)	...[b]	...[b]
Residues in most favored regions (%)	97%	97%
Residues in additionally allowed regions (%)	3%	3%
PDB-ID	**...**	**...**

Values in parentheses are for the highest resolution shell: [a](1.85-1.80), [b](1.64-1.60).

[†] $R_{meas} = (\Sigma (n/(n-1) \Sigma |I - (I)|)/ \Sigma I \times 100$, where I is intensity of a reflection and (I) is its average intensity.

[‡] $R_{factor} = \Sigma |F_o - F_c| / \Sigma |F_o| \times 100$.

[§] R_{free} is calculated on 5% randomly selected reflections, for cross-validation.

Table 2. Relative mRNA levels of ectopically overexpressed TgpA wt and C404A mutant

Strain	OD_{600}	0% Ara	0.1% Ara
PAO1-pHERD28T	0.8	1*	1
PAO1-pHERD28T-TgpA wt	0.8	16	544
PAO1-pHERD28T-C404A	0.8	11	363

*Values represent $2^{-\Delta\Delta CT}$ values of the ectopic expression of *tgpA* mRNAs

Table 3. Binding constants for PGN ligands. The equilibrium dissociation constants (K_d) are given in µM. NS: Not Significative

	K_d (µM)	
	P. aeruginosa	*B. subtillis*
TG domain	39± 2	210 ± 4
Helicase	NS	1800± 390

Supplementary information

Mass spectrometry analysis

Bands of interest were excised from SDS-PAGE and digested with trypsin and other peptidases, and analysed with LC-MS in the Protein Microsequencing Facility (PROMIFA-San Raffaele Scientific Institute-Milan).

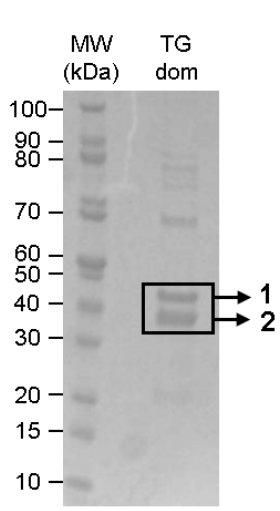

Band 1

MGSDKIHHHHHHHHHHGVR LGPLWSLPMP GNKGVTGLSE
201 SMAPGDIAEL GRSAELAFRV RFEGALPPRE QLYWRALTME RFDGRRWAQA
251 PQWSGEDALH WQKRGPELRY DVIMQPSSQP WLFALDVAQT DQTDTRLMSD
301 FHLQRRQPVE QRLFYRVSSW PQALRESSID PRTRWRNLQL PMHGNPRARA
351 LADELRQAHA QPQALVAALL QRFNHEPFAY TLKPPATGAD GVDDFLFDTR
401 SGFCAHYAGA MAFVLRAAGI PARVVAGYQG GELNPAGNYL LVHQFDAHAW
451 VEYWQPEQGW LSVDPTYQVA PERIEQGLEQ ALAGDSEYLA DAPLSPLRYR
501 GLPWLNDMRL AWDSLNYGWQ RWVLAYQGEQ QGAFLQRWFG GLDP

Band 2

MGSDKIHHHHHHHHHHGVR LGPLWSLPMP GNKGVTGLSE
201 SMAPGDIAEL GRSAELAFRV RFEGALPPRE QLYWRALTME RFDGRRWAQA
251 PQWSGEDALH WQKRGPELRY DVIMQPSSQP WLFALDVAQT DQTDTRLMSD
301 FHLQRRQPVE QRLFYRVSSW PQALRESSID PRTRWRNLQL PMHGNPRARA
351 LADELRQAHA QPQALVAALL QRFNHEPFAY TLKPPATGAD GVDDFLFDTR
401 SGFCAHYAGA MAFVLRAAGI PARVVAGYQG GELNPAGNYL LVHQFDAHAW
451 VEYWQPEQGW LSVDPTYQVA PERIEQGLEQ ALAGDSEYLA DAPLSPLRYR
501 GLPWLNDMRL AWDSLNYGWQ RWVLAYQGEQ QGAFLQRWFG GLDP

Fig S1. Mass spectrometry analysis of the two bands obtained during the TG domain purification. In Red are highlighte all the peptides generated by tripsin digestion and identified with mass analysis. In Green are highlithed those peptides generated by digestion with other peptidases different from trypsin.

PART III

F. Preliminary results

F.1 TgpA *In silico* docking

Molecular docking has become an increasingly important tool for drug discovery. This approach can be used to model the interaction between a small molecule and a protein at the atomic level, which allows characterizing the behaviour of small molecules in the binding site of target proteins as well as to elucidate fundamental biochemical processes.

A search was maid through molecular docking ligand-protein complexes by exploring the conformational space of a library of ligands within the active site of the TG domain. A scoring function was used to approximate the free energy of binding between the protein and the ligand in each docking pose. Docking and scoring produced a series of ranked compounds, with which were subsequently evaluated *in vivo*.

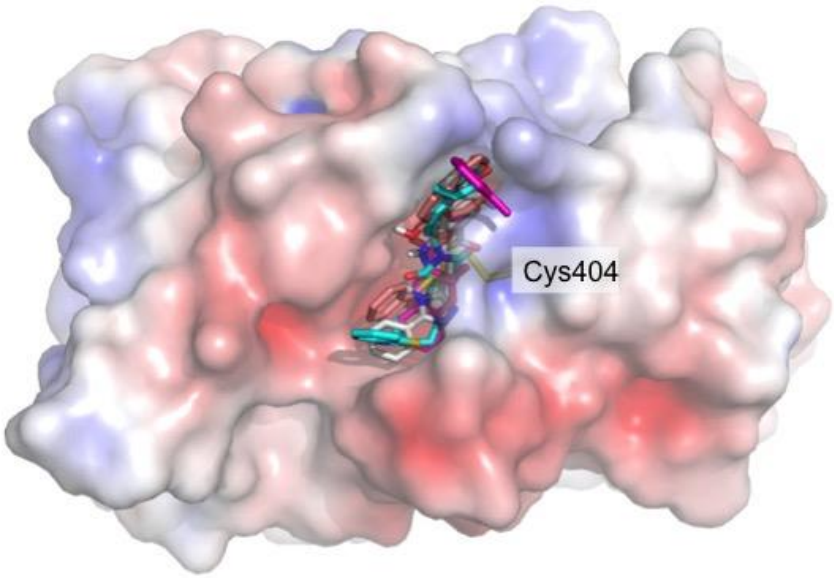

Figure F1. Representation of putative inhibitory compounds found during *In silico* docking, located inside the catalytic core of the TG domain structure.

In the TG domain 3D structure it is possible to identify a putative ligand-binding cavity displaying open or closed structure, regulated by the conformation of the C-terminal tail of the domain. Using the 3D structure of the protein in the open state (Hg bound) it was analysed *in silico* a medium size library of commercially available compounds (Hit2lead with 30,000 molecules) identifying eight potential binders with predicted K_i in the nM range.

The library was first analysed with the program AutoDock Vina (fast screening) exploring a protein region around Phe403 (with extension of 23 Å in every direction) to extract the top molecules (161 molecules, 0.5% of the library). In a second run the chosen compounds have been ranked more accurately with the program AutoDock (slow screening) identifying the best eight molecules that are listed in Table F1.

For *in vivo* evaluation, overnight cultures of PAO1 and *E. coli* strain M1655 were diluted in LB 50% to OD_{600} 10^{-6} and inoculated in microtiter wells with serial dilutions of each compound per triplicated, starting from 100 µM to 0.05µM. Culture growths were monitored in real-time by absorbance measurement at OD_{600} for 20 hrs and the percentage of inhibition was calculated considering 100% the growth of the control PAO1 and *E. coli* M1655 in the absence of compounds.

The compound #8 could not be evaluated because it was not soluble. The other seven compounds tested in PAO1 and in *E. coli* M1655, did not show a significant inhibition; none of them showed an inhibition of growth higher than 50% (Table F1).

The percentage of inhibition observed in *E. coli* M1655, generally higher than that observed in PAO1, suggests that the inhibition might not be specific to the function that TgpA fulfills in PAO1, since *E. coli* M1655 shares no homologs with TgpA.

The compound #2 shows inhibition of around 17% in *P. aeruginosa*, which is not trivial for a first screening.

In order to continue with the search for possible inhibitory molecules of the TgpA activity, which consequently inhibit the growth of *P. aeruginosa*, the search and evaluation of new compounds must be performed.

Table F1. 2D chemical structures of the eight top-scoring compounds found during *in silico* docking of the TG domain, and its percentage of inhibition in PAO1 *and E. coli* strain M1655. NT: Not tested

Compund	K_i (nM)	Structure	Percentage (%) of inhibition	
			PAO1	*E. coli* M1655
1	25.2	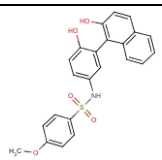	0	8±0.07
2	9.3	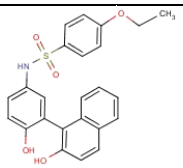	17±0.07	14±0.09
3	348	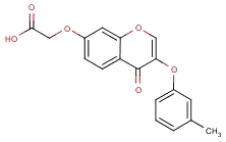	13±0.06	29±0.1
4	42.3	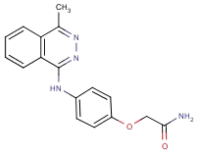	10±0.04	25±0.1
5	33	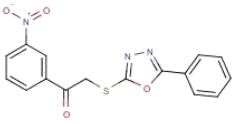	10±0.03	21±0.05
6	375	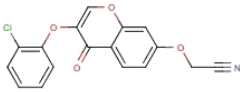	5±0.04	17±0.05
7	343	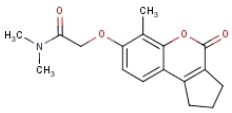	3±0.03	23±0.04
8	71.2	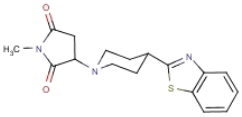	NT	NT